

ENGINEERING EXPERIMENT STATION
COLLEGE OF ENGINEERING

SOLAR-ASSISTED REFRIGERANT-FILLED
COLLECTOR HEAT PUMPS

BY

MICHAEL P. O'DELL

MASTER OF SCIENCE
(MECHANICAL ENGINEERING)

UNIVERSITY OF WISCONSIN-MADISON
1982



SOLAR-ASSISTED REFRIGERANT-FILLED
COLLECTOR HEAT PUMPS

by

MICHAEL P. O'DELL

A thesis submitted in partial fulfillment of the
requirements for the degree of

MASTER OF SCIENCE
(Mechanical Engineering)

at the

UNIVERSITY OF WISCONSIN-MADISON

1982

ABSTRACT

This thesis presents a general procedure for estimating seasonal performance of heat pump systems with refrigerant-filled collectors. The procedure is based on the "bin" method for weather statistics and accounts for variations in collector design and orientation and for heat pump capacity and efficiency. The "sol-air" temperature concept is utilized and hourly weather data is needed in order to generate the necessary bins. The design procedure presented in this thesis is applicable to most applications of collector heat pumps without energy storage.

The results from this design procedure for space heating and process water heating applications for uncovered and covered collector heat pump systems will be compared against performance results for a conventional heat pump and liquid-based solar heating system. The effects of changes in system parameters (collector design, convection loss coefficient and orientation, heat pump size and COP, load type and location) on performance are presented. Methods for improving overall system performance such as optional collector control and thermal storage are discussed. The effects of convection and solar radiation on the collector performance is presented. Performance degradation due to heat pump cycling is discussed. Also presented is an economic analysis of the uncovered collector system for space heating and the performance of such a system in the cooling

mode.

The results for heating performance indicate that uncovered collector heat pump systems have somewhat better performance than conventional air-source heat pumps and covered collector heat pump systems at a wide range of collector areas. Conventional solar systems surpass the performance of the heat pump systems at large collector areas. Thermal storage greatly enhances the performance of collector heat pump systems, especially the covered collector systems which have inferior performance without storage. Economic considerations reduce the attractiveness of collector heat pump systems. Cooling performance of the solar-assisted heat pump systems is below the performance of conventional air-source heat pumps.

A heat pump system with a refrigerant-filled collector/evaporator is best utilized if the collector is not covered and exposed on both sides. This system can have a reasonably small collector area and no storage is needed for satisfactory performance.

ACKNOWLEDGMENTS

I sincerely express my gratitude for the guidance of Professors J. W. Mitchell, W. A. Beckman, S. A. Klein and J. A. Duffie in this work. I especially appreciate the enthusiasm, encouragement and knowledge shown by Professor Mitchell. I would also like to thank the other graduate students and staff of the Lab for their many helpful suggestions and advice.

The financial support of the Solar Heating and Cooling Research and Development Branch, Office of Conservation and Solar Applications, U. S. Department of Energy is appreciated. Bonnie Albright and the State of Wisconsin Energy Office also deserve thanks for financial support.

Finally, I would like to thank my mother and other family members, friends and God, who gave me the necessary understanding and support when it was needed.

TABLE OF CONTENTS

	<u>Page</u>
ABSTRACT	ii
ACKNOWLEDGMENTS	iv
LIST OF FIGURES	vii
LIST OF TABLES	x
NOMENCLATURE	xi
1.0 INTRODUCTION	1
1.1 Background	1
1.2 Objectives	5
2.0 SYSTEM MODEL	7
2.1 System Description	7
2.2 System Model for Heating Performance	9
3.0 DESIGN METHOD	20
3.1 Sol-Air Temperature Bin Method	20
4.0 SPACE HEATING PERFORMANCE	31
4.1 Base Case Space Heating Applications	31
4.2 Collector Control Strategy	59
4.3 Collector Convection and Radiation Heat Transfer	64
4.4 Performance Upper Bound with Storage	75
4.5 Building Thermal Capacitance	78
4.6 Performance Degradation Due to Cycling	81
4.7 Economic Considerations	91
5.0 SPACE COOLING APPLICATIONS	96
5.1 System Model for Cooling Performance	96
5.2 TRNSYS Simulation Results	100
6.0 HIGH TEMPERATURE PROCESS WATER HEATING APPLICATIONS	104
6.1 Base Case Process Heat Applications	104
6.2 Collector Control	113
6.3 Performance Upper Bound with Storage	113

TABLE OF CONTENTS (continued)	<u>Page</u>
7.0 CONCLUSIONS	117
APPENDIX A: DESIGN METHOD PROGRAMS	121
A.1 Sol-Air Temperature Bin Generation Method	122
A.2 Performance Simulation-Space and Process Water Heating	125
APPENDIX B: COOLING MODEL TRNSYS COMPONENT	128
BIBLIOGRAPHY	131

LIST OF FIGURES

<u>Figure</u>	<u>Page</u>
2.1.1 Refrigerant-Filled Collector Heat Pump System	8
2.2.1 Heat Pump Performance	18
3.1.1 Sol-Air Temperature Bin Distribution for Uncovered Collector in January--Madison	22
3.1.2 Effect of Sol-Air Temperature on COP	25
4.1.1 Base Case Space Heating Performance--Madison	33
4.1.2 Base Case Space Heating Performance--Albuquerque	34
4.1.3 Base Case Space Heating Performance--New York	35
4.1.4 Base Case Space Heating Performance--Seattle	36
4.1.5 Effect of U_L on Heating Performance--Madison	40
4.1.6 Effect of Heat Pump Size on Uncovered Collector System F_{NP} --Madison	43
4.1.7 Effect of Heat Pump Size on Covered Collector System F_{NP} --Madison	44
4.1.8 Effect of Heat Pump Size on Uncovered Collector System COP--Madison	46
4.1.9 Effect of Heat Pump Size on Covered Collector System COP--Madison	47
4.1.10 Effect of Maximum COP on Collector Heat Pump Performance--Madison	50
4.1.11 Effect of Maximum COP on Collector Heat Pump Performance--Albuquerque	51
4.1.12 Effect of 25% COP Improvement on Heat Pump Performance--Madison	53
4.1.13 Effect of 25% COP Improvement on Heat Pump Performance--Albuquerque	54

LIST OF FIGURES (continued)

<u>Figure</u>		<u>Page</u>
4.2.1	Effect of Collector Performance Control--Madison	61
4.2.2	Fraction of Hours During Which Evaporator Temperature Exceeds Ambient for Collector Heat Pump Systems--Madison	63
4.3.1	Summary of "Free" Energy Gained by Collector Heat Pumps--Madison	66
4.3.2	Overall COP by Energy Gain Modes for Uncovered Collector Heat Pump--Madison	67
4.3.3	Overall COP by Energy Gain Modes for Covered Collector Heat Pump--Madison	68
4.3.4	Fraction of Operating Hours by Energy Gain Modes--Madison	69
4.3.5	Temperature Bin Distribution for Uncovered Collector in January--Madison	70
4.3.6	Critical Level for Convection Heat Transfer to Collector	73
4.4.1	Upper Bound Performance with Storage for Collector Heat Pumps--Madison	77
4.6.1	Typical Heating Load and Heat Pump Capacity vs. Ambient Temperature	82
4.6.2	Effect of Degradation Coefficient on Uncovered Collector Heat Pump--Madison	87
4.6.3	Effect of Degradation Coefficient on Covered Collector Heat Pump--Madison	88
4.7.1	Additional Cost for Uncovered Collector System Collector Cost for Zero Life Cycle Savings vs. Conventional Heat Pump--Madison	94
5.2.1	Overall Cooling COP--Madison	101

LIST OF FIGURES (continued)

<u>Figure</u>		<u>Page</u>
5.2.2	Overall Cooling COP--Albuquerque	102
6.1.1	Base Case Process Heating Performance--Madison	107
6.1.2	Base Case Process Heating Performance--Albuquerque	108
6.1.3	Effect of Shading Incident Radiation on Uncovered Collector Process Heat Performance--Madison	110
6.1.4	Energy Delivered to Load by Collector Heat Pumps--Madison	111
6.1.5	Energy Delivered to Load by Collector Heat Pumps--Albuquerque	112
6.2.1	Effect of Collector Performance Control for Process Heating Load--Madison	114
6.3.1	Upper Bound with Storage for Process Heat Load--Madison	116

LIST OF TABLES

<u>Table</u>	<u>Page</u>
2.2.1 Heat Pump Model Empirical Curve Fit Constants	17
2.2.2 Effect on Heat Pump Performance	19
4.1.1 System Simulation Parameters--Space Heating	32
4.1.2 Conventional Heat Pump Performance--Madison Simulation	45
4.1.3 Effect of Collector Slope on System Performance	58
4.5.1 Improved Results with Storage--Madison	80
4.6.1 Cycling Performance--Madison	89
4.6.2 Effect of Cycling Rate on COP	91
5.1.1 System Simulation Parameters--Cooling	99
6.1.1 System Simulation Parameters--Process Heating	105

NOMENCLATURE

A_c	Collector area
C_p	Specific Heat Constant
C_D	Degradation coefficient
C_{Fl}	First year unit energy cost
COP	Heat pump coefficient of performance
COP_{cyc}	Heat pump coefficient of performance during cycling
COP_{ss}	Heat pump steady-state coefficient of performance
E_c	Initial investment cost for conventional heat pump
E_s	Initial investment cost for solar-assisted heat pump
f_{cyc}	Fraction of "on-time" with heat pump cycling
f_{ss}	Fraction of "on-time" with steady-state heat pump operation
F'	Collector efficiency factor
F_{np}	Fraction of load met by non-purchased energy
F_{np-c}	Non-purchased fraction for a conventional heat pump
F_{np-s}	Non-purchased fraction for a solar-assisted heat pump
F_R	Collector heat removal efficiency factor
h_{rad}	Radiation heat transfer coefficient
h_{wind}	Wind convection heat transfer coefficient
I_T	Rate of solar radiation incident on the collector
L	Annual heating load
LCS	Life-cycle cost savings for installed equipment
\dot{m}	Mass flow rate

NOMENCLATURE (continued)

P_1	Ratio of life-cycle fuel cost savings to first year fuel cost savings
P_2	Ratio of additional life-cycle expenditures due to capital investment to the initial investment
Q_{abs}	Rate of energy absorbed by the collector
Q_{AUX}	Rate of energy supplied by the auxiliary source
Q_{COOL}	Rate of capacity by the heat pump in the cooling mode
Q_{cyc}	Heat pump capacity during cycling
Q_{DEL}	Rate of capacity by the heat pump in the heating mode
Q_L	Rate of heating load
Q_{NOM}	Nominal heat pump capacity
Q_{ss}	Heat pump steady-state capacity
Q_u	Rate of useful energy collection
T_a	Outdoor ambient temperature
T_c	Heat pump saturated condensing temperature
T_e	Heat pump saturated evaporating temperature
$T_{f,i}$	Collector fluid inlet temperature
T_p	Collector plate surface temperature
T_{sa}	Collector sol-air temperature
T_{sky}	Equivalent blackbody sky temperature
T_R	Room temperature
$(UA)_e$	Evaporator heat exchanger overall heat transfer coefficient
$(UA)_o$	Overall heat transfer coefficient for space heating

NOMENCLATURE (continued)

U_B	Collector bottom loss coefficient
U_L	Collector overall loss coefficient
U_T	Collector top loss coefficient
V_{wind}	Wind velocity
W	Heat pump electrical input
W_{cyc}	Heat pump electrical input during cycling
W_{ss}	Heat pump steady-state electrical input

Greek Symbols

ε	Collector emittance
σ	Stephan-Boltzman constant
$(\tau\alpha)$	Effect product of the transmittance of the cover system and the absorptance of the collector plate

1.0 INTRODUCTION

1.1 Background

Electrically driven air-to-air heat pumps and solar heating systems have proven to be practical means for reducing consumption of fossil fuels for space heating and water heating purposes. The potential advantages of combining the "free" low-grade sources of energy used by heat pumps and solar collectors have been of great interest to researchers and designers in recent time.

Much previous research on systems which use solar radiation with heat pumps has involved concepts in which a solar collection system operates in an independent "loop," while interfacing in some manner with the halocarbon refrigerant heat pump. The three basic configurations of this type that have been investigated can be differentiated according to the arrangement of the solar collection system and the heat pump with respect to the heating load. In the "series" system [1,2], the solar collection system and heat pump act in series with respect to the load. The energy stored by the solar system is used by the evaporator of the heat pump to allow operation at elevated temperatures. The "parallel" system [1,3] consists of independent heat pump and solar heating systems. Each system delivers to the load directly. The "dual source" system [1] allows the heat pump to utilize either the solar source or an ambient source to drive its evaporator. It is possible to combine the advantages of the series and parallel system this way.

One of the recent developments in the area of heat pump and solar technology is the use of refrigerant-filled solar collectors in place of the air source evaporator in a heat pump system. The rest of the system employs standard materials and components currently utilized in the refrigeration and air conditioning industry. This configuration is practical because of the widespread experience and use of the technology applied to its design, and the simplicity of the design itself relative to other solar-heat pump combined systems.

The flat plate used as the heat pump evaporator combines wind and natural convection along with incident solar radiation for transferring heat to the halocarbon refrigerant inside the collector/evaporator. From a solar viewpoint, the working fluid undergoes a phase change at a relatively low constant temperature. This yields a higher collector efficiency than that of a conventional liquid or air solar collector which operates at higher temperatures. Collection efficiencies near 100 percent can be achieved if the collector operates at temperatures close to the ambient, which is possible with refrigerant-filled collectors. Collector efficiency is also improved due to the fact that two phase flow is occurring, resulting in high heat transfer coefficients. From a heat pump standpoint, the effect of incident solar radiation is to raise the evaporating temperature, resulting in increased heat pump coefficient of performance (COP) and capacity delivered to the load. When the evaporator temperature exceeds the ambient temperature, convection losses from the collector/

evaporator occur, resulting in lowered collector efficiency. When no solar radiation is available, heat transfer to the collector is by convection alone. In this situation the system will operate like a conventional heat pump in the respect that the evaporator temperature will be lower than the ambient temperature. Since the collector/evaporator must depend on free convection heat transfer when solar radiation is unavailable collector heat pump performance may suffer relative to conventional heat pumps, which are designed for forced convection heat transfer to the evaporator. Another factor which might be detrimental to collector heat pump performance is the greater pressure drop due to two phase refrigerant flow in the collector passages which will hurt compressor performance. The collector heat pump concept does allow the elimination of the defrost cycle characteristic of air-to-air heat pumps. Due to the nature of collector design and solar absorption, the frost layer on the collector will not become thick enough to warrant defrost capability.

Taking the above analysis into account, there are reasons to expect that refrigerant-filled collector heat pump systems can be designed adequately to yield performance superiority over conventional heat pump and solar systems. Industrial process water heating applications have been shown to be thermally and economically attractive [4] for heat pumps, which may indicate a potential use for solar-aided heat pumps for daytime operation. Studies of refrigerant-filled collectors alone [5] and the resulting heat pump performance with elevated evaporating temperatures [6] have been

done, but not used in system performance estimates in this thesis. Charturvedi, Chiang and Roberts [5] concluded that collector efficiency was important in overall system design and a balance should be struck between improved system performance and reduced collector efficiency at increasing collector area for an optimum economic return. Kush [6] stated that existing heat pump technology and components could be used to obtain consistently high heat pump COP when operating with an elevated evaporator source temperature.

A design point analysis was made by Krakow and Lin [7] but the results do not indicate seasonal performance. Krakow and Lin discovered that heat pump systems with collectors without covers performed better than systems with covered collectors at low levels of solar radiation and high ambient temperatures, while covered collector system performed better at high levels of solar radiation and low ambient temperatures. Their conclusion, based on comparisons of performance with one collector area and one heat pump size, was that covered collector heat pump systems were better suited for cold climates than uncovered systems.

In a study by Hito [8], experimental work was performed on a custom-designed refrigerant-filled collector heat pump system. The author concluded that the system is technically feasible and that there is potential for using the system to cool as well as heat. Hito also mentioned the indispensibility of obtaining accurate computer simulations. Dixon [9] concluded that a water storage system with an uncovered collector heat pump system should not be recom-

mended because heat losses and parasitic power consumption actually reduced overall system performance in an experimental situation. Dixon also stated that the system could be practical for cooling applications, but suggested that the heat pump operate at night only, or some form of collector plate cooling be used.

Although refrigerant-filled collector heat pump systems are being manufactured and marketed, there is no information available to compare the seasonal performance of these systems to conventional heat pumps or solar heating systems.

1.2 Objectives

The first objective of this work is the development of a computer simulation model for heating applications with sufficient accuracy and simplicity to be used in many long term performance simulations. The model is flexible enough to permit changes in parameters such as system size and efficiency and collector area, orientation and collector properties. Next, a design method based on the collector "sol-air" temperature and the use of temperature bins was created. The sol-air temperature bin method, which can be used in locations for which hourly weather data are available, was useful in much of the following analyses of solar-aided and conventional heat pump performance.

In Chapter 4 of this thesis the results of performance simulations in space heating applications are presented. The principle application of refrigerant-filled collector heat pumps is in residential space heating where the systems are in direct competition with

conventional heat pump and solar systems, as well as fossil-fueled systems. The primary performance parameter revealed in this section is the amount of "free" energy delivered to the load. Thus seasonal performance comparisons are made between collector heat pump and conventional heat pump and solar systems. The effect of system parameters such as collector convection heat transfer coefficient, maximum COP, heat pump size and collector slope are discussed. Methods of improving system performance which include storage, use of building thermal capacitance and selective collector control are presented. Performance degradation due to heat pump compressor cycling is discussed. The contributions of convection heat transfer and radiation heat transfer to the collector will be compared for uncovered and covered collector heat pump systems. The computer model and corresponding results for collector heat pumps in cooling mode operation are presented in Chapter 5. In Chapter 6, the collector heat pump system will be applied to process water heating applications and an account will be made of the effect of various parameters on system performance. The performance differences between the space heating and process heat applications for these systems will be analyzed in the concluding section of this thesis. General recommendations for optimizing the design of refrigerant-filled collector heat pumps will also be included.

2.0 SYSTEM MODEL

2.1 System Description

The basic configuration of the refrigerant-filled collector heat pump system for which the computer model is derived is shown in Figure 2.1.1. System control is typical of most space heating heat pump installations in that the heat pump compressor is switched "on" anytime there is a call for heat from the room thermostat.

The heat pump evaporator is a refrigerant-to-air heat exchanger which absorbs available solar radiation. A collector/evaporator may have cover plates ("covered collector") to reduce convection losses during periods in which incident radiation raises the plate temperature above ambient. A bare collector/evaporator ("uncovered collector") will allow plate exposure to wind and natural convection. The performance of the uncovered collector is expected to be more uniform than the covered collector because of the effect of convection. For both types of collectors the ambient air acts as a convective heat source or sink, depending on whether the refrigerant temperature is higher or lower than the ambient temperature.

The system requires some form of refrigerant flow regulator between its high and low pressure sides in order to provide a refrigerant vapor superheat level at the compressor inlet. Thermal expansion valves are best suited for this specification because they are designed to sense and maintain a relatively constant superheat throughout a wide range of operating pressures. The heat pump compressor is of the hermetically sealed, reciprocating piston variety and is de-

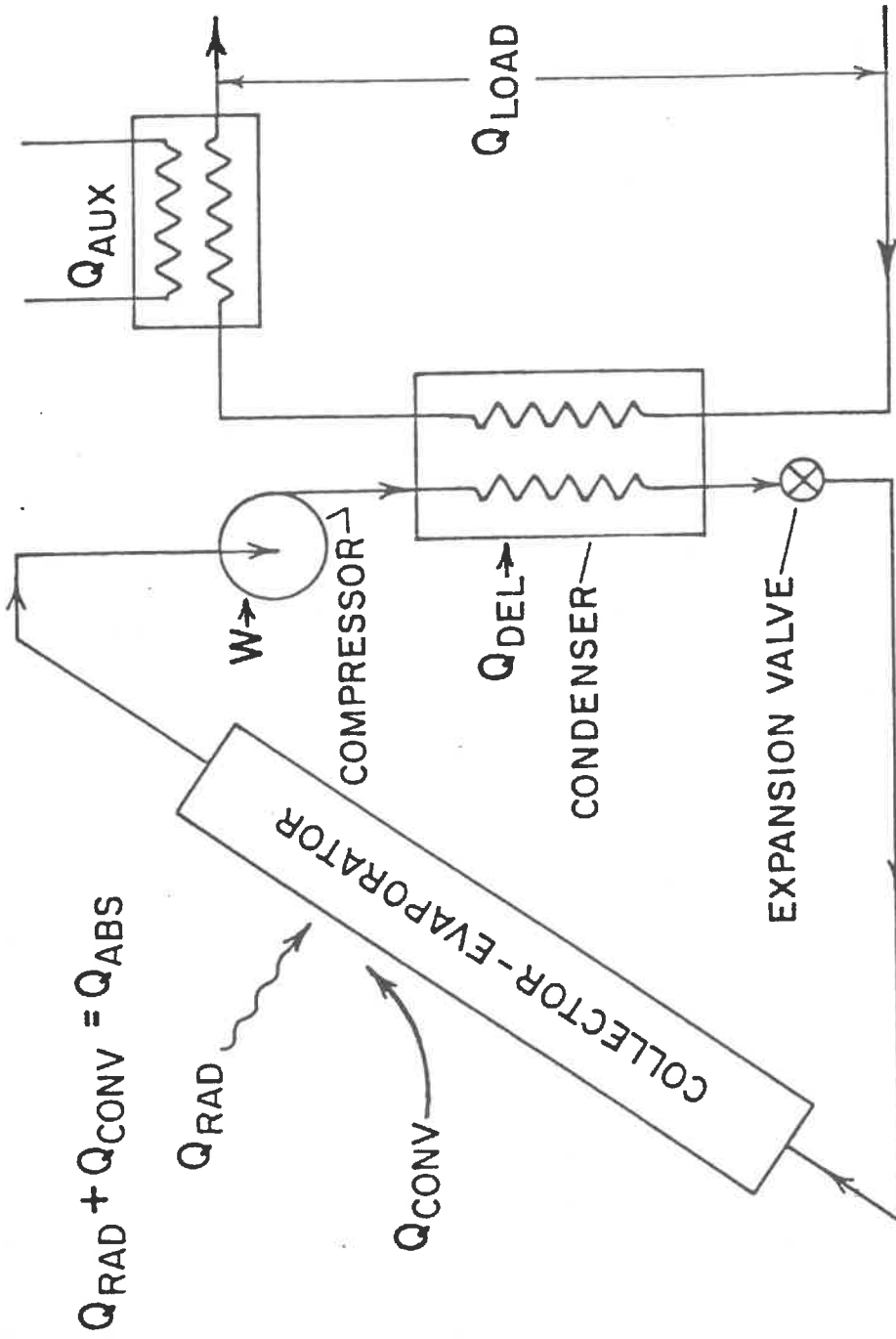


Figure 2.1.1 Refrigerant-Filled Collector Heat Pump System

signed to operate with a specific type of refrigerant. A refrigerant receiver and/or accumulator may also be included in the system to help in controlling the refrigerant distribution. The energy rejected by the condenser after refrigerant compression contributes to the load requirements through a refrigerant-to-air or refrigerant-to-water heat exchanger. The remainder of the load demand is met by an auxiliary source. An energy storage media for rejected condenser heat is not ordinarily included for space heating applications in these installations. However, the effects of storage on system performance will be discussed.

2.2 System Model for Heating Performance

Refrigerant-Filled Collector Heat Pumps--The flat plate evaporator is modeled with the Hottel and Whillier collector equation for useful energy gain [10]

$$Q_u = A_c F_R [(\tau\alpha) I_T - U_L (T_{f,i} - T_a)] \quad 2.2.1$$

where Q_u is the useful energy collector, A_c is the collector plate area, F_R is the collector heat removal factor, $(\tau\alpha)$ is the transmittance-absorptance product, I_T is the incident solar radiation, U_L is the loss coefficient, and $T_{f,i}$ and T_a are the fluid inlet and ambient temperatures, respectively.

The heat removal factor, F_R , is limited by the value of the collector efficiency factor, F' . At a particular location on the collector, F' represents the ratio of the actual useful energy gain to the useful energy gain that would result if the collector plate sur-

face had been at the local fluid temperature [11]. In the case where a collector contains a refrigerant undergoing boiling heat transfer, resistance to heat transfer between the boiling fluid and ambient air is quite small. Inside film coefficients are higher than ones in single phase flow. The film coefficient for a typical halocarbon refrigerant, R-12, in two-phase flow is approximately three times the film coefficient of liquid refrigerant in the same flow application. Coupled with the reasoning that refrigerant flow rates in heat pump applications are on the same order as flow rates in conventional liquid collection system and the assumption of negligible metal bond resistance leads to the belief that the collector efficiency factor is nearly, if not equal to unity. This assumption of unity collector efficiency is optimistic for a practical collector design and may yield results which are slightly greater than what is achievable. The heat removal factor, F_R , is the ratio of the actual useful energy gain by the collector to the useful gain if the whole collector were at the inlet fluid temperature. It is related to the collector efficiency factor by

$$F_R = \frac{\dot{m} C_p}{A_c U_L} \left[1 - e^{-\frac{A_c U_L F'}{\dot{m} C_p}} \right] \quad 2.2.2$$

where \dot{m} is the mass flow rate through the collector and C_p is the specific heat constant of the collector fluid. In two phase flow through the collector, the refrigerant temperature remains at the saturation temperature until all of the refrigerant has evaporated.

A small portion of the collector/evaporator will have superheated refrigerant in it prior to entering the compressor, but the effect on overall heat removal factor is assumed to be negligible. The argument for the collector uniform temperature assumption is enhanced by the reasoning that the collector has a high inside film coefficient due to refrigerant boiling and the design of the collector passages is such that there is insignificant temperature gradient in the collector plate. In all of the simulations reported in this thesis, the value used for F_R is unity. This is a reasonable assumption, given the above arguments and the uncertainty in estimating other collector parameters, such as $(\tau\alpha)$ and U_L .

The fluid inlet temperature to the collector is the evaporator temperature, T_e , and the useful energy collected is the absorbed energy for the heat pump, Q_{abs} . Equation 2.2.2 can be rewritten as

$$Q_{abs} = A_c [(\tau\alpha) I_T - U_L (T_e - T_a)] \quad 2.2.3$$

The loss coefficient or convection coefficient, U_L , is the sum of the collector top and bottom loss coefficients, U_T and U_B . The covered collector loss coefficients are treated in the same manner as conventional solar collectors [11,12]. The top of the collector is covered with at least one glazing and the bottom is insulated. Both sides of the uncovered collector are exposed to wind and natural convection currents while only the top is exposed to solar radiation. U_L for the uncovered collector is due primarily to convection and is a strong function of wind velocity. The wind convection coefficient

is determined by [11]:

$$h_{\text{wind}} = 3.74 V_{\text{wind}}^{0.6} \quad 2.2.4$$

where V_{wind} is the wind velocity in meters/second and h_{wind} has units of watts/(meters)²C.

Radiation emitted from the plate is accountable by [11]:

$$h_{\text{rad}} = \sigma \epsilon (T_p^4 - T_{\text{sky}}^4) \quad 2.2.5$$

where σ is the Stephan-Boltzman constant, ϵ is the plate emissivity, T_p is the plate temperature (equal to T_e) and T_{sky} is the equivalent surrounding blackbody temperature. T_{sky} is determined by [11]:

$$T_{\text{sky}} = 0.0552 T_a^{1.5} \quad 2.2.6$$

The overall convection coefficient for an uncovered collector is estimated by:

$$U_L = U_T + U_B = (h_{\text{wind}} + h_{\text{rad}}) + h_{\text{wind}} \quad 2.2.7$$

The equations used in determining heat pump capacity and COP for the computer model are curve fits derived from manufacturer's data for conventional air-to-air heat pumps. Energy rejected by the heat pump condenser and delivered to the load by the heat pump is of the form

$$Q_{\text{DEL}} = F(T_e) = (a_1 + a_2 T_e + a_3 T_e^2) Q_{\text{NOM}} \quad 2.2.8$$

where Q_{NOM} is the nominal heat pump capacity and a_1 , a_2 and a_3 are

empirical constants. In heating applications the saturated condensing temperature remains relatively constant because of the constant sink temperature of the fluid entering the condenser. If the condenser is a refrigerant-to-air heat exchanger, the sink temperature is typically 20°C. The actual heat pump capacity is assumed to be only a function of the evaporator temperature for loads met on a demand basis, therefore. System coefficient of performance is also a strong function of saturated evaporating temperature and is defined by

$$\text{COP} = \frac{Q_{\text{DEL}}}{W} = b_1 + b_2 T_e \quad 2.2.9$$

where W is the electrical input to the heat pump compressor and b_1 and b_2 are empirically derived constants. The energy delivered to the load is given by the sum of energy absorbed by the collector/evaporator and the heat pump compressor work:

$$Q_{\text{DEL}} = Q_{\text{abs}} + W \quad 2.2.10$$

To obtain the steady state system performance at any ambient condition, equations 2.2.3 through 2.2.10 are utilized. Since the number of unknown values equals the number of equations used, an iterative process is required to solve for the value of evaporator temperature which will satisfy all of the equations. Newton's iteration technique was used in this work.

In space heating applications, the load is determined by the usual steady-state expression:

$$Q_L = (UA)_o (T_R - T_a) \quad 2.2.11$$

where $(UA)_o$ is the overall building conductance-area product and T_R is the inside room temperature. If the application is an industrial process heat load, the load is determined from whatever time-dependent function is used. Any shortfall in meeting the load is made up with an auxiliary electric heat source with COP of 1.0. Thus

$$Q_L = Q_{DEL} + Q_{AUX} \quad 2.2.12$$

The performance totals for any period of interest may be reduced to a measure which is the ratio of the free energy obtained through absorption by the collector/evaporator divided by the load. This "non-purchased fraction" is:

$$F_{np} = 1 - \frac{W + Q_{AUX}}{Q_L} = \frac{Q_{DEL} - W}{Q_L} \quad 2.2.13$$

Each value included in equation 2.2.13 is the sum total for each particular parameter for the time period.

Conventional Heat Pump--The conventional air-source heat pump is assumed to have a constant outdoor coil size and airflow. The evaporating temperature at constant entering condenser fluid temperature is subsequently only a function of outdoor ambient temperature. The relationship for T_e as a function of T_a was derived empirically from manufacturer's data and is of the form:

$$T_e = c_1 T_a + c_2 \quad 2.2.14$$

Justification for Equation 2.2.14 can be made by studying the heat pump equations. The energy absorbed by the evaporator of a heat pump is proportional to the difference between the evaporator temperature and the ambient temperature and is defined by:

$$Q_{abs} = (UA)_e (T_a - T_e) \quad 2.2.15$$

where $(UA)_e$ is the overall heat transfer coefficient of the evaporator. Equation 2.2.15 can be rewritten in terms of T_e :

$$T_e = T_a - \frac{Q_{abs}}{(UA)_e} \quad 2.2.16$$

Q_{abs} can be defined in terms of the heat pump capacity, Q_{DEL} , and COP which are functions of T_e .

$$Q_{abs} = Q_{DEL}(T_e) \left[\frac{COP(T_e) - 1}{COP(T_e)} \right] \quad 2.2.17$$

Equation 2.2.17 can be substituted into equation 2.2.16:

$$T_e = T_a - \frac{Q_{DEL}(T_e)}{(UA)_e} \left[\frac{COP(T_e) - 1}{COP(T_e)} \right] \quad 2.2.18$$

The difference between T_e and T_a is a function of T_e and therefore not constant. The empirical correlation for the conventional heat pump which indicates a linear relationship between T_e and T_a thus becomes credible for modeling purposes.

$$T_e = c_1 T_a + c_2 \quad 2.2.14$$

Equations 2.2.8 and 2.2.9 together with equation 2.2.14 are used to obtain the COP and capacity of the conventional heat pump.

From a computer model standpoint the only differences between the collector heat pump and the conventional heat pump are the characteristics of the outdoor heat exchanger. Simulation comparisons will then show the relative advantage or disadvantage of the solar-aided heat pumps.

System Performance Maps--Table 2.2.1 indicates the values for constants used to obtain heating performance results.

Figure 2.2.1 shows the corresponding performance curves for COP, Q_{DEL} and W as functions of evaporator temperature. The COP is limited to a maximum value of 4.0 to prevent unrealistic system performance.

The equilibrium evaporator temperature in refrigerant-filled collector heat pumps is affected in nearly the same manner as in conventional heat pumps when design or weather parameters are altered, with the exception of solar radiation, which has negligible effect on conventional systems. Table 2.2.2 illustrates the general effect that increasing specific parameters has on the equilibrium performance of collector heat pump systems. T_c is the heat pump condensing temperature. This table can be used as a reference in understanding the performance results.

Table 2.2.1

Heat Pump Model Empirical Curve Fit Constants

<u>Constant</u>	<u>Value</u>
a_1	12.86 MJ/HR
a_2	0.43 MJ/HR-C
a_3	0.0034 MJ/HR-C ²
b_1	0.06/C
b_2	2.9
c_1	0.83
c_2	-7.4 C

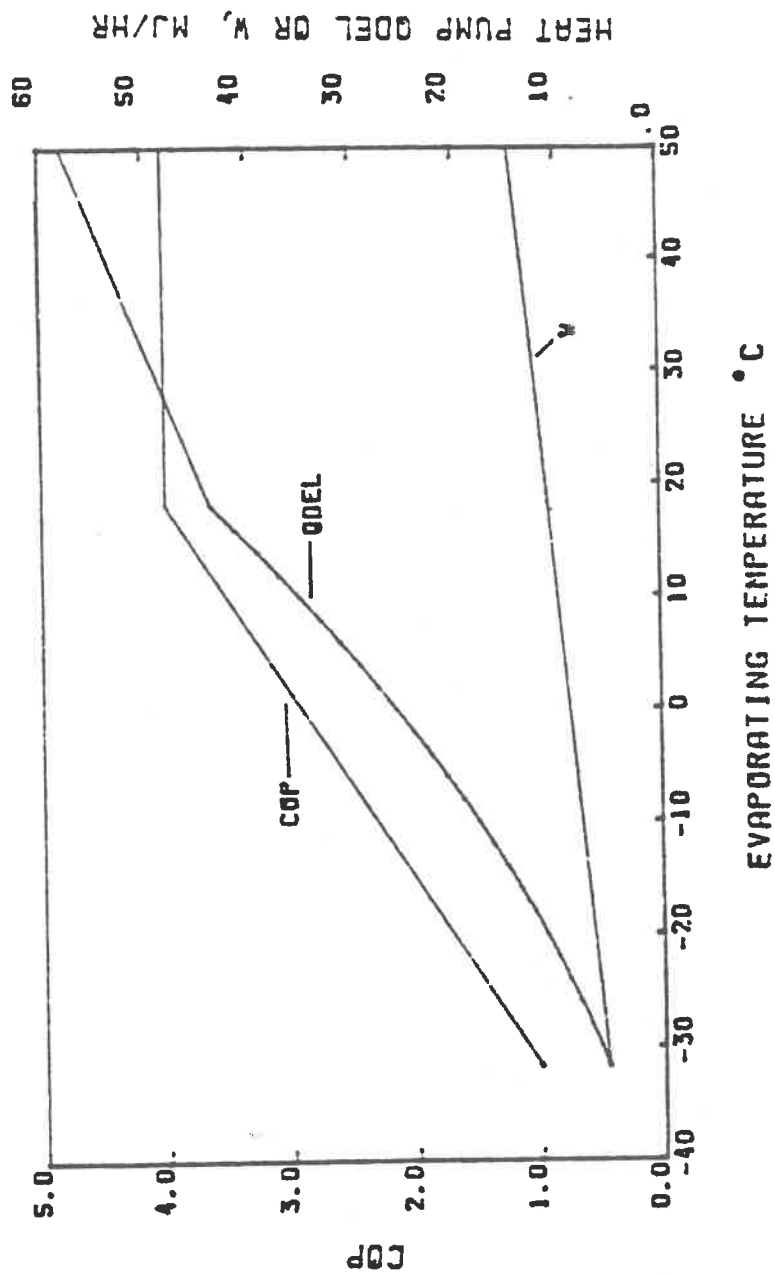


Figure 2.2.1 Heat Pump Performance

Table 2.2.2
Effect on Heat Pump Performance

<u>Parameter Increased</u>	<u>Effect on</u>		
	<u>T_e</u>	<u>T_c</u>	<u>COP</u>
Evaporator Heat Exchanger Area	Increase	Increase	Increase
Condenser Heat Exchanger Area	Decrease	Decrease	Increase
Compressor Efficiency	Increase	Decrease	Increase
Compressor Capacity	Decrease	Increase	Decrease
System Refrigerant Charge	Increase	Increase	Unknown
Evaporator Source Temperature	Increase	Increase	Increase
Condenser Sink Temperature	Increase	Increase	Decrease
Incident Radiation of Evap/Collector	Increase	Increase	Increase
U _L (convection coefficient)			
1. T _e < T _a (low radiation)	Increase	Increase	Increase
2. T _e > T _a (high radiation)	Decrease	Decrease	Decrease

3.0 DESIGN METHOD

The load model and the heat pump relations of Chapter 2 are all based on quasi-steady state operation. There is no energy storage or thermal capacitance in the system which will cause carry-over of the effect of system operation from one hour to the next. A method for estimating long-term performance of collector heat pumps which is based on the standard bin method for conventional heat pumps can be employed. The effect on heat pump performance by start-up transients will be discussed in Section 4.6.

3.1 Sol-Air Temperature Bin Method

This method is developed by starting with the collector equation for these systems:

$$Q_{abs} = A_c [(\tau\alpha) I_T - U_L (T_e - T_a)] \quad 2.2.3$$

Equation 2.2.3 can be rearranged:

$$Q_{abs} = A_c U_L \left[\left(T_a + \frac{(\tau\alpha) I_T}{U_L} \right) - T_e \right] \quad 3.1.1$$

Collector properties and weather conditions can be combined into a property known as the "sol-air" temperature, defined as

$$T_{sa} = \left(T_a + \frac{(\tau\alpha) I_T}{U_L} \right) \quad 3.1.2$$

The ambient temperature (T_a) and radiation on a horizontal surface are necessary weather data. The horizontal surface radiation needs to be converted to incident radiation on the collector surface (I_T)

by some method, such as in [11]. The collector transmittance-absorptance product ($\tau\alpha$) is needed, along with the collector loss coefficient (U_L). After substituting Equation 3.1.2 into 3.1.1 the resulting collector equation is:

$$Q_{\text{abs}} = A_c U_L (T_{\text{sa}} - T_e) \quad 3.1.3$$

Equation 3.1.3 illustrates how the amount of energy absorbed by the collector/evaporator can be increased by increasing incident solar radiation. As incident radiation increases the collector sol-air temperature increases. The interaction with the heat pump will cause the evaporator temperature to increase, but not as much as the sol-air temperature has increased. The result is more "free" energy transferred to the refrigerant in the evaporator and higher system COP caused by the increase in T_e .

The sol-air temperature concept allows hourly weather data to be converted into two-dimensional bins which contain the number of hours corresponding to an ambient temperature range and a sol-air temperature range. It is necessary and convenient to use a constant estimated "average" value of U_L for the bin method. For a monthly simulation, most of the bins which contain any number of hours will most likely have a total of more than one. The wind velocities for the hours in each bin will not be the same, so an estimate of the loss coefficient for a particular collector will make bin data generation and use easier. An example of the hourly distribution by sol-air and ambient temperature bins is shown in Figure 3.1.1 for an

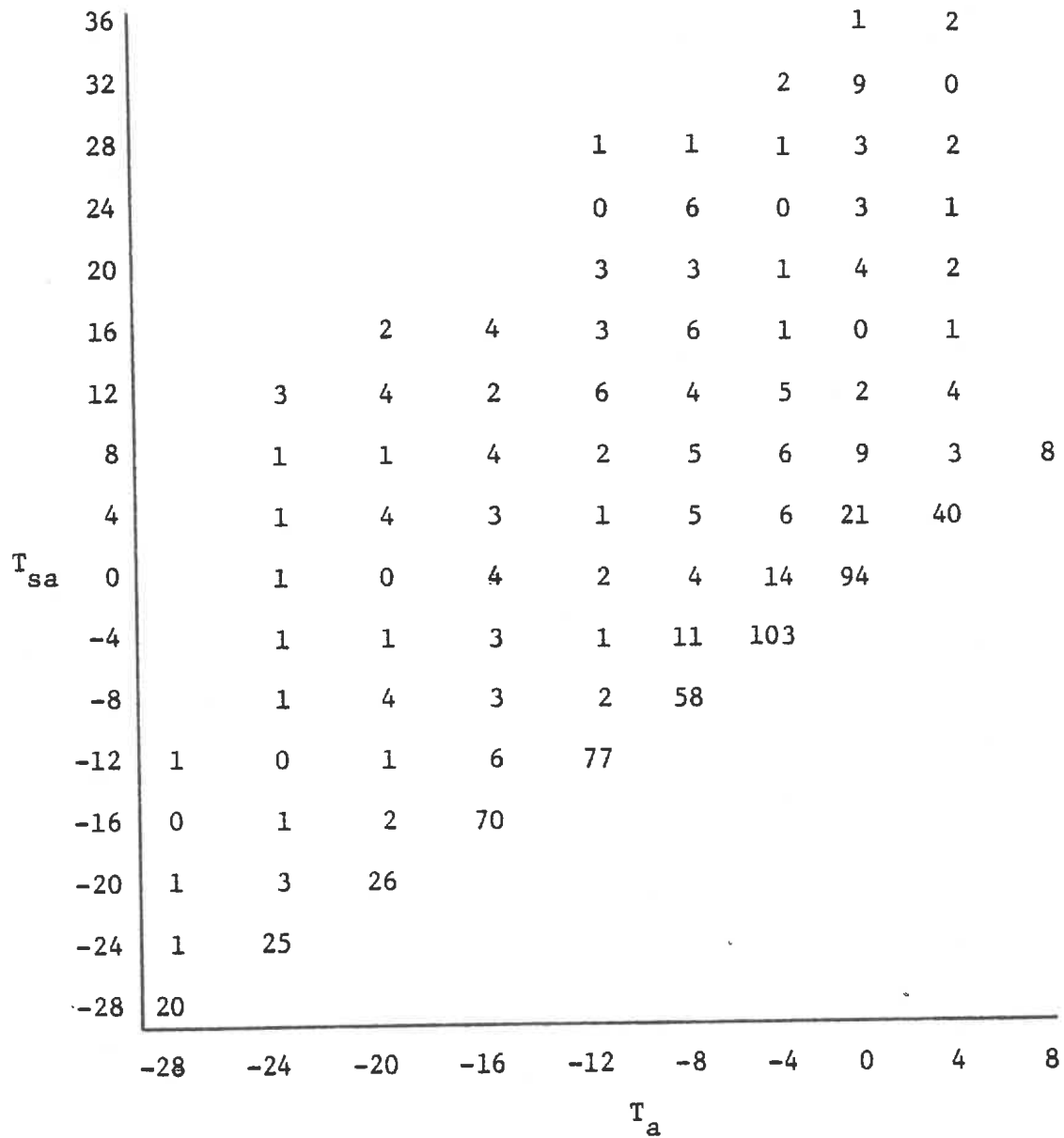


Figure 3.1.1 Sol-Air Temperature Bin Distribution for Uncovered Collector in January--Madison

uncovered collector in Madison, WI for the month of January. Each bin has a width of 4°C for both the ambient temperature and sol-air temperature scales. The numbers on each scale correspond to temperature values at the midpoint of each bin. The number in each bin is the actual number of hours within the temperature ranges specified for the bin during the entire month.

The bin method procedure is convenient when resolving refrigerant-filled collector heat pump performance for space heating or process heat applications. In space heating applications, the load can be determined by the ambient temperature at the midpoint of the bin ambient temperature range. Alternative heating loads could include loads which are a function of sol-air temperature or loads which are a function of time, such as a constant process heat load. System performance is obtained by using the mid-point sol-air temperature of the same bin for which the load is determined. Equations 2.2.8 through 2.2.10, along with Equation 3.1.3 are used to solve for simultaneous results. Performance totals for the time period for which bin data is available are obtained by summing all of the contributions from each bin.

This same bin method can be used to generate conventional heat pump performance by ignoring the sol-air temperature and using the ambient temperature bin data for both performance and load calculations. Equations 2.2.10 through 2.2.14 are used to obtain conventional heat pump performance. Another method for estimating conventional heat pump performance is outlined by Anderson [13]. This

method was not used for any of the results presented in this thesis because it was easier to use existing sol-air and ambient temperature bins adapted for conventional heat pump calculations.

In all of the simulations employing the sol-air temperature bin method in this study, bin data and results were ascertained on a monthly basis and the range used for the ambient temperature and sol-air temperature bins was 2°C.

The effect of sol-air temperature on COP for an uncovered collector heat pump system is illustrated in Figure 3.1.2 for several collector areas. The figure indicates that increased sol-air temperatures result in higher system COP's. The larger collector areas have greater increases in COP, indicating that the evaporator temperature is nearer to the sol-air temperature. The evaporator temperature is equal to the sol-air temperature for a collector of infinite area. The infinite area curve in Figure 3.1.2 defines the upper limit of heat pump performance with collector area as a variable.

Weather Data Tapes--Solmet [14] TMY hour-by-hour weather data were used in this design study. The data provided by these weather tapes were the hourly ambient temperature and wind velocity and the total hourly radiation on a horizontal surface.

TRNSYS Simulations--The transient simulation program TRNSYS [12] was also used to perform detailed hour-by-hour simulations of system performance for refrigerant-filled collector heat pump systems. This provided a basis for comparing results obtained by the sol-air bin

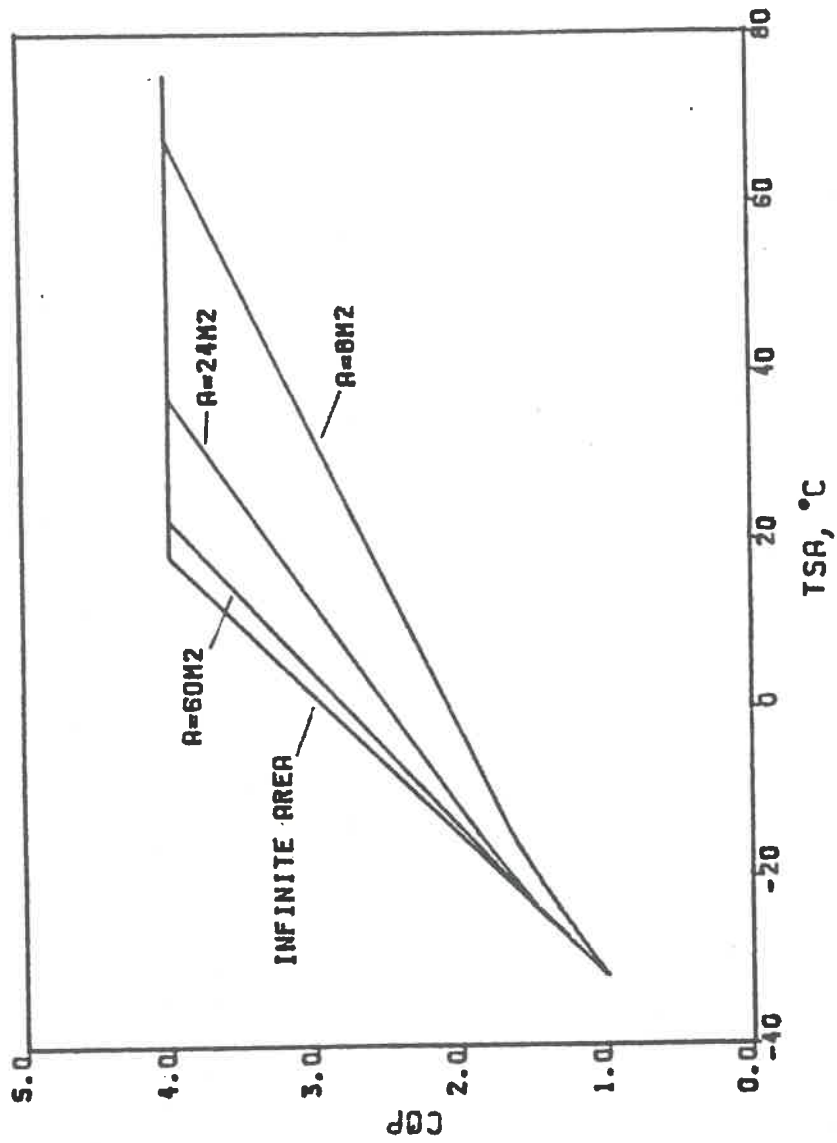


Figure 3.1.2 Effect of Sol-Air Temperature on COP

method. The basic TRNSYS components used include weather data input, a Data Reader (Type 9), heating load (Type 12), Radiation Processor (Type 16), monthly summary output components and a specially written heat pump model component containing Equations 2.2.8 through 2.2.10, along with 2.2.3, the collector equation. The TRNSYS simulations were similar to sol-air bin method simulations in the following respects:

- a) The same hour-by-hour weather data were used for both methods.
- b) The calculations used in determining the incident solar radiation on the collector surface were identical to the calculations used in the TRNSYS radiation processor.
- c) The equations for determining heat pump performance in both cases were taken from the model developed here and therefore had the same origin.
- d) The load model used in the TRNSYS simulations is the same load model for space heating applications as used in the bin method, and is given by Equation 2.2.11.

Any differences in the results obtained by each method is attributable only to error caused by the bin temperature range chosen for bin method calculations. When TRNSYS simulations were compared with those of the bin method with 2°C bin widths, the results were essentially identical. This justifies the use of the sol-air bin method as a design procedure to obtain realistic long term performance calculations for refrigerant-filled collector heat pumps.

Design Method Summary--This design method determines heat pump performance on a monthly basis and will work with any location for which hourly weather data are available. The method is outlined by steps:

- 1) Convert collector/evaporator properties and weather data for each month into a two-dimensional bin array containing the total number of hours for the month in each bin. 2°C width bins are recommended for an array specifying ambient temperature and sol-air temperature. The sol-air temperature is defined by

$$T_{sa} = \left(T_a + \frac{(\tau\alpha) I_T}{U_L} \right) \quad 3.1.2$$

with terms defined previously. It is necessary that a constant value for U_L be used. Appendix A.1 contains a FORTRAN computer program which will achieve this result with SOLMET TMY weather tapes.

- 2) Heat pump performance data for capacity (Q_{DEL}) and COP as a function of evaporator temperature (T_e) is needed. The data may be curve fit as in Equations 2.2.8 and 2.2.9 or they may be a series of data points for which values between points are determined by linear interpolation.
- 3) The heat pump performance is used with the collector equation to achieve heat pump balance points:

$$Q_{abs} = A_c U_L (T_{sa} - T_e) \quad 3.1.3$$

An additional relation which is required for an overall heat pump energy balance is defined by Equation 2.2.10:

$$Q_{\text{DEL}} = Q_{\text{abs}} + W \quad 2.2.10$$

Thus for each calculation there are four unknown values:

- a) heat pump heating capacity (Q_{DEL})
- b) heat pump coefficient of performance (COP)
- c) energy transferred to the collection (Q_{abs})
- d) evaporator temperature (T_e)

There are four relations:

- a) $Q_{\text{DEL}} = f(T_e)$
- b) $\text{COP} = Q_{\text{DEL}}/W = f(T_e)$
- c) $Q_{\text{abs}} = f(T_e)$
- d) $Q_{\text{DEL}} = Q_{\text{abs}} + W$

An iteration procedure will result ultimately in an evaporator temperature which will satisfy all of the relations. This procedure is performed for each bin generated in Part 1 of this method. In addition, the load must be determined for each bin, based on ambient temperature or some other method. The contribution to all performance parameters from each bin is added to its appropriate total to obtain monthly results. This procedure is repeated for all months and the combined total will be the yearly results. A FORTRAN program which will calculate monthly and yearly performance results from bin data is listed in Appendix A.2. This program utilizes curve fit equations

for heat pump performance but can be adapted for use with tabular performance data.

Example Steady-State Performance Calculation--Presented here is a sample calculation for an uncovered collector heat pump system. One bin selected from Figure 3.1.1 is selected and the empirical constants of Table 2.2.1 will be used to determine performance. System parameters and bin information include the following:

$$\begin{aligned} Q_{\text{NOM}} &= 2 \text{ tons of refrigeration} \\ A_c &= 24 \text{ m}^2 \\ U_L &= 20 \text{ W/m}^2 \text{ C} \\ T_a &= -4^\circ\text{C} \\ T_{\text{sa}} &= 8^\circ\text{C} \\ N &= 6 \text{ hours stored in bin} \\ (UA)_o &= 0.83 \text{ MJ/hr-}^\circ\text{C} \\ T_R &= 20^\circ\text{C} \end{aligned}$$

The heat pump performance equations are:

$$\begin{aligned} \text{COP} &= .06 T_e + 2.9 \\ Q_{\text{DEL}} &= 2(12.86 + .43 T_e + .0034 T_e^2) \text{ MJ/hr} \\ Q_{\text{abs}} &= 20 \times 24 (8 - T_e) \times .0036 \text{ MJ/hr} \\ Q_{\text{DEL}} &= Q_{\text{abs}} + \frac{Q_{\text{DEL}}}{\text{COP}} \text{ (heat pump energy balance)} \end{aligned}$$

The load for a space heat application is

$$Q_L = 0.83 (20 - (-4)) = 19.92 \text{ MJ/hr}$$

An initial guess that $T_e = T_a = -4^\circ\text{C}$ does not yield an accurate heat pump energy balance and is not correct. After adjusting T_e upward until an energy balance is obtained the resulting value for evapor-

ator temperature is -1.2°C . The results are summarized:

$$Q_L = 19.92 \text{ MJ/hr}$$

$$Q_{\text{DEL}} = 24.70 \text{ MJ/hr}$$

$$\text{COP} = 2.83$$

$$W = 8.73 \text{ MJ/hr}$$

$$Q_{\text{abs}} = 15.97 \text{ MJ/hr}$$

The heat pump hourly capacity is greater than the load and the performance results must be reduced proportionally since the heat pump will not be operating during the entire hour.

$$Q_{\text{DEL}} = 19.92 \text{ MJ/hr}$$

$$\text{COP} = 2.83$$

$$W = 7.04 \text{ MJ/hr}$$

$$Q_{\text{abs}} = 12.88 \text{ MJ/hr}$$

$$Q_{\text{AUX}} = 0.$$

The corresponding contributions to the monthly total for heat pump delivered energy and electrical input, load and auxiliary energy are:

$$Q_L = 6 \times 19.92 = 119.52 \text{ MJ}$$

$$Q_{\text{DEL}} = 6 \times 19.92 = 119.52 \text{ MJ}$$

$$W = 6 \times 7.04 = 42.24 \text{ MJ}$$

$$Q_{\text{AUX}} = 0.$$

The "non-purchased" fraction for this bin is:

$$F_{\text{np}} = \frac{Q_{\text{abs}}}{Q_L} = \frac{12.88}{19.92} = 0.65$$

4.0 SPACE HEATING PERFORMANCE

4.1 Base Case Space Heating Applications

The systems for which performance was compared include the uncovered and covered types of collector/evaporator heat pump systems, a conventional air source heat pump system and a conventional solar collection system. The space heating systems were evaluated for the heating season in four U.S. locations. These locations along with the parameters used in the base case performance comparisons are shown in Table 4.1.1

The performance of conventional solar heating systems was determined by the f-chart [15] method. A liquid collection system was chosen due to the similarity of collector design to the refrigerant-filled collector. The conventional solar system operates at a higher average plate temperature than the covered collector heat pump system and subsequently will experience more heat losses [11]. The value of $F_R U_L$ used in the conventional solar system simulations is $4.22 \text{ W/m}^2\text{-C}$ and the value used for the covered collector heat pump system is $3.0 \text{ W/m}^2\text{-C}$. Storage was used with the conventional solar simulations because of the commonality of storage use with space heating solar systems.

Figures 4.1.1 through 4.1.4 show comparisons between the four types of heating systems described and the four locations listed in Table 4.1.1. The yearly non-purchased fraction is plotted against collector area for the conventional solar and solar-aided heat pump systems. The non-purchased fraction for an air-to-air

Table 4.1.1

System Simulation Parameters--Space Heating

<u>System Type</u>	$F_R - U_L$ <u>(W/M²C)</u>	$F_R (\tau\alpha)$ <u></u>	<u>Collector Slope</u>	<u>Collector Area (m²)</u>	<u>Heat Pump Size (MJ)</u>
Covered Collector	3.0	.72	60°	0-100	25.3
Uncovered Collector	20.0	.80	60°	0-100	25.3
Conventional Heat Pump	-	-	-	-	25.3
Conventional Solar (Liquid System)	4.22	.70	60°	0-100	-
Collector Plate Emissivity				0.1	
Conventional Heat Pump COP @ 8°C				2.85	
Building Loss Coefficient (UA, W/C)				231	
Storage Capacity for Conventional Solar (KJ/°C-m ²)				350	
Room Temperature (°C)				20	
Collector Orientation				South Facing	
Locations:	Madison, WI	Seattle, WA			
	Albuquerque, NM	New York, NY			

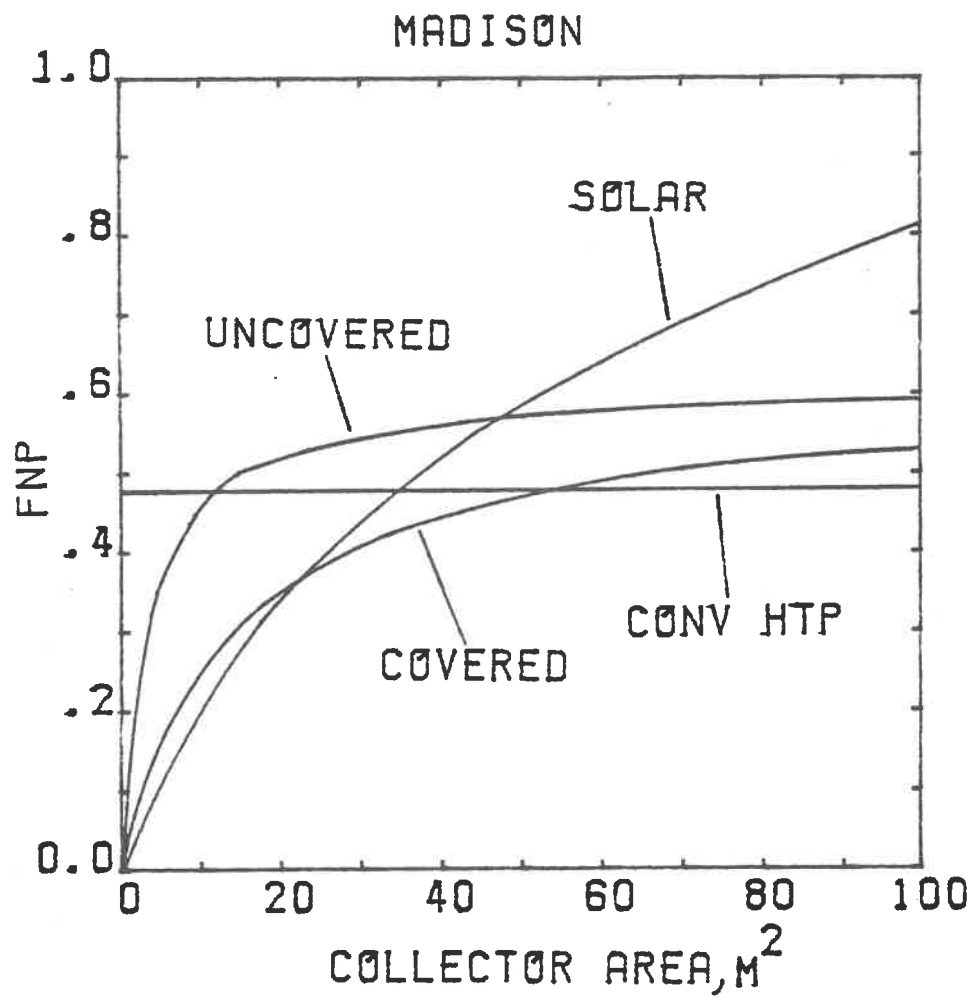


Figure 4.1.1 Base Case Space Heating Performance--Madison

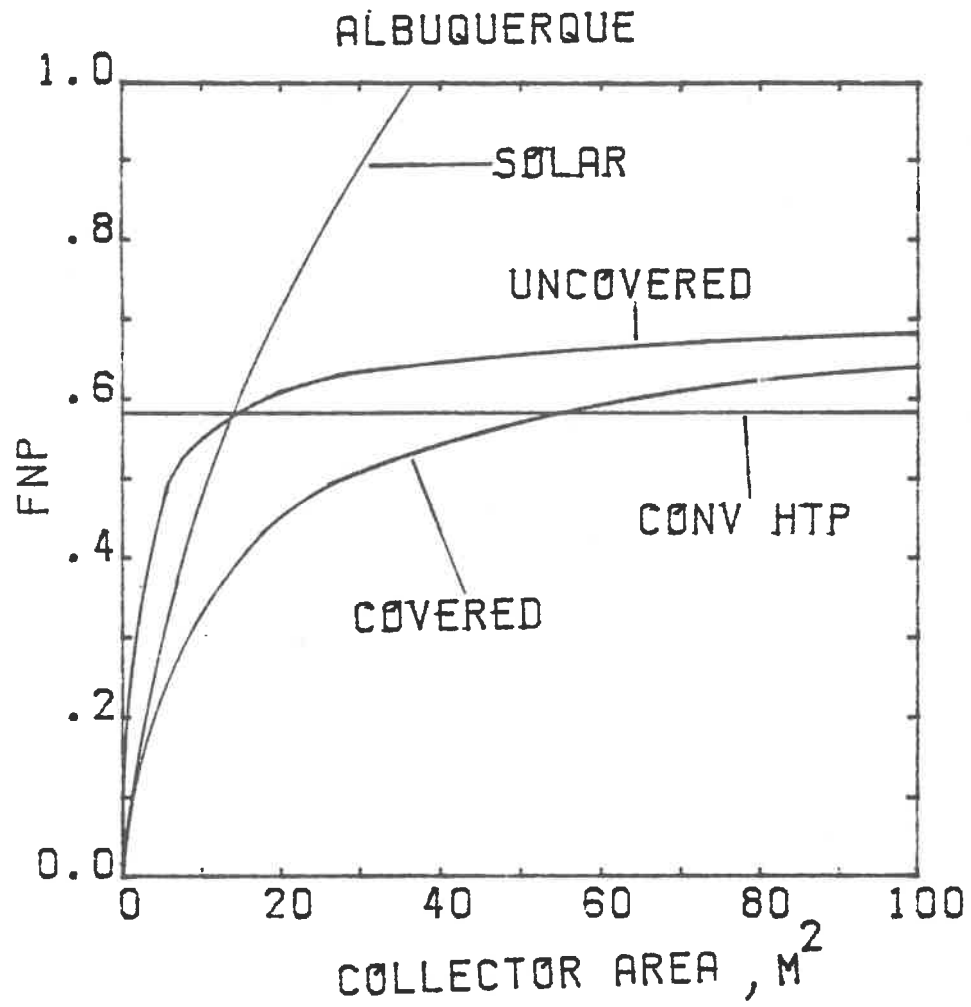


Figure 4.1.2 Base Case Space Heating Performance--Albuquerque

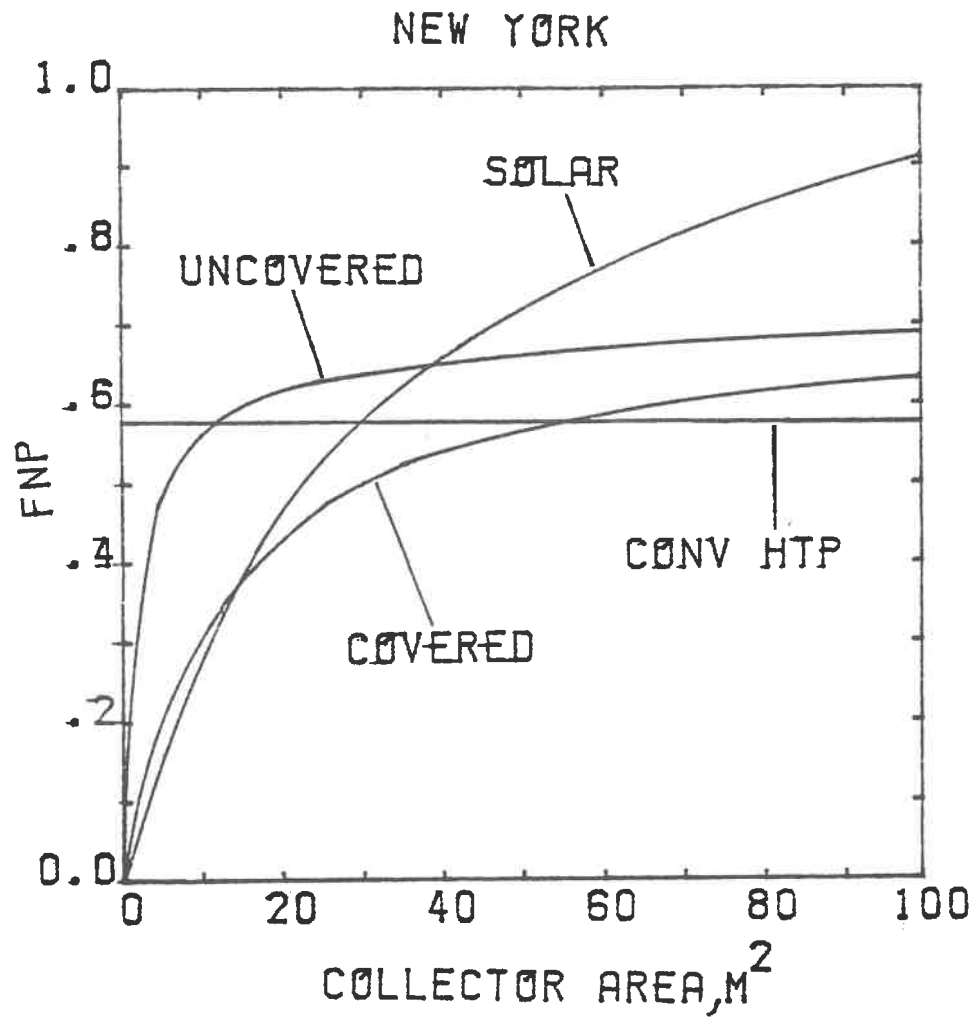


Figure 4.1.3 Base Case Space Heating Performance--New York

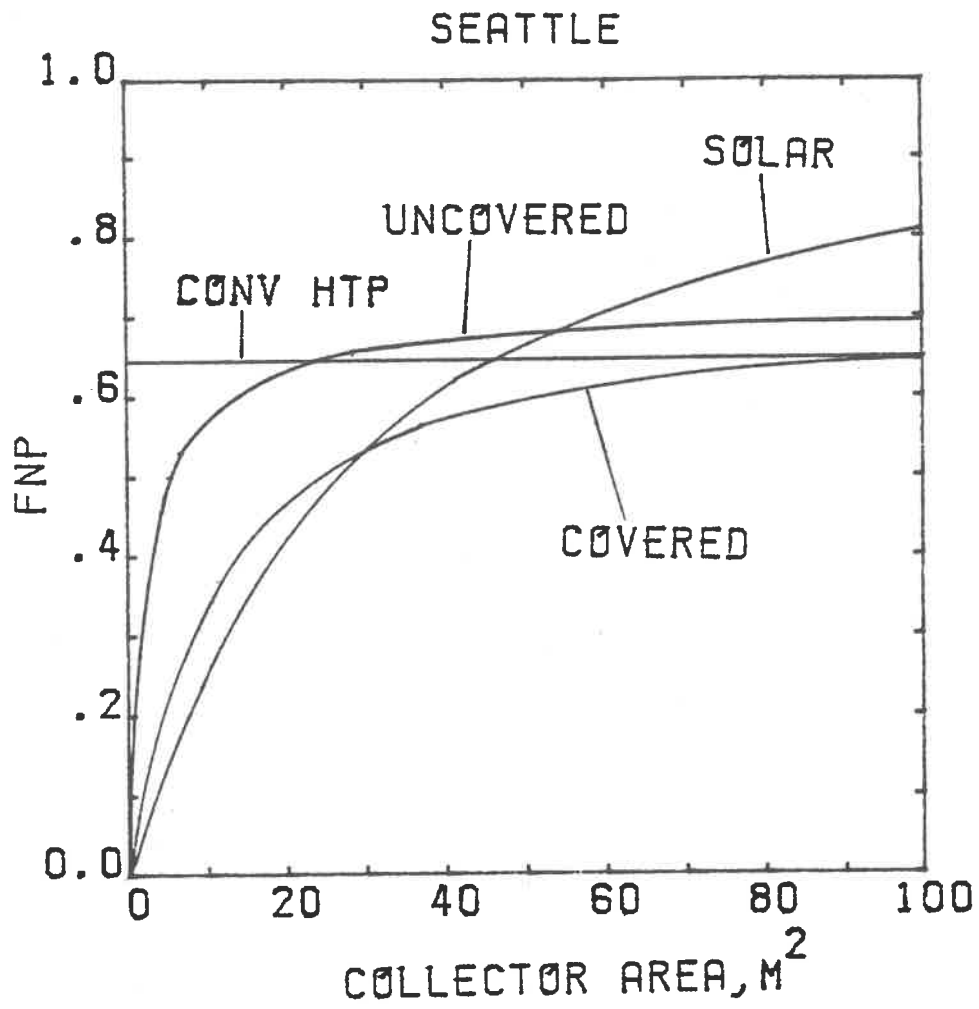


Figure 4.1.4 Base Case Space Heating Performance--Seattle

heat pump system is a horizontal line since the physical size of all heat pump components is assumed constant.

The non-purchased fraction for uncovered collector systems in all locations increases rapidly at low collector areas and is better than the conventional heat pump at large areas. The points at which the uncovered collector system performance exceeds the conventional heat pump performance occur at a collector area of 11 to 13 m² in all four cities. Since the non-purchased fraction curves are rising steeply at this point, it would seem that the addition of less than 10 m² of collector area to the area necessary to equal conventional heat pump performance will give a definite performance advantage to the uncovered collector heat pump system and still maintain technically feasible collector areas. In Madison, this advantage at 22 m² is 5% of the load. The performance of the conventional solar system is the lowest at small collector areas, but is better than the other systems at larger areas. The covered collector system performance for the space heating loads is low for small collector areas and does not equal that of the conventional heat pump until areas exceed 50 m² in Madison, New York, and Albuquerque and 100 m² in Seattle. The performance of covered collector heat pump systems is consistently lower than the uncovered systems in all locations. The difference is greatest for collector areas below 40 m², which includes the range for currently installed applications corresponding to the nominal heat pump size used in these applications.

The greater performance of the uncovered over the covered systems was not anticipated. The covered system was expected to have the advantage of being able to operate at higher evaporator temperatures with a higher system COP during periods of solar radiation. The covered system does operate better during periods when solar insolation is high. However, with low levels of radiation, the primary energy source is convection from ambient air. The lower loss coefficient of the covered collector will drive the evaporator temperature lower than that for the uncovered collector, with a consequent reduction in COP. Periods during which little or no solar radiation is available occur the majority of the time at all locations. In addition, higher space heating loads may occur at times of low radiation levels leading to the realization that a covered collector heat pump system will have poor performance when compared with other heat pump systems.

The overall performance difference between the conventional solar system and the heat pump systems was significantly greater in Albuquerque than in the other three locations. The fact that Albuquerque receives more solar radiation than the other locations greatly benefitted the performance of the conventional solar system in that location but did not seem to contribute much to the performance of the collector heat pump systems. The performances of both collector heat pump types in Seattle is nearly the same as the results obtained for Albuquerque. Of the four locations studied, Seattle has the least amount of available solar radiation during

the winter months, when the majority of the space heating load occurs.

All of the above suggests that convection heat transfer is considerably more important to the performance of refrigerant-filled collector heat pump systems than solar radiation.

Effect of Convection Coefficient--There is uncertainty in estimating U_L for the uncovered and covered collector heat pumps. The effect of this coefficient on performance was studied. The results obtained in Figure 4.1.5 for Madison are generated with parameters from Table 4.1.1 with the exception of U_L . The values of U_L for the uncovered collector were taken to be 10, 20, and 30 W/m^2C , which reflects variations of local average wind speed and structural effects of the installation. For the covered collector, differences in the "tightness" of the covers and insulation were estimated using loss coefficient values of 3.0 and 1.0 W/m^2C . Loss coefficients as low as 1.0 could be achieved because of the small difference between plate temperature (T_e) and ambient temperature during operation and the non-reflective property of collector plates used in solar applications. The results in Figure 4.1.5 show that reducing the covered collector loss coefficient decreases the yearly space heating performance of the system considerably. This shows that convection is the primary energy source.

The uncovered collector results show a diminishing return for higher convection coefficients. This result has two causes:

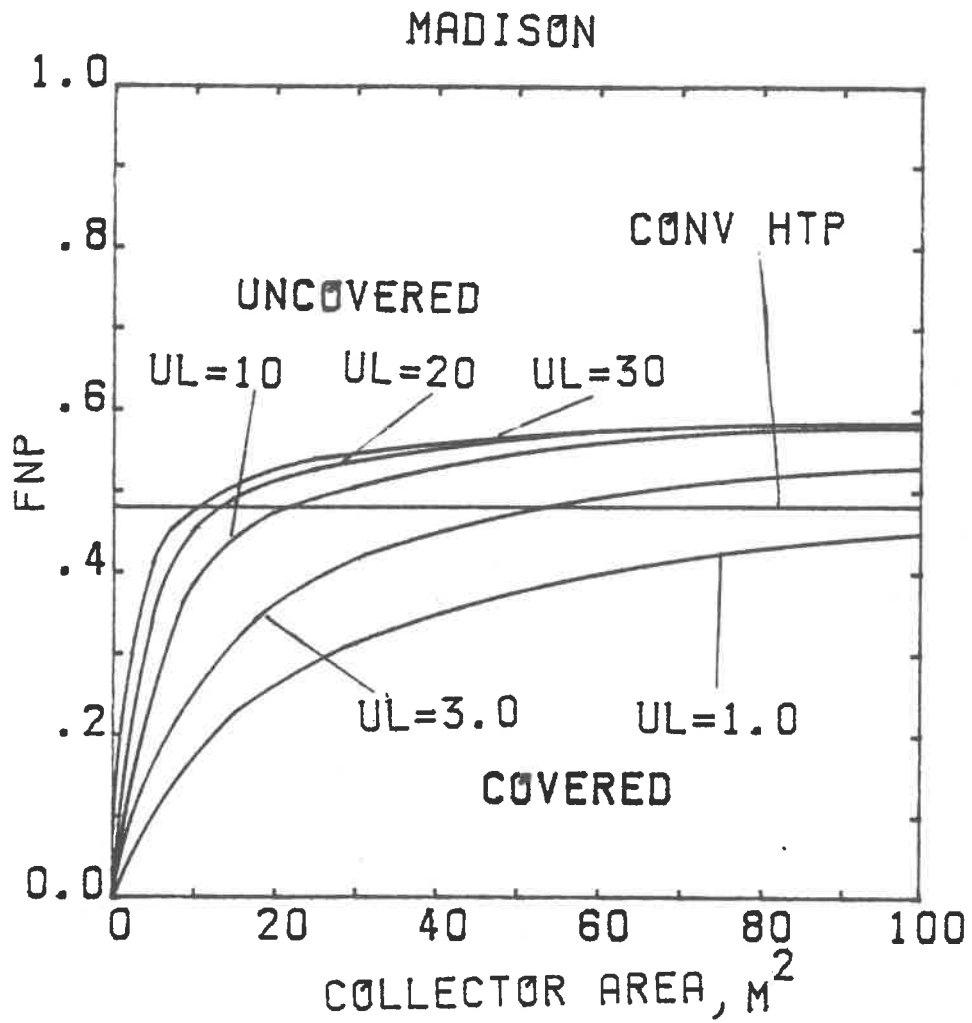


Figure 4.1.5 Effect of U_L on Heating Performance—Madison

1. At high radiation levels, performance at high values of convection coefficient suffers because of higher convection losses from the plate. This occurs more often at larger collector areas because of the relative ease with which evaporator temperature may be raised with increased insolation.
2. During night-time or during periods of low radiation levels, a higher convection coefficient will tend to drive up the evaporating temperature. In this case however, the evaporator temperature must remain lower than the ambient temperature in order to obtain sufficient heat transfer to evaporate refrigerant in the collector. Thus each incremental increase in convection coefficient will result in less increase in evaporating temperature, COP and system heating capacity.

The results for variations in U_L do show some effect in the 10-40 m^2 collector area range especially for values of U_L from 10 to 20. The performance for $U_L = 10$, which approximates natural convection on the bare collector, results in performance superior to all covered collector systems. The horizontal line representing conventional heat pump performance intersects the performance curve for $U_L = 10$ at 22 m^2 . This indicates that with minimal wind convection, uncovered collector performance remains adequate at appropriate collector areas.

Effect of Heat Pump Size--Performance was estimated at various nominal heat pump sizes for the covered and uncovered collector heat pumps and the conventional heat pump. The results are shown in Figures 4.1.6 and 4.1.7 for the Madison space heating application. Nominal sizes studied include 12.7, 25.3, 50.6 and 63.3 MJ, corresponding to 1, 2, 4 and 5 tons of refrigeration, respectively. Results for the conventional heat pump are shown in Table 4.1.2.

Results for the uncovered collector system indicate that the 50.6 MJ heat pump size has the best overall performance from a non-purchased fraction standpoint. The 25.3 and 63.3 MJ sizes are slightly lower in performance and the 12.7 MJ size is poorest of all. However, plots of overall COP vs. collector area (Figures 4.1.8 and 4.1.9) show that the smaller sizes have the highest COP with COP's decreasing progressively from the smallest to the largest size. This is sensed in the fact that at any given ambient condition and collector area, refrigerant flow in the collector/evaporator will be less for a smaller size heat pump with a compressor of lower volumetric capacity. This will result in a larger amount of liquid and vapor refrigerant in the evaporator, causing its temperature and pressure to be greater. The higher evaporating pressure allows the compressor to operate at higher volumetric efficiency and the lesser difference between suction and discharge pressures for the smaller size causes greater system COP. The results for non-purchased fraction do not correspond to those for COP because of the interaction of the load with the heat pump.

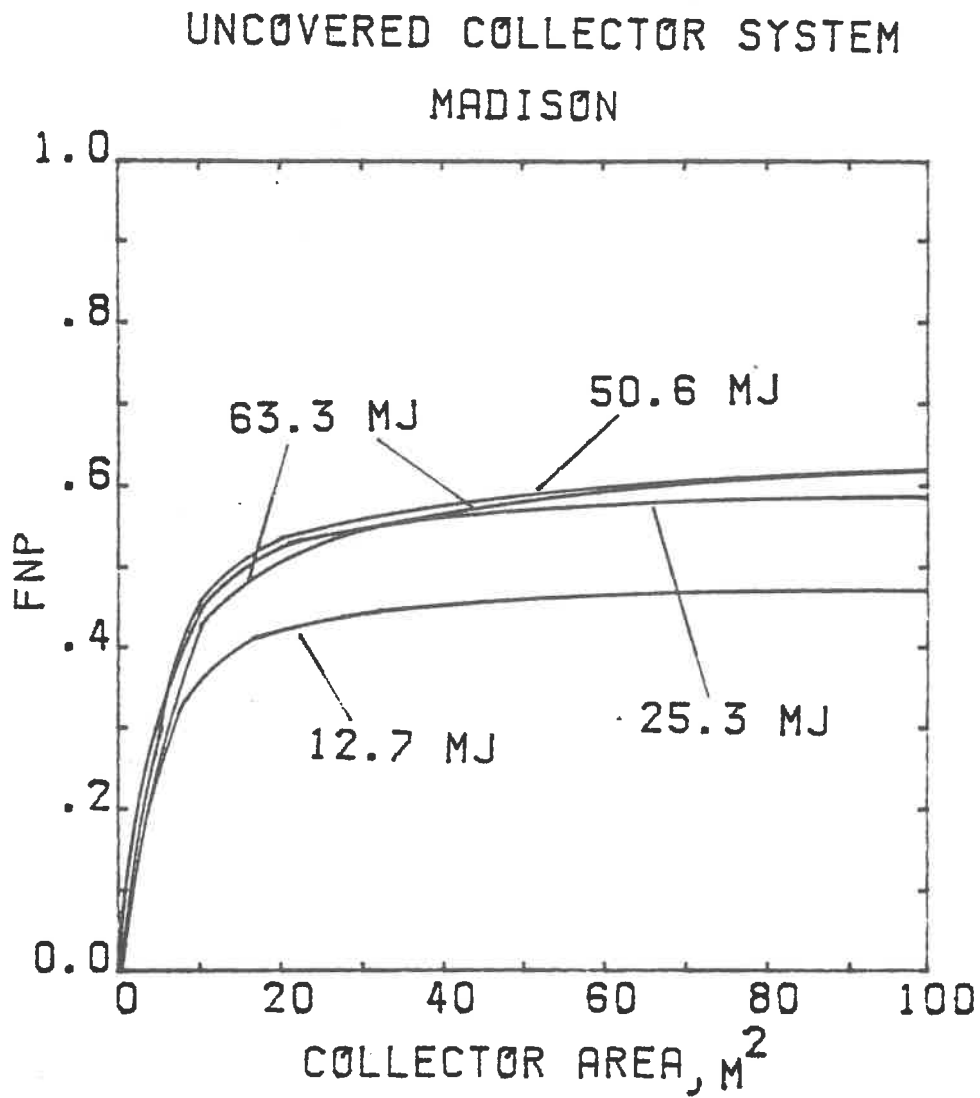


Figure 4.1.6 Effect of Heat Pump Size on Uncovered Collector System F_{np} --Madison

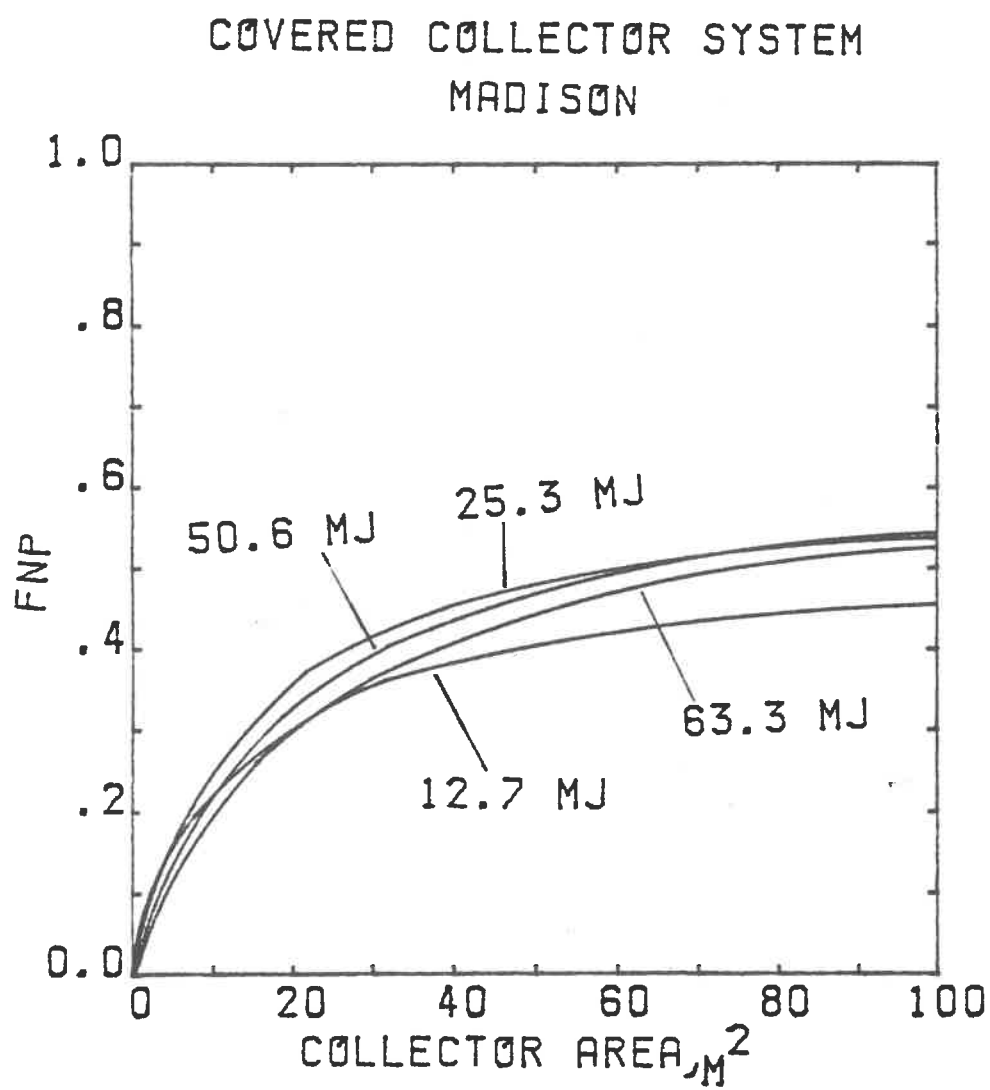


Figure 4.1.7 Effect of Heat Pump Size on Covered Collector System F_{np} --Madison

Table 4.1.2

Conventional Heat Pump Performance--Madison Simulation

<u>Size (MJ)</u>	<u>F_{NP}</u>	<u>COP</u>
12.7	.332	2.49
25.3	.477	2.39
50.6	.543	2.30
63.3	.549	2.28

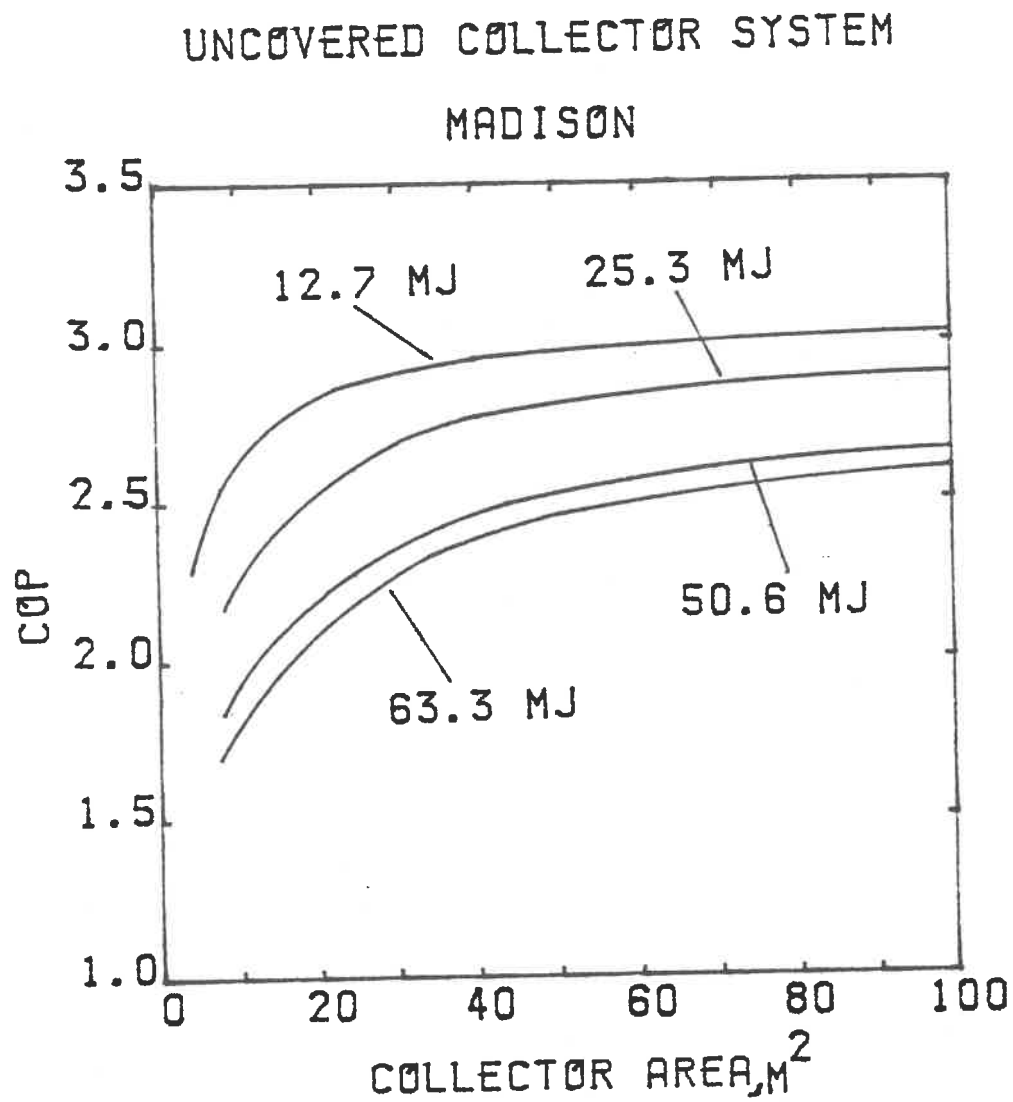


Figure 4.1.8 Effect of Heat Pump Size on Uncovered Collector System COP--Madison

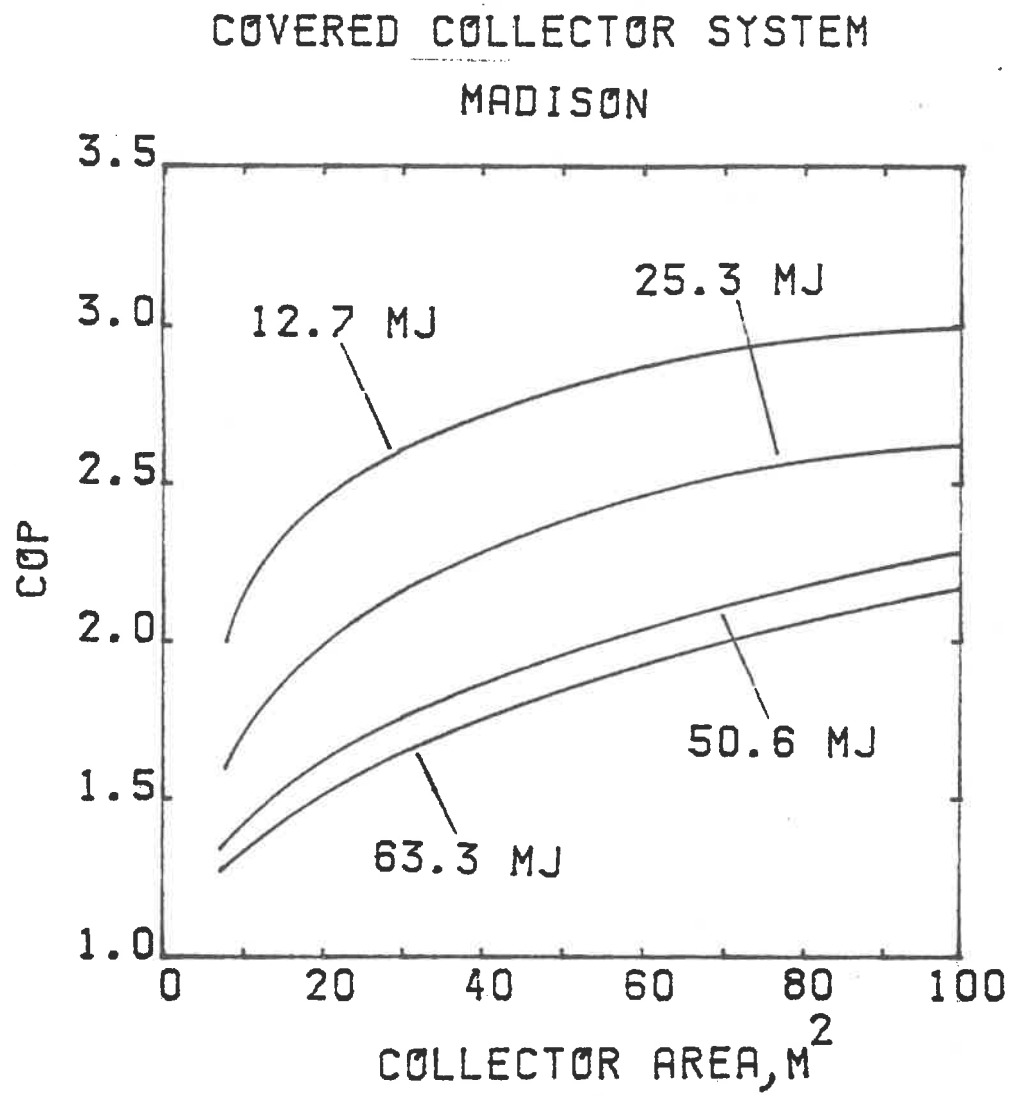


Figure 4.1.9 Effect of Heat Pump Size on Covered Collector System COP--Madison

For the uncovered collector system, the non-purchased fraction for the 12.7 MJ system is low because its capacity is less than the load more often. The increase in auxiliary energy needed more than offsets any COP advantage. The 50.6 MJ size achieves the highest non-purchased fraction at the collector area range of 10-60 m² because it has the best balance between COP advantage over the 63.3 MJ size and use of less auxiliary over the smaller sizes. The non-purchased fraction of the 63.3 MJ size approaches that of the 50.6 MJ size at higher collector areas because of the decreasing COP differential between the two sizes with a larger evaporator and the increasing ability of the larger size heat pump to extract more capacity with increasing collector areas.

For the collector area range of 10-60 m² in the covered collector system, the 25.3 MJ size has the highest non-purchased fraction. The overall COP advantage of smaller sizes is greater for the covered system than the uncovered system. The primary reason for this is that for the same ambient conditions, collector area and heat pump size, the difference between the collector "sol-air" temperature (ambient temperature if at night-time) and evaporator temperature during operation is greater for the covered system than the uncovered system. If a large size heat pump is replaced by a smaller size, the potential increase in evaporator temperature is greater for the covered system than the uncovered system. In the limit, a heat pump of zero size will have complete evaporator flooding and the evaporator temperature will equal the sol-air temperature. Since the sol-air

temperature of the covered system is equal to or greater than the sol-air temperature of the uncovered system at any given condition due to its lower "convection" coefficient it is apparent why the covered system experiences greater improvement with smaller sizes. The difference between non-purchased fraction for the 12.7, 25.3, and 50.6 MJ sizes in the covered application becomes less at higher collector areas because the COP differences due to size becomes less important and the capacity advantage of the larger sizes becomes more important. Results for the conventional heat pump show that the COP advantage of smaller sizes does not offset the size advantage for the sizes considered in the Madison study. The steady-state COP for all heat pump sizes will be identical at the same ambient temperature. Each heat pump size is assumed to have an appropriate evaporator heat exchanger area to obtain this result. The overall seasonal COP disadvantage due to large size for air-to-air heat pumps is because a large heat pump size will deliver more energy to the load at lower ambient temperatures than smaller sizes. Above the temperature at which heat pump capacity exceeds the load for a small heat pump, the capacity and COP contributions of a small and large size heat pump will be equal. Steady-state COP's are low at lower ambient temperatures, which causes overall COP's to be low for the larger heat pump size.

Effect of Maximum COP--In order to take full advantage of high daytime sol-air temperatures during operation, an analysis of system performance was made with a maximum allowable COP of 20.0 instead of

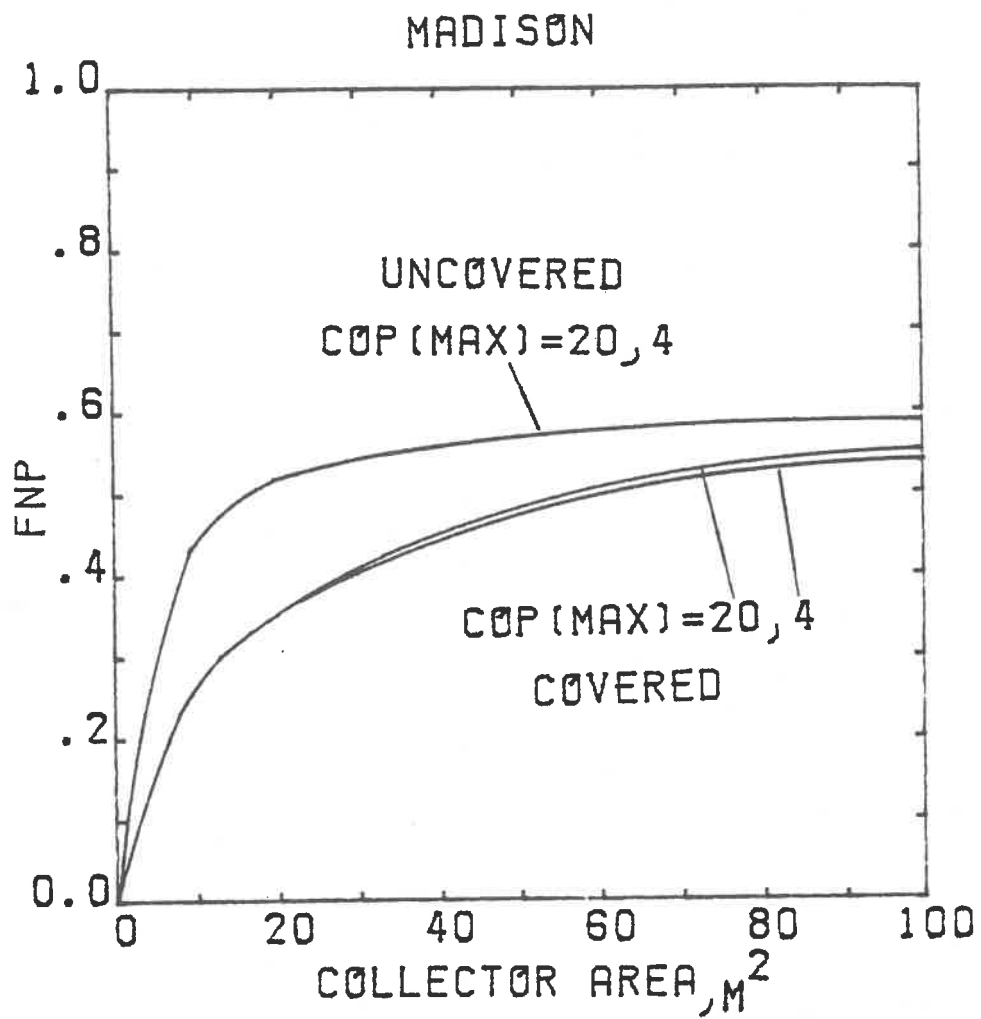


Figure 4.1.10 Effect of Maximum COP on Collector Heat Pump Performance--Madison

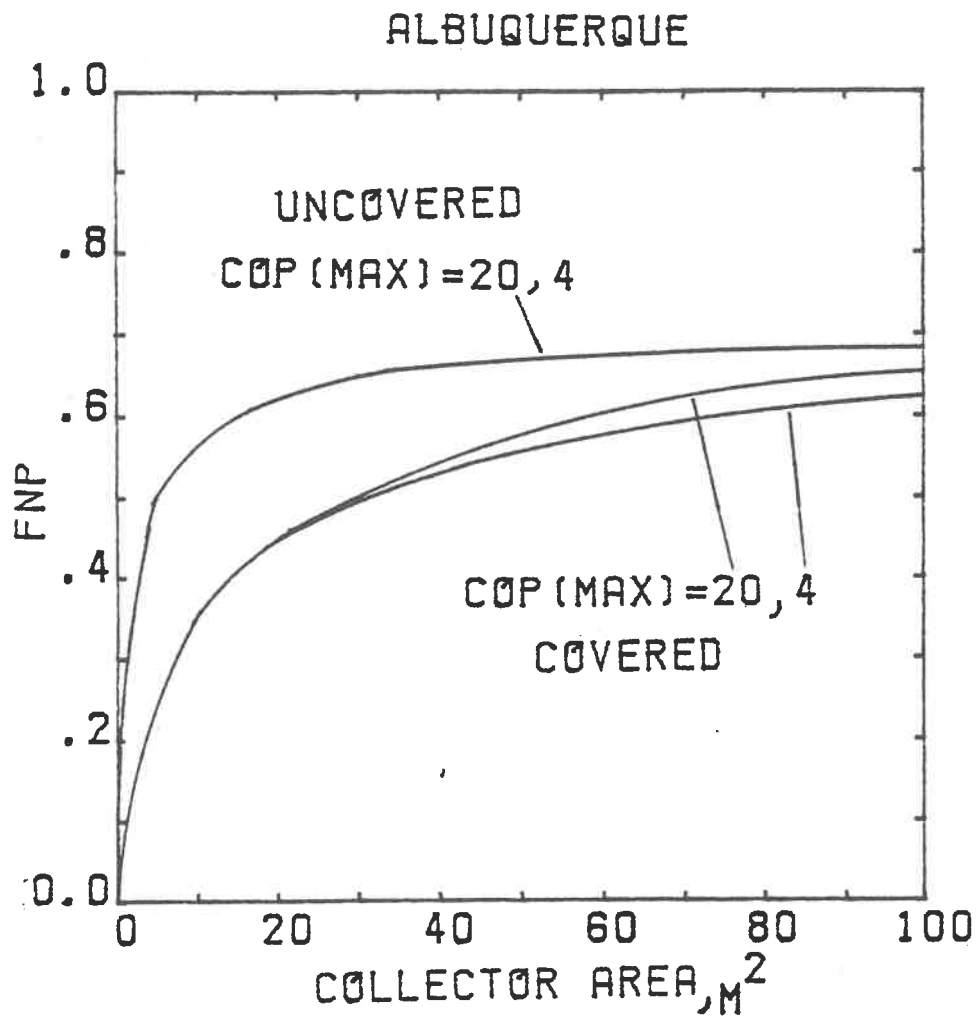


Figure 4.1.11 Effect of Maximum COP on Collector Heat Pump Performance--Albuquerque

the value 4.0, which was used in the base case studies. The performance curves of Figure 2.2.1 were altered to allow continuous performance improvement past the 4.0 COP point for this comparison. Other system characteristics remained the same as in Table 4.1.1, as were the characteristic equations for heat pump performance as a function of evaporator temperature. Figures 4.1.10 and 4.1.11 show the comparisons made for the space heating simulations in Madison and Albuquerque. The results show that there is little overall performance improvement for the covered system and none for the uncovered system. This is a consequence of the need for high sol-air temperatures for COP improvement. The fraction of hours for which COP's greater than 4.0 were achieved were almost none for the uncovered system and quite small for the covered systems.

Effect of Improved COP--System performance was determined for the heat pumps systems with the COP improved 25% over that used for the base case simulations. In these simulations the heat pump COP is 25% higher at each evaporator temperature, with a maximum COP of 5.0. All other system and load characteristics remained the same. Figures 4.1.12 and 4.1.13 show the comparison of results with improved COP against the original COP for the uncovered, covered and conventional heat pumps in Madison and Albuquerque. The dashed lines are results for the original COP and the solid lines are for the improved COP.

The results for non-purchased fraction in Madison indicate that the conventional heat pump improved by 7% of the load at the higher

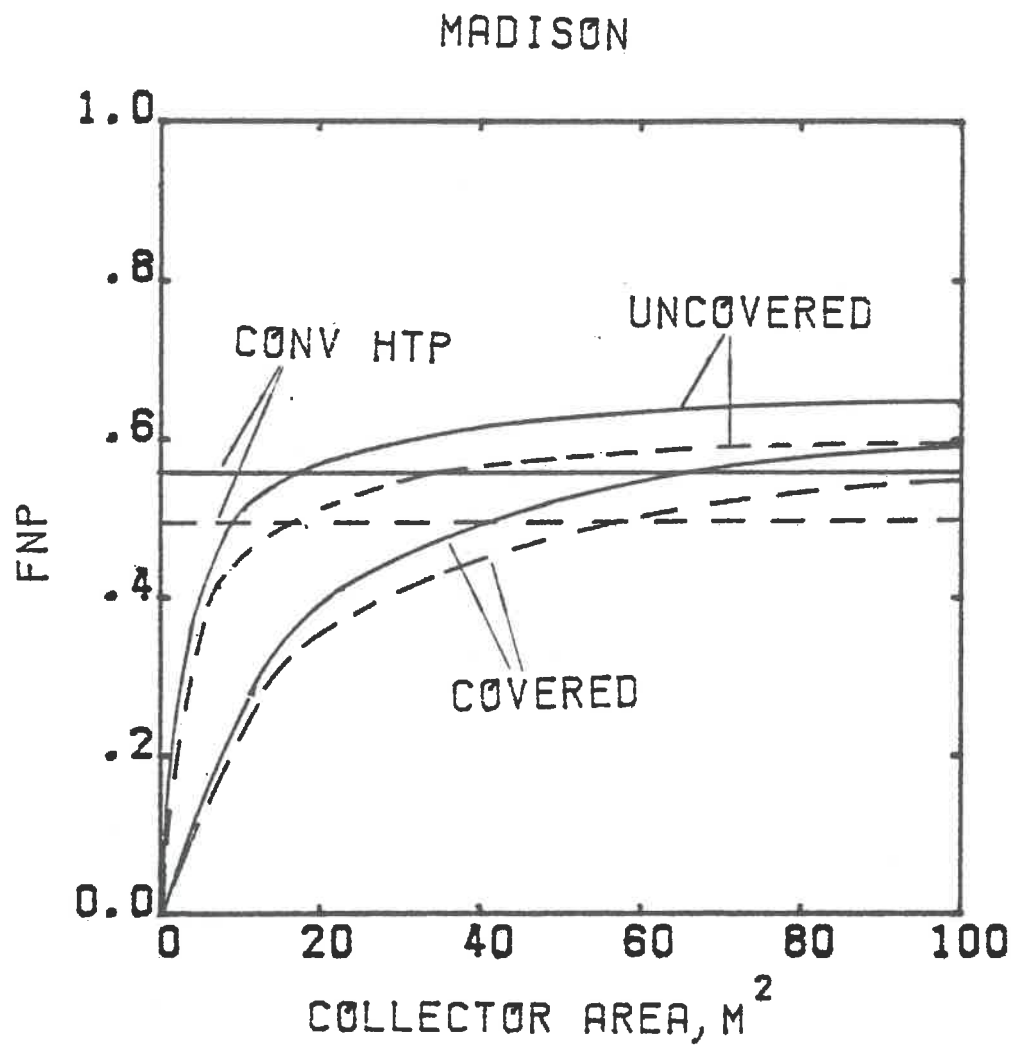


Figure 4.1.12 Effect of 25% COP Improvement on Heat Pump Performance--Madison

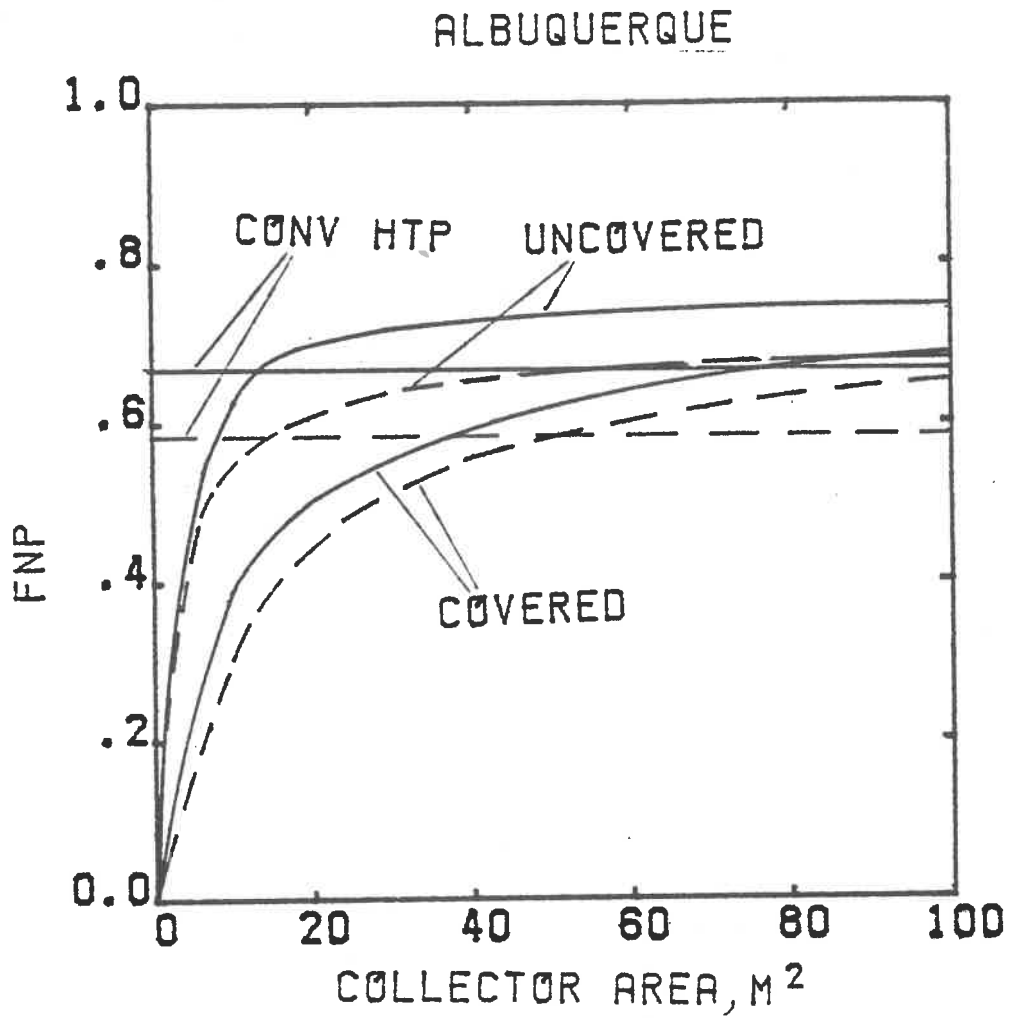


Figure 4.1.13 Effect of 25% COP Improvement on Heat Pump Performance--Albuquerque

COP, while at 24 m^2 collector area the uncovered system experienced an improvement of 6% of the load and covered system gained 5%. In the Albuquerque results the conventional heat pump, 24 m^2 uncovered and 24 m^2 covered heat pump systems gained 11%, 7% and 4%, respectively. The performance improvement for the conventional heat pump, which depends only on convective heat transfer is the greatest, while the covered collector heat pump, which depends on convection the least showed the least improvement.

The results can be explained in terms of the heat pump energy balance. As the system COP at a constant evaporator temperature (T_e) is raised, the heat pump capacity (Q_{DEL}) remains the same and the compressor work input (W) decreases. The energy absorbed by the evaporator (Q_{abs}) increases to maintain an overall energy balance ($Q_{\text{abs}} + W = Q_{\text{DEL}}$). When comparing the heat pump energy balances for high and low COP systems under the same weather and load conditions, it is apparent that the high COP system, which is trying to deliver the same capacity as the low COP system needs to have its collector/evaporator absorb more energy than the low COP system. This tends to drive down the evaporator temperature of the high COP system relative to the low COP system, because the amount of energy absorbed by refrigerant boiling in the evaporator is proportional to the difference between the sol-air (or ambient) temperature and the evaporator temperature. The lower steady-state evaporator temperature of the high COP system causes its steady-state COP to be less than expected and the heat pump capacity delivered to the load will

be less than the capacity for the low COP system with the same ambient conditions.

Since the convection coefficient (U_L) of the covered collector heat pump system is less than the convection coefficient of the uncovered collector heat pump system, the evaporator temperature of the covered system is more sensitive to changes in the weather and changes in system performance characteristics. As the steady-state COP of the heat pump increases, the effort to increase the amount of energy absorbed by the collector/evaporator of the covered system to maintain its energy balance causes the evaporator temperature to decrease a greater amount than with the uncovered system. A review of the collector equation helps to show this:

$$Q_{\text{abs}} = A_c U_L (T_{\text{sa}} - T_e) \quad 3.1.3$$

The covered collector heat pump system thus experiences the least overall improvement in both locations. The conventional heat pump has the highest convection coefficient and therefore experiences the greatest performance improvement with the higher COP.

The differences in performance increases between systems was more dramatic in Albuquerque than in Madison. The fact that non-purchased fraction for the conventional heat pump in Albuquerque improved so much more than in Madison is because the annual space heating load in Albuquerque is significantly less than the load in Madison. Any system performance changes are more likely to have a greater effect on non-purchased fraction for a smaller load. This also is

the primary reason why the uncovered system improved more in Albuquerque than in Madison. The covered collector system in Albuquerque had the lowest performance improvement of all. This is partially due to availability of more hours with high sol-air temperatures in Albuquerque than in Madison. The covered system operating with a high sol-air temperature already has a high COP. The effect of increasing system COP is going to decrease the steady-state evaporator temperature more dramatically because of the large amount of absorbed energy (Q_{abs}) needed for the heat pump energy balance. The result is little, if any performance gain for the covered system.

Effect of Collector Slope--Yearly space heating performance was obtained for Madison and Albuquerque with the collector slope altered to 90° from the horizontal for comparison with the results obtained with a 60° collector slope. The rest of the Table 4.1.1 parameters are the same. The results are summarized in Table 4.1.3 for 24 m^2 collector area. The comparisons for other collector areas are nearly the same.

The results indicate that the month of the simulation has no bearing on the difference in performance between the two collector orientations for both systems. The 60° collector tilt is better for both systems during all months at all collector areas in both Madison and Albuquerque. Since these results represent a potentially wide range of solar azimuth angles, it is apparent that the 60° slope will give consistently better results for all refrigerant-filled collector heat pump applications. The improvement in non-purchased frac-

Table 4.1.3
 Effect of Collector Slope on System Performance
 Collector Area--24 m²

	<u>Period</u>	<u>Collector Slope Angle</u>	<u>Madison</u>		<u>Albuquerque</u>		
			<u>COP</u>	<u>F_{np}</u>	<u>COP</u>	<u>F_{np}</u>	
Uncovered Collector	December	60	2.42	.508	2.73	.604	
	December	90	2.41	.507	2.71	.602	
	March	60	2.61	.540	2.84	.627	
	March	90	2.57	.533	2.80	.622	
	Year	60	2.58	.529	2.83	.630	
	Year	90	2.56	.526	2.81	.627	
	Covered Collector	December	60	1.91	.300	2.20	.438
		December	90	1.89	.295	2.18	.436
March		60	2.18	.394	2.23	.481	
March		90	2.14	.384	2.19	.473	
Year		60	2.07	.377	2.19	.473	
Year		90	2.04	.369	2.16	.467	

tion is typically less than one percent of the load, though.

4.2 Collector Control Strategy

The potential for overall heat pump performance improvement by combining the convective heat exchange properties of the coverless collector and the insulative properties of the covered collector into one system was investigated. The steady-state system COP can be maximized by selecting which of the two modes--covered or convective--will be the most efficient. In actual operation a collector would be utilized for both modes. Convective heat transfer with the collector plate surface would be obtained by blowing outdoor air between the covers and collector plate containing the evaporating refrigerant. In the convective mode, the system behaves much like a conventional air source heat pump, with the added benefit of available incident solar radiation. The covered mode is obtained by sealing off possible convection to air circulating between the collector plate and covers from the outside. The back of the collector/evaporator is insulated to prevent convection losses. Heat loss from the collector would be by the same means as conventional covered solar collectors.

The convection heat transfer coefficient of the collector plate is dependent on parameters such as collector size and dimensions, and air flow rate. By using reasonable estimates for air flow rate between cover and plate and selecting a 24 m^2 collector for the 25.3 MJ system, the forced convection coefficient for flow between two plates can be estimated by methods such as in [11]. The calculated

value for the convection coefficient in this application ranges from 10 to $20 \text{ W/m}^2\text{C}$. The value used for the convective mode simulations is $20 \text{ W/m}^2\text{C}$ to allow comparison with the uncovered collector heat pump results discussed in Section 4.1. It was found that the actual value used for the forced air convection coefficient has little effect on the conclusion in this study.

In selecting a control strategy, it was determined that the evaporator temperature is the parameter which will determine which mode--covered or convective--would be used. When utilizing the sol-air bin method, the steady-state evaporator temperature can be calculated for both modes for a particular bin. Since the system COP increases with evaporator temperature the mode which has the highest evaporator temperature will be used to generate performance results. The result of the mode selection process is that when the evaporator temperature is greater than the ambient temperature for the covered mode, it is used because convection losses from the plate can be limited. Otherwise, the convection mode is used. The collector heat pump will operate more like a conventional heat pump when the evaporator temperature is less than the ambient temperature. The results are shown in Figure 4.2.1 for the space heating load in Madison using the parameters of Table 4.1.1. The performance improvement of this type of control over the uncovered collector system is only slight.

Since the covered mode is used only when the evaporator temperature exceeds the ambient temperature, its use is limited to the

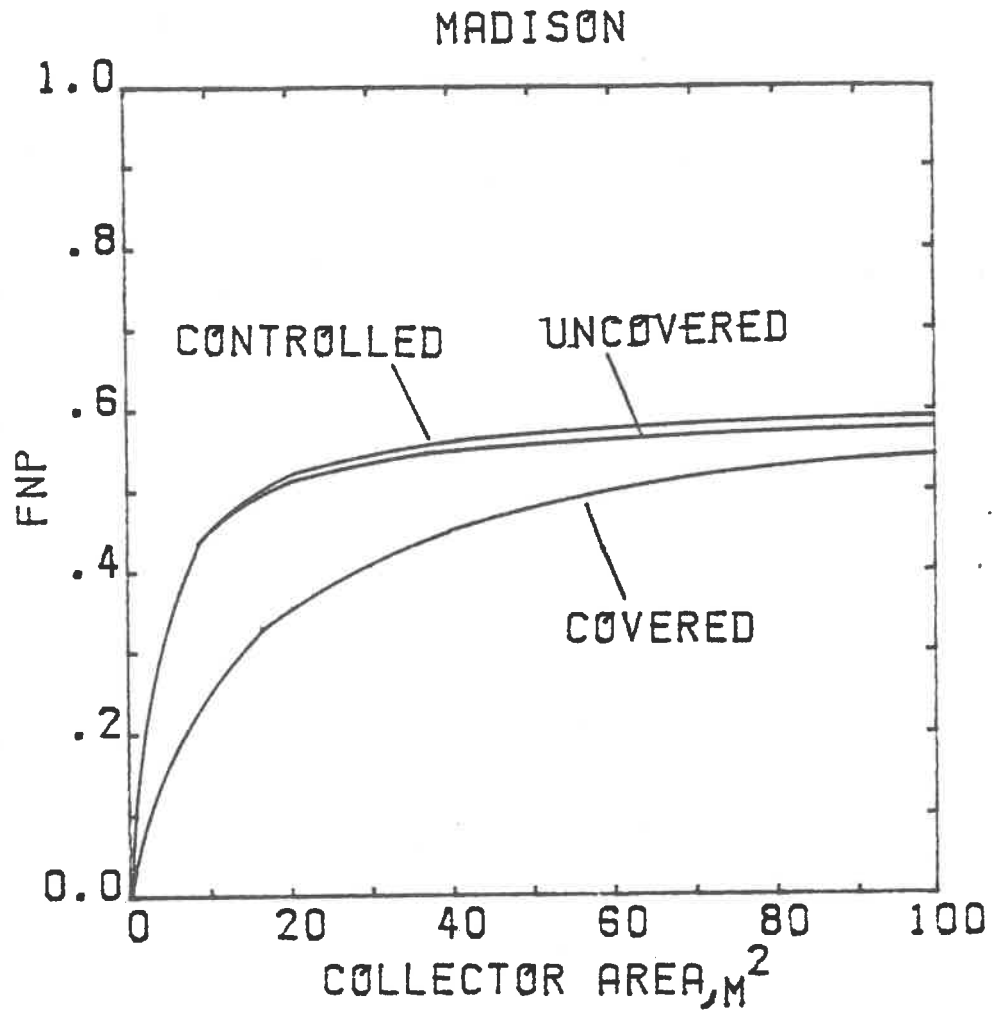


Figure 4.2.1 Effect of Collector Performance Control--Madison

fraction of hours shown in Figure 4.2.2 for the covered system. The other curve in the figure is for an uncovered collector. The difference in fractions between collector types is due to transmission losses through covers for the covered collector. It is apparent from Figure 4.2.2 that the number of hours of forced convection mode operation is almost the same as the number of hours for which T_e is less than T_a for the uncovered collector simulation. The convective and covered modes both have the effect of transmission losses through glass covers for the collector control application. The number of hours for which T_e is greater than T_a will be equal for both modes.

The fraction of hours of covered mode operation in Madison is less than 20% for collector areas less than 40 m^2 . Space heating loads are typically small during periods of available solar radiation. At low temperatures such as those experienced in Madison, lower radiation levels will cause a switchover to the covered mode, though. Generally the percentage of the load which will see a performance improvement with this type of collector control when compared with an uncovered collector application will not be very great. As a specific example, for a 24 m^2 collector in Madison the percentage of hours with covered mode operation is only 14%, which corresponds to the fraction of the heating load met by operation of the heat pump in this mode.

It will be shown in Section 4.3 that only incident radiation, not U_L , determines whether convection heat transfer will aid or hurt collector performance.

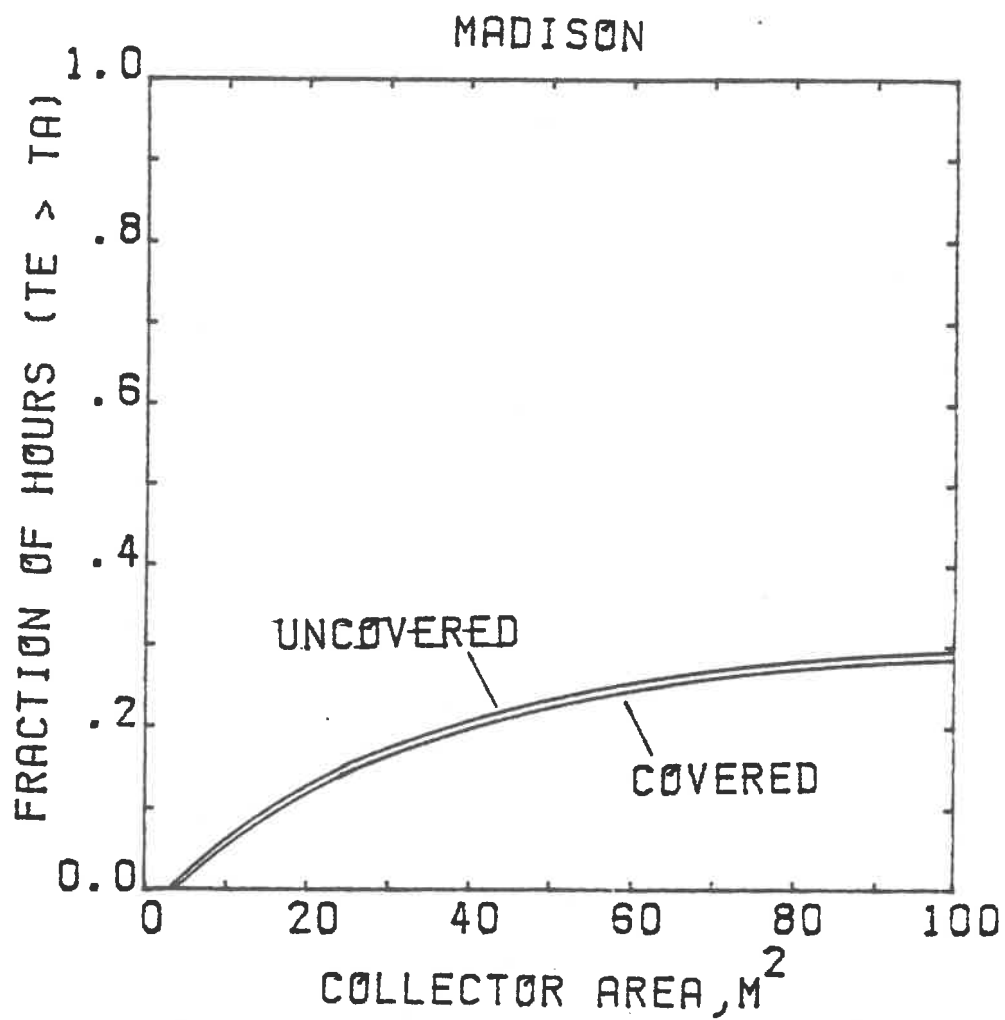


Figure 4.2.2 Fraction of Hours During Which Evaporator Temperature Exceeds Ambient for Collector Heat Pump Systems--Madison

4.3 Collector Convection and Radiation Heat Transfer

The two principle sources of energy transfer to the collector/evaporator plate in refrigerant-filled collector heat pumps are convection and solar radiation. The interaction of convection and radiation and the effect on system performance is not the same for different collector types. The performance of an uncovered collector system will depend more on convection heat transfer than will that of a covered collector heat pump system. The absorption of solar radiation is less vital to the performance of an uncovered collector system than a covered collector system.

The combination of convection and radiation that affects the heat pump can be divided into three categories:

1. Solar radiation with convective losses. During this daytime condition, the evaporator temperature is driven above the ambient temperature and convection from the collector reduces the amount of energy transferred to the boiling refrigerant in the collector.
2. Solar radiation with convective gains. The amount of incident radiation is less than in (1) and the evaporator temperature is less than the ambient temperature.
3. Convection Gain Only. This is a nighttime condition and all heat transfer occurs by wind or natural convection. The collector heat pump behaves like a conventional air-source heat pump.

Figure 4.3.1 indicates how much "free" energy was obtained by the three possible combinations for two collector types in the Madison bin method simulation. The corresponding overall COP plots are in Figures 4.3.2 and 4.3.3 and the fraction of hours for each combination is shown in Figure 4.3.4. Figure 4.3.5 shows an example of this distribution for bin hours in Madison.

When radiation levels are high and convection reduces collector performance, the covered system has the advantage of higher COP's. The amount of non-purchased energy obtained in this case is not necessarily greater for the covered system for these reasons:

1. The covered system has greater efficiency and capacity at radiation levels which allow the evaporator temperature to exceed the ambient temperature. The system operates less of the time since the capacity exceeds the load and less radiation is utilized. The uncovered system actually utilizes more incident radiation during the year in this case.
2. The maximum COP restriction occurs more often for the covered system. This further reduces the amount of radiation utilized because a maximum of 75% of the heat pump capacity can be attributable to absorbed radiation with a maximum COP of 4.0.

The amount of time during which convection gain and radiation are coincident is relatively small at large collector areas but is significant at smaller collector areas where the total absorbed

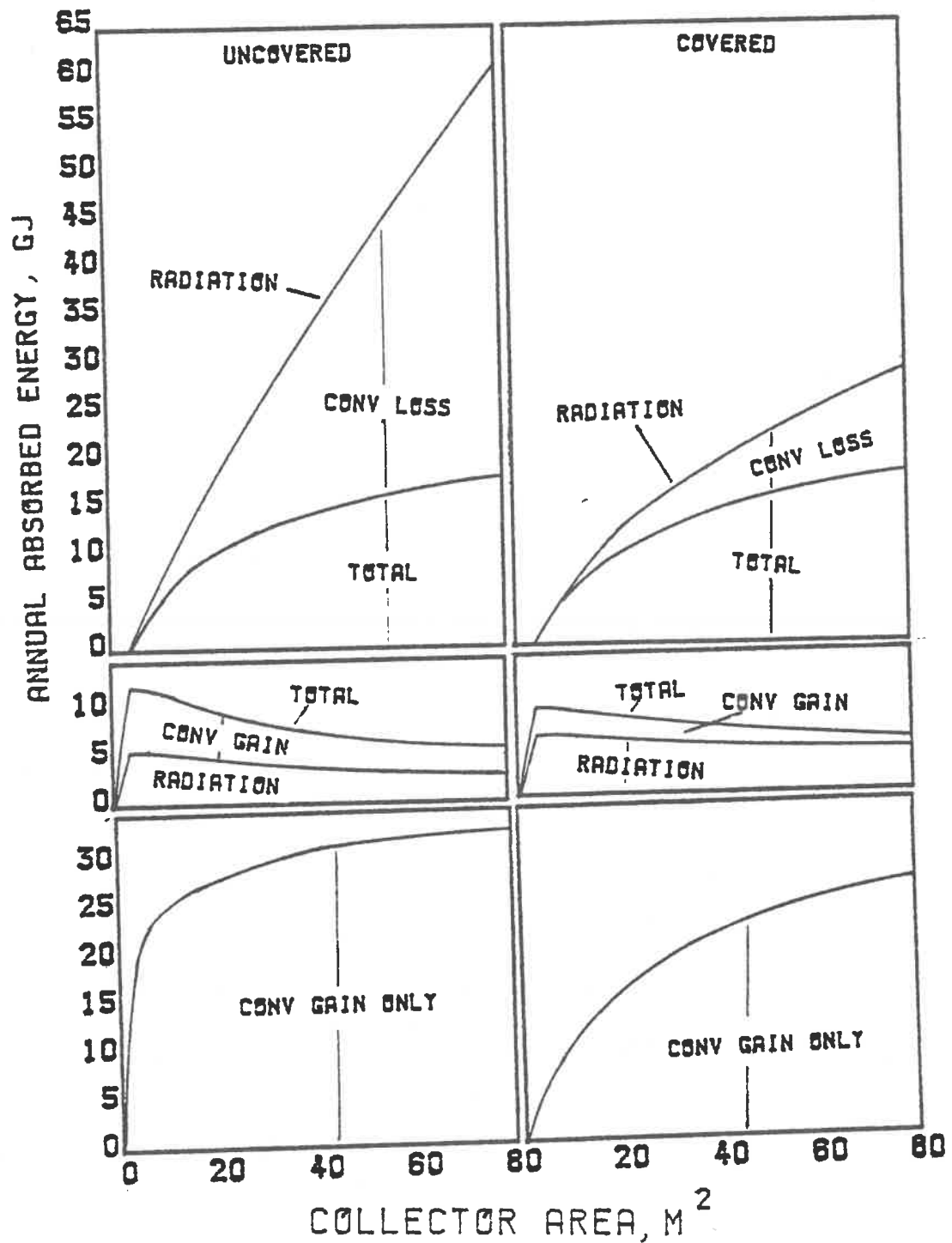


Figure 4.3.1 Summary of "Free" Energy Gained by Collector Heat Pumps--Madison

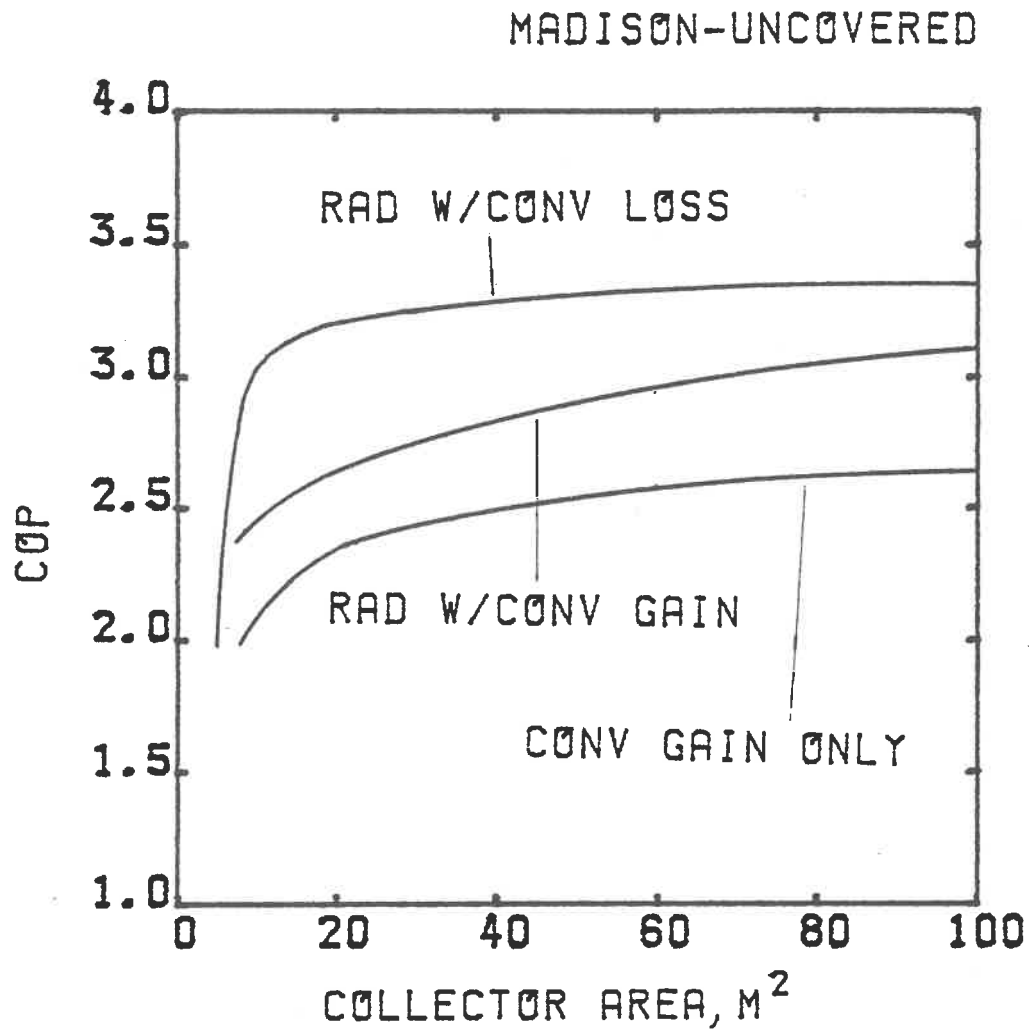


Figure 4.3.2 Overall COP by Energy Gain Modes for Uncovered Collector Heat Pump--Madison

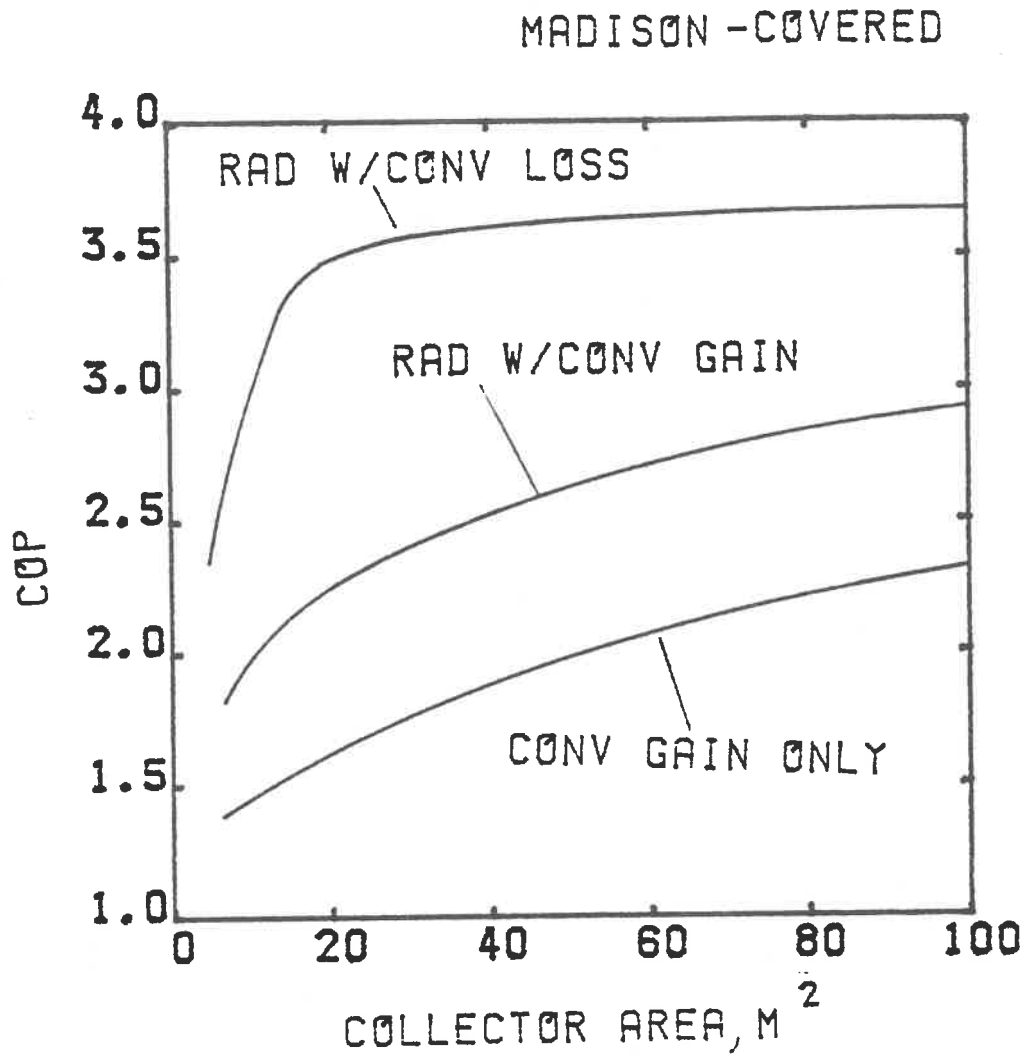


Figure 4.3.3 Overall COP by Energy Gain Modes for Covered Collector Heat Pump—Madison

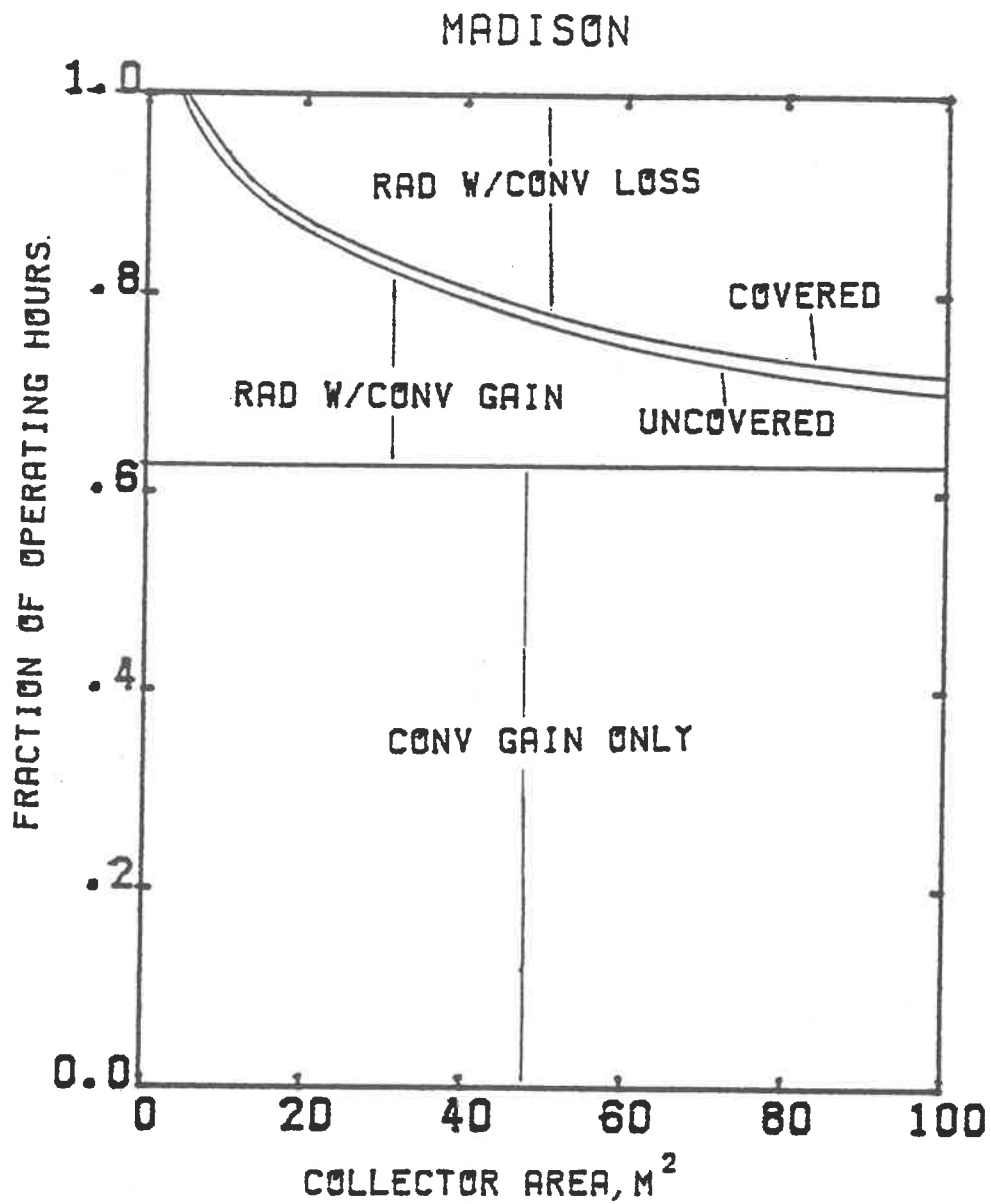


Figure 4.3.4 Fraction of Operating Hours by Energy Gain Modes--
Madison

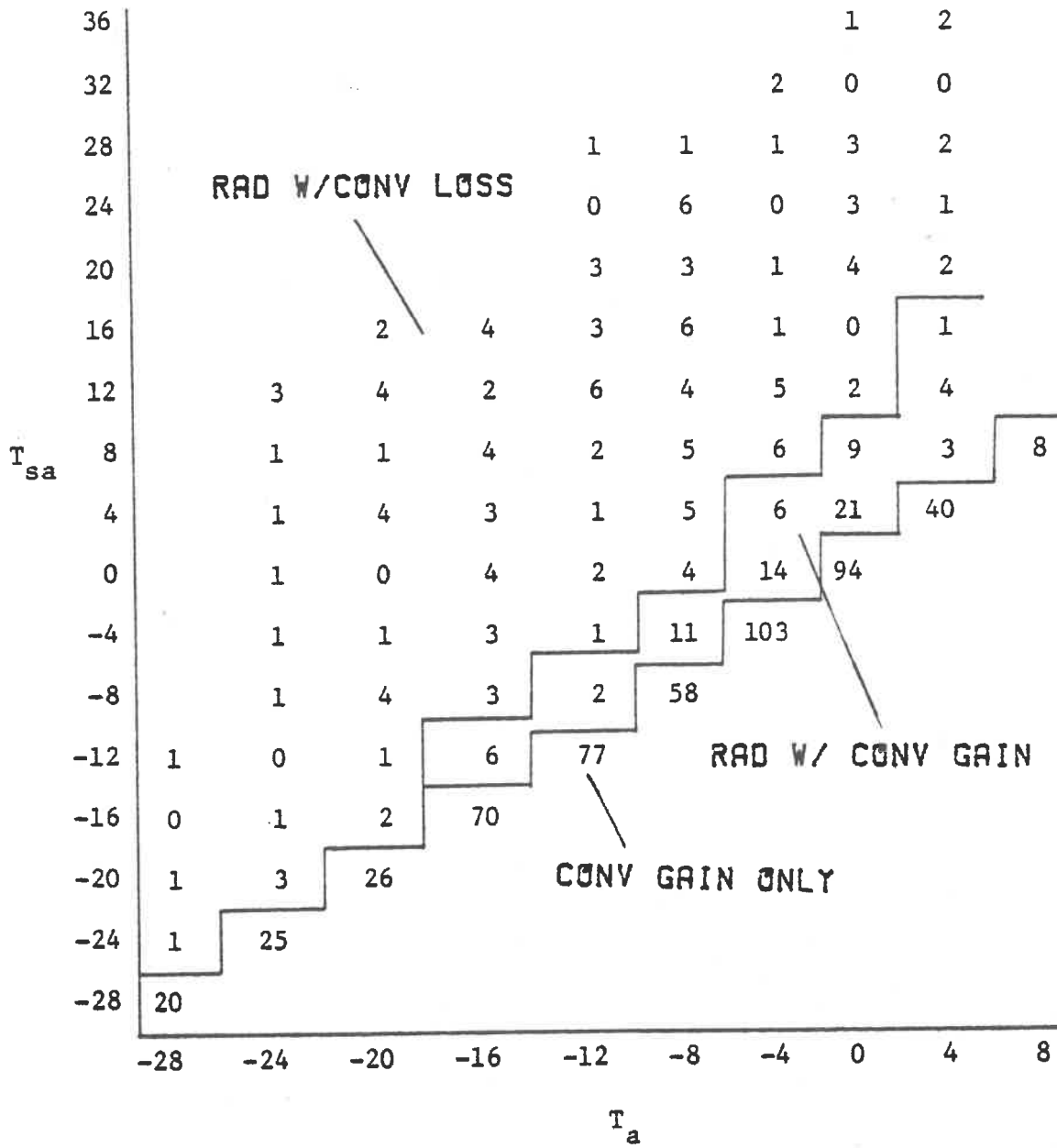


Figure 4.3.5 Temperature Bin Distribution for Uncovered Collector in January—Madison

radiation is less likely to raise the evaporator temperature above ambient. In this case the uncovered collector system has the performance edge because of its higher convection heat transfer coefficient.

The majority of hours of heat pump operation occur when there is no available radiation. The uncovered system performs much better than the covered system in this circumstance. The uncovered system is able to generate substantial non-purchased energy at small collector areas with convection only. The benefit of increasing collector area from a non-purchased energy standpoint for the uncovered system diminishes for two reasons:

1. Increased heat pump cycling as the capacity increases with larger collector areas. The load limits the amount of "free" convection energy used.
2. As the area increases the evaporator temperature tends to increase, thereby increasing the COP. However, the upper limit for evaporator temperature is the ambient temperature for the convection gain only mode. The amount of energy transferred to the evaporator is $Q_{abs} = U_L A_c (T_a - T_e)$. As T_e increases, $(T_a - T_e)$ decreases, tending to limit the amount of convection heat transfer to the collector. This affects both system types but is better illustrated with the covered system which has the lower loss coefficient. The heat transfer capacity of the collector in the covered system is more sensitive to changes in evaporator

temperature.

Critical Radiation Level for Convection--For a heat pump with a refrigerant-filled collector/evaporator, there is a radiation level corresponding to each ambient temperature above which the evaporator temperature will be greater than the ambient temperature. A relationship for the locus of "critical" points at which evaporator and ambient temperatures are equal can be derived by substituting T_a for T_e in the collector equation (Eq. 2.2.3). The heat pump energy balance then becomes

$$Q_{abs} = A_c (\tau\alpha) I_T = Q_{DEL} - W \quad 4.3.1$$

where Q_{DEL} and W are functions of the ambient temperature (defined to be equal to the evaporator temperature). Upon substituting the heat pump COP into Equation 4.3.1 and rearranging terms, the absorbed radiation level can be defined in terms of known model parameters:

$$A_c (\tau\alpha) I_T = \frac{Q_{DEL}(T_a) \times [COP(T_a) - 1]}{COP(T_a)} \quad 4.3.2$$

Figure 4.3.6 shows this relationship for the heat pump model used in the simulations reported in this thesis. The plotted line is appropriate for both covered and uncovered collector types because absorbed radiation, which accounts for collector properties is plotted on the vertical scale. Above the level at which the evaporator and ambient temperatures are equal, the collector will ex-

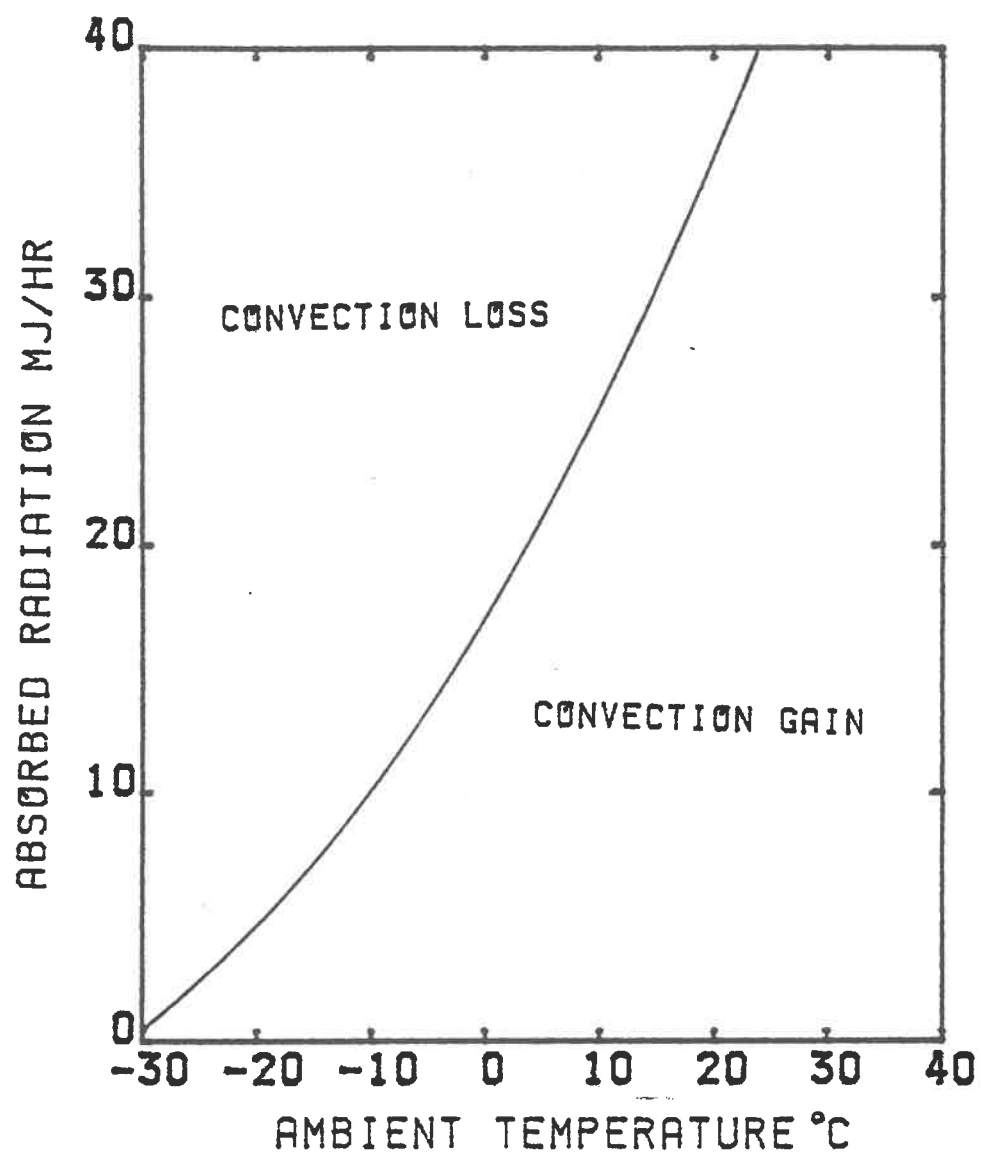


Figure 4.3.6 Critical Level for Convection Heat Transfer to Collector

perience convection loss. This benefits the covered collector system from an overall performance standpoint. Below the critical level, the uncovered system benefits because its properties are better suited to take advantage of convection gains. This plot should further enhance the understanding of the collector control strategy application results reported in Section 4.2 and should also aid in determining the ambient conditions which cause the distribution of hours shown in Figure 4.3.4. Figure 4.3.6 is graphical evidence for the fact that covered collector heat pump systems are better suited for cold temperatures and high radiation levels while uncovered systems perform better with warmer temperatures and less radiation.

Upon reviewing Equation 4.3.2 it is obvious that the "critical" radiation level can be moved by changing heat pump model characteristics. The critical level can be reduced and hence aid covered system performance relative to the uncovered system by reducing Q_{DEL} . Since the heat pump capacity at constant ambient temperature will primarily be affected by changes in nominal heat pump size, it is beneficial to the covered system to reduce the heat pump size. This result corresponds with the conclusions drawn in the discussion of the effect of heat pump size in Section 4.1.

Another inference that can be made by observing Equation 4.3.2 is that reducing average system COP will also reduce the critical absorbed radiation. This will improve the covered system performance relative to the uncovered system performance. General conclusions

can be made for both collector types in regard to heat pump performances:

1. Covered collector systems work well with small heat pump sizes, large collector areas and plenty of solar radiation. When this determination is taken to the limit, the compressor can be replaced with a refrigerant pump and an energy storage media can be added to the system to take maximum advantage of solar radiation. Covered system design will then be similar to a conventional solar heating system.
2. Uncovered collector systems are more strongly affected by changes in the ambient temperature than solar radiation levels. This lends credence to the argument that uncovered collector heat pumps operate much like conventional air source heat pumps.

4.4 Performance Upper Bound with Storage

In many solar applications the effect of energy storage is to enhance overall system performance. Active liquid and air collection systems in residential applications operate poorly without some form of storage. Most commercially available heat pumps, on the other hand, do not utilize storage and depend on auxiliary sources to supply the remaining energy to match loads which exceed the heat pump capacity. The air source heat pump, however, will always be able to operate at capacity, thereby meeting all or a substantial portion of the load at all times. The need for storage is much less

apparent for air-to-air heat pumps than conventional solar systems, especially considering the increased cost of a storage subsystem.

The potential for storage with refrigeration-filled collector heat pumps is more substantial than that for conventional heat pumps because of the ability to take advantage of higher daytime COP. Energy delivered during daytime operation can be stored for use at night.

The upper bound on system performance is determined on a monthly basis using the sol-air temperature bin method described earlier. The method utilizes the bins with highest available sol-air temperatures. The bin array is "scanned" first at the highest sol-air temperature and the heat pump capacity and electrical input contributions are totaled. The scanning continues at the next lowest sol-air temperature bin and continues descending in sol-air temperature until the total energy delivered equals the total monthly load. Thus the method has the effect of utilizing the highest heat pump performance available during the month to satisfy the total monthly load requirement. A storage system which would store any amount of energy without losses is assumed implicitly with this method. It is also assumed that some type of "sensor" is used which knows when the collector/evaporator sol-air temperature is high enough to operate the heat pump. Distribution of weather data and load throughout the month is ignored because of the above assumptions.

Upper bound performance results are plotted for the yearly Madison space heating load in Figure 4.4.1 along with the corres-

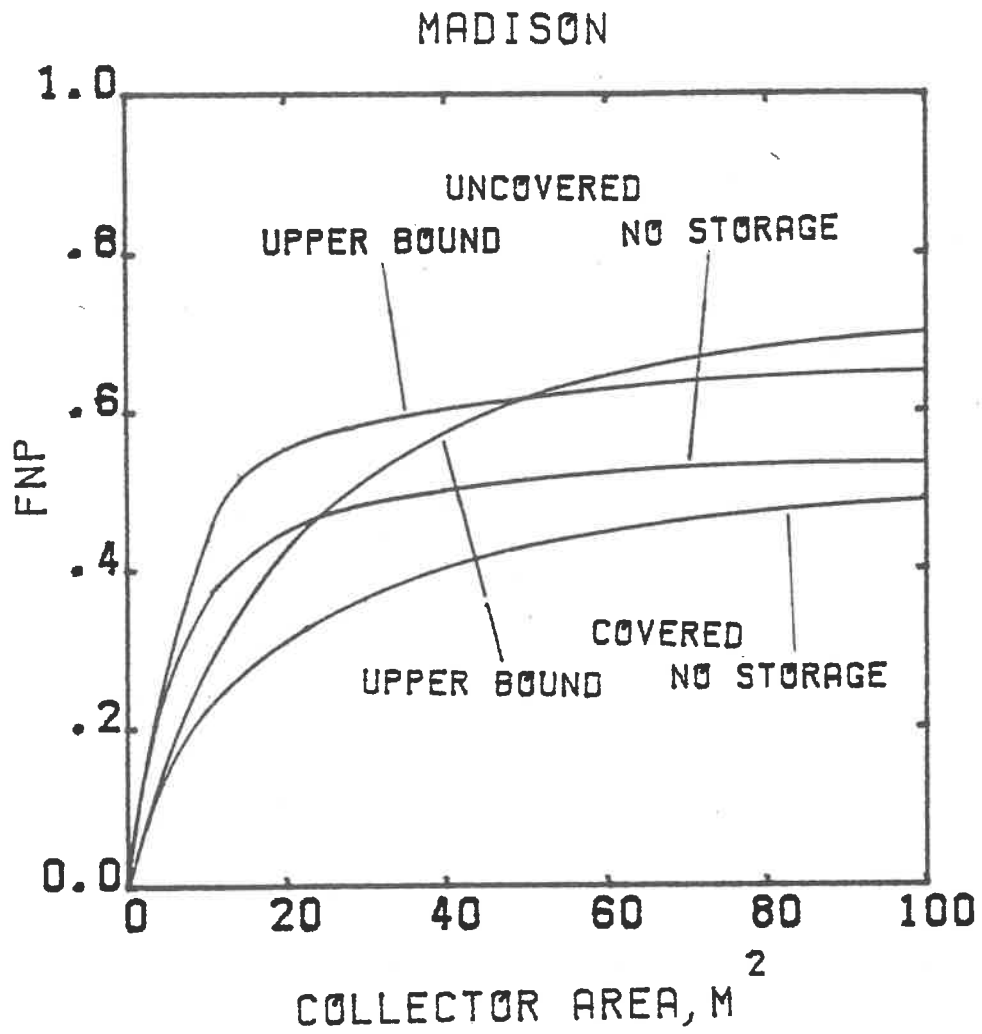


Figure 4.4.1 Upper Bound Performance with Storage for Collector Heat Pumps--Madison

ponding performance curves for the non-storage simulations described earlier. The results show a potential for substantial improvement with storage, especially for covered collector heat pump systems. Upper bound performance of the covered collector system exceeds that of the uncovered collector system in this example above 60 m² collector area.

Clearly, it can be stated that some form of storage will improve the overall performance of both collector heat pump systems, especially the covered system. In many cases, however, installed systems are of the uncovered collector type with no storage for space heating. These are typically retrofit installations in which the collector heat pump system is added on to a previously installed furnace and delivery system, where it may have been difficult to justify the added cost and space of the storage arrangement. In the next section, the effect of using building thermal mass as a storage media will be discussed.

4.5 Building Thermal Capacitance

All of the heat pump simulation results presented thus far have used energy rate control. The load has been directly proportional to the difference between room temperature and ambient temperature. To determine the effect of house capacitance on the overall performance of refrigerant-filled collector heat pumps in space heating situations, TRNSYS simulations were performed with these systems and a house load model. The TRNSYS components used in the simulations include weather data input, a Data Reader (Type 9), Radiation Pro-

cessor (Type 16), Walls (Type 17), Roof (Type 18), Room (Type 19) and the heat pump model used in the TRNSYS simulation discussed in Section 3.1. The effective room thermal capacitance in the one node capacitance room model is 20000 KJ/°C. The overall UA and infiltration rate of the room were adjusted until the total monthly load for this method was approximately the same as in the bin method for Madison.

The storage of energy in the building thermal mass was achieved by allowing the room temperature to vary over a range of either 5°C or 10°C. The control strategy permitted continuous system operation in daytime until the maximum room temperature was reached. During the night, the heat pump system and the necessary auxiliary energy were used to maintain the minimum room temperature. The minimum and maximum room temperatures used in the simulations were 18°C and 23°C, respectively, for the 5°C range, and 16°C and 26°C, respectively, for the 10°C range.

The performance of the uncovered and covered collector systems with building capacitance was compared with bin method results for Madison. The results for room temperature ranges of 5°C and 10°C are shown with bin methods results for no-storage and upper-bound storage simulations in Table 4.5.1.

By utilizing energy storage in the form of thermal mass in the building, the system performance for space heating loads can be improved significantly. The minimum non-purchased fraction increase is 1.5% of the load with the uncovered collector system at 24 m² collector area and a 5°C room temperature range. An increase in

Table 4.5.1

Improved Results With Storage--Madison

<u>System</u>	<u>Simulation Type</u>	<u>Seasonal Non-Purchased Fraction</u>
Uncovered Collector 24 m ²	Base Case (no storage)	.460
	Bldg. Capacitance 5°C range	.475
	Bldg. Capacitance 10°C range	.505
	Upper Bound	.555
Uncovered Collector 48 m ²	Base Case (no storage)	.495
	Bldg. Capacitance 5°C range	.510
	Bldg. Capacitance 10°C range	.545
	Upper Bound	.610
Covered Collector 24 m ²	Base Case (no storage)	.345
	Bldg. Capacitance 5°C range	.375
	Bldg. Capacitance 10°C range	.440
	Upper Bound	.475
Covered Collector 48 m ²	Base Case (no storage)	.410
	Bldg. Capacitance 5°C range	.460
	Bldg. Capacitance 10°C range	.525
	Upper Bound	.610

non-purchased fraction over the no-storage case of as much as 11.5% of the load is achievable with the covered collector system of 48 m² collector area and a 10°C range. The additive advantage of increased heat pump COP and capacity due to daytime solar input to the collector/evaporator becomes realizable when thermal mass storage is used.

4.6 Performance Degradation Due to Cycling

All of the previous performance calculations discussed in this thesis have assumed that heat pumps attain steady-state operation instantaneously upon being switched "on." The effect of deviation from steady-state performance due to heat pump cycling will be presented in this section.

When a heat pump operates above the balance point, the steady-state capacity of the heat pump exceeds the load and the compressor of the unit will cycle on and off. Figure 4.6.1 illustrates how the capacity increases with ambient temperature for a typical heat pump in a space heating application, while the load decreases. To the left of the balance point, auxiliary sources must be used to match the load. Above the balance point, or to the right, heat pump cycling occurs. The amount of degradation increases as the ratio of load to steady-state capacity decreases and is a maximum at zero load. Due to complex design and thermodynamic considerations the overall integrated COP of the heat pump during a period of cycling will be less than the expected steady-state COP during that same period. In typical commercially available heat pumps, the factors that affect cycling include:

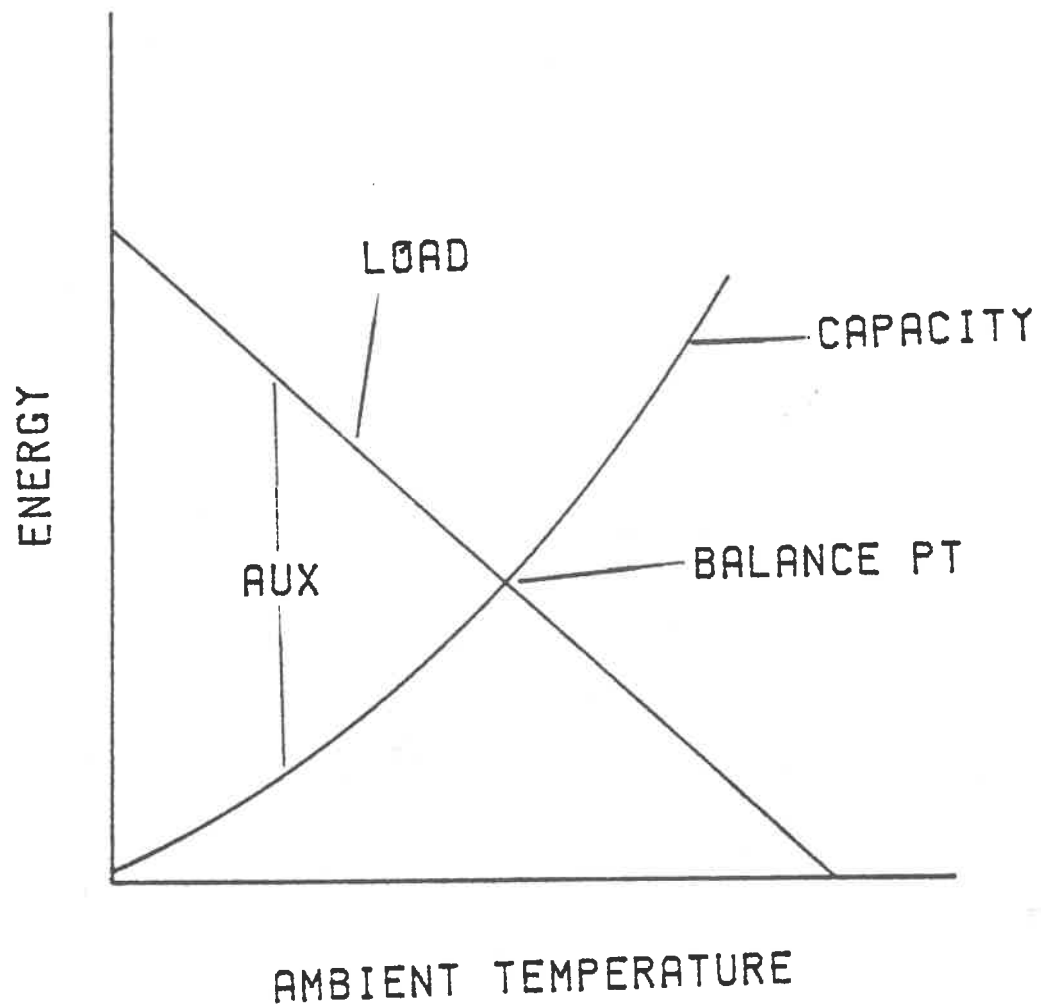


Figure 4.6.1 Typical Heating Load and Heat Pump Capacity vs. Ambient Temperature

1. Refrigerant distribution. Without any check valves or solenoid valves to prevent movement, most of the system refrigerant charge will ultimately migrate to the heat pump heat exchanger coil which has the coldest surrounding temperature during an "off" period. It may require minutes for the refrigerant to be re-distributed to steady-state proportions within the system upon start-up. This may be especially harmful to performance in the heating mode because the evaporator coil, which is outdoors and therefore is exposed to colder temperatures than the condenser coil, contains much less refrigerant than the condenser coil during steady-state operation. The compressor is forced to begin re-distributing the charge after start-up and system capacity will be lower than steady-state capacity until steady-state conditions are reached. A side-effect of the refrigerant charge distribution problem is the mechanical harm done to the compressor by the initial pumping of liquid refrigerant, or "slugging."
2. High compressor electrical current draw upon start-up. The compressor must work harder than normally after starting in order to bring the refrigerant vapor pressure in the compressor suction line down to a level at which the compressor was designed to operate at. The momentum of refrigerant flow must also be established, which also causes high power consumption initially.

3. Lost capacity after shut-down. Without any special arrangements once the heat pump stops, its capacity immediately goes to zero. The indoor heat exchange coil which has been at a temperature suitable for delivery to the load maintains a high temperature for a period after shut-down. Migrating refrigerant will remove most of this available heating capacity and reject it outdoors. Upon start-up the coil must again return to its steady-state temperature.

Since the degradation characteristics of different heat pump models and types are typically not the same, it is advantageous to develop a method of estimating degradation for heat pump types for which information is not available. In the Department of Energy guidelines [16], an industry-wide method used for estimating reduced heating and cooling performance from cycling is outlined. The "degradation coefficient," C_D , is defined for any particular operating point as follows:

$$C_D = \frac{1 - \frac{COP_{cyc}}{COP_{ss}}}{1 - \frac{Q_{cyc}}{Q_{ss}}} \quad 4.6.1$$

where COP_{cyc}/COP_{ss} is the ratio of overall cyclic COP to steady-state COP and Q_{cyc}/Q_{ss} is the ratio of cyclic to steady-state capacity over the same time period. Equation 4.6.1 can be rearranged to evaluate COP during cycling as

$$\text{COP}_{\text{cyc}} = \text{COP}_{\text{ss}} \left[1 - C_D \left(1 - \frac{Q_{\text{cyc}}}{Q_{\text{ss}}} \right) \right] \quad 4.6.2$$

Over a suitable time period such as one hour, the energy delivered, Q_{cyc} , will equal the load. Equation 4.6.2 can be written as

$$\text{COP}_{\text{cyc}} = \text{COP}_{\text{ss}} \left[1 - C_D \left(1 - \frac{Q_L}{Q_{\text{ss}}} \right) \right] \quad 4.6.3$$

Equation 4.6.3 is applicable to bin method performance calculations because all of the terms are determined under the conditions defined by a particular bin.

It is assumed that a refrigerant-filled collector heat pump operating in the same manner as a conventional residential heat pump will have similar performance degradation due to cycling. The collector/evaporator plate temperature requires a finite amount of time to stabilize upon start-up and the long length of refrigerant lines between the evaporator and the rest of the heat pump add to the transient effect at the beginning of each "on" cycle. No actual data is available to allow calculation of a degradation coefficient for collector heat pumps. It is assumed, therefore, that a reasonable value for these systems would be in the range of 0.25 to 0.40, which is the practical range for conventional split-system heat pumps.

The performance was obtained for the Madison yearly space heating simulation with degradation coefficient values of 0.0, 0.25 and

0.40. The results showing non-purchased fraction as a function of collector area for the uncovered and covered collector systems are shown in Figures 4.6.2 and 4.6.3. Comparisons between the results for these systems at 24 m^2 collector area and conventional heat pumps is shown in Table 4.6.1. The COP reduction is the percentage decrease in overall COP against the $C_D = .0$ case. F_{np} reduction is the magnitude in percent of the load.

None of the system types stands out as having substantially worse performance with cycling losses when compared with the others. The uncovered system had a higher COP reduction because it had the highest overall COP and consequently was likely to have the greatest COP and F_{np} decrease. The covered system with a 24 m^2 collector had the lowest overall COP and the least amount of COP decrease. The results show that accounting for cycling losses tends to lessen the performance differences between different types of heat pump systems with equal degradation coefficients. There is no indication that having a refrigerant-filled collector/evaporator has any effect on cycling performance.

Effect of Reduced Average COP on Cycling Rate--There is reason to believe that the method for estimating degradation performance outlined above is conservative and predicts the lowest possible heat pump COP due to cycling. In this discussion a more lenient approach is taken to achieve the highest potential cycling COP based on the degradation coefficient concept.

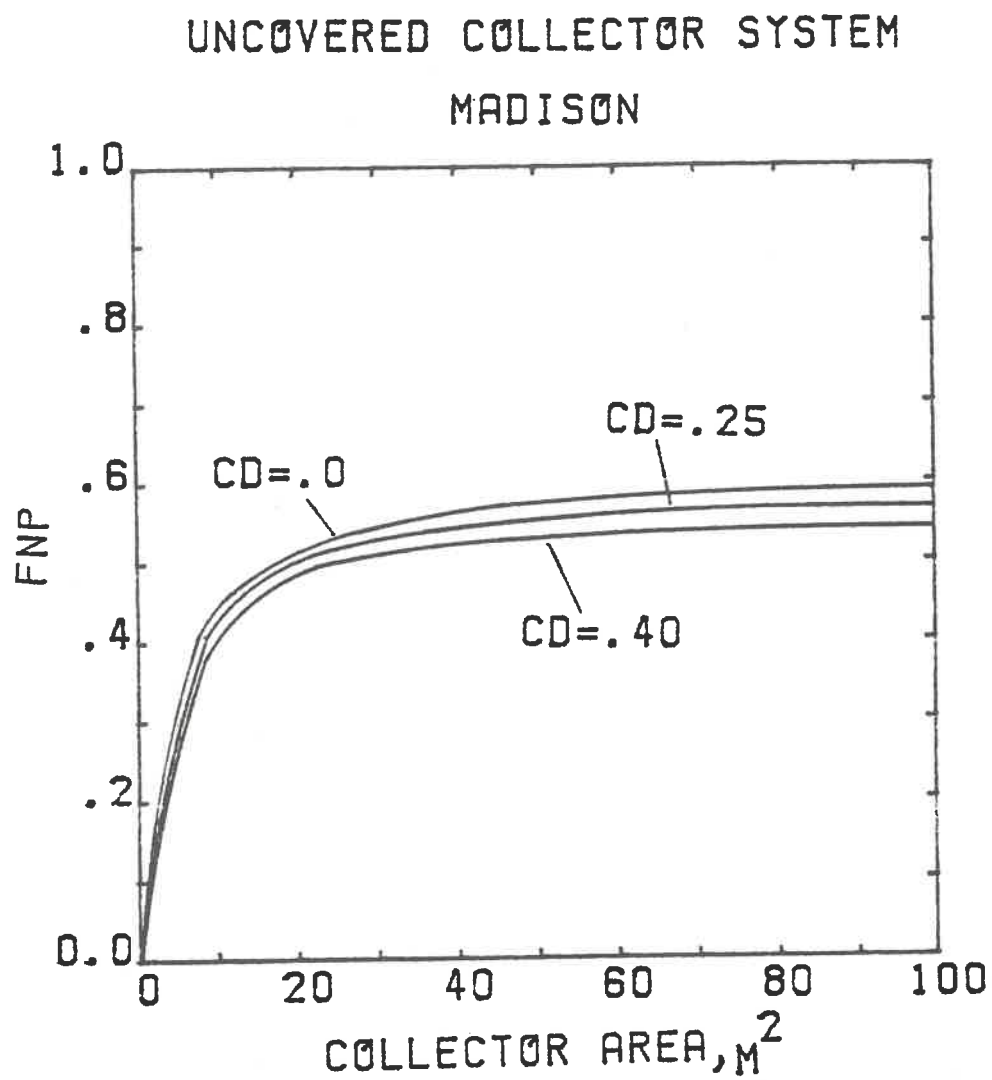


Figure 4.6.2 Effect of Degradation Coefficient on Uncovered Collector Heat Pump--Madison

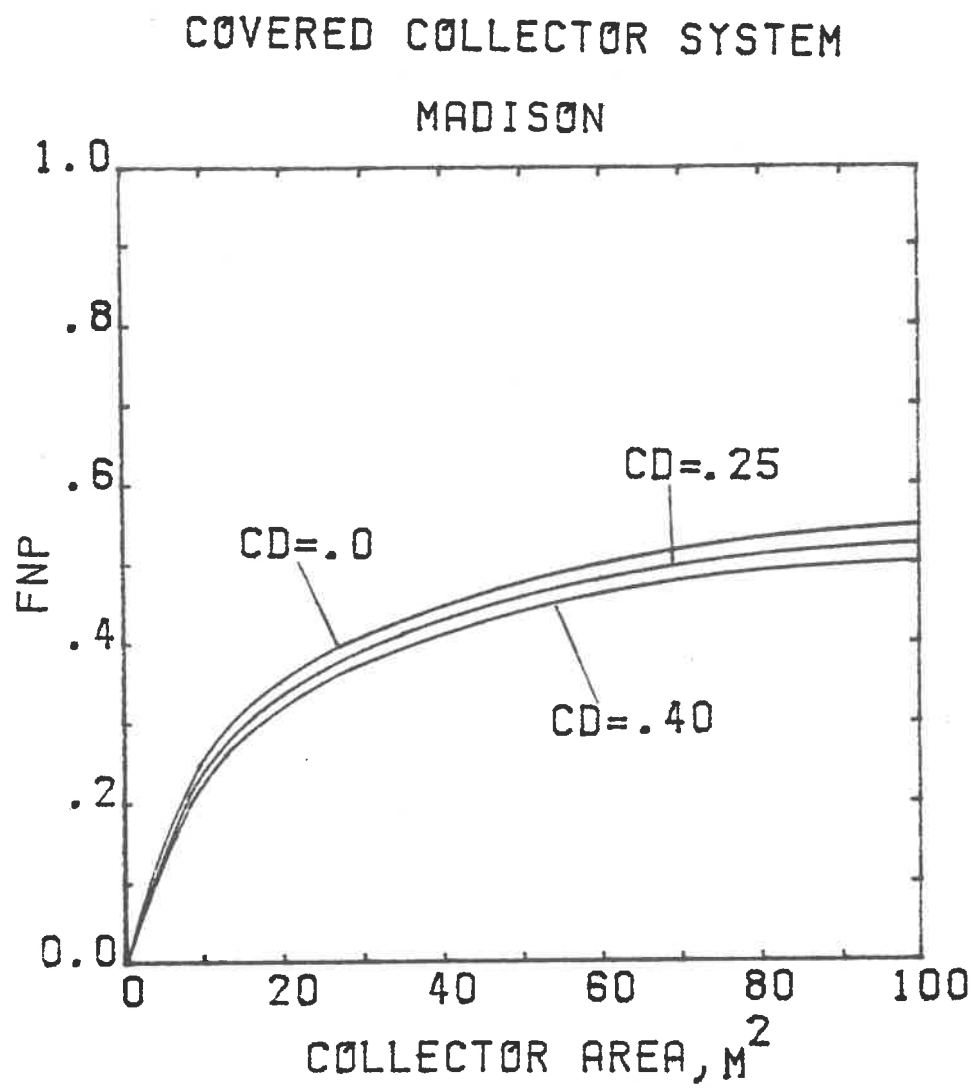


Figure 4.6.3 Effect of Degradation Coefficient on Covered Collector Heat Pump--Madison

Table 4.6.1
Cycling Performance--Madison

<u>System</u>	<u>$C_D = .25$</u>		<u>$C_D = 0.40$</u>	
	<u>COP Reduction</u>	<u>F_{np} Reduction</u>	<u>COP Reduction</u>	<u>F_{np} Reduction</u>
Uncovered (24m ²)	6.5%	2.3%	11.9%	4.2%
Covered (24m ²)	4.8	1.8	8.1	3.2
Conventional	5.4	2.0	9.5	3.7

In the method utilizing equation 4.6.3, the underlying assumption is that the fraction of heat pump "on" time is equal to the load divided by the steady-state capacity. An alternative would be to consider a "cyclic" heat pump capacity which is greater than the steady-state capacity by the additional amount of the electrical energy needed for cycling over the amount used to generate steady-state capacity. Thus fraction of "on" time based on steady-state capacity is:

$$f_{ss} = \frac{Q_L}{Q_{ss}} \quad 4.6.4$$

and the "on" time fraction based on cyclic capacity is

$$f_{cyc} = \frac{Q_L}{Q_{cyc}} = \frac{Q_L}{Q_{ss} + (W_{cyc} - W_{ss})} \quad 4.6.5$$

Upon substituting $W_{cyc} = \frac{Q_L}{COP_{cyc} f_{cyc}}$ and $W_{ss} = \frac{Q_L}{COP_{ss} f_{ss}}$ into equation 4.6.5 and rearranging terms, the ratio of "on" fractions can be determined.

$$\frac{f_{cyc}}{f_{ss}} = \frac{COP_{ss}}{COP_{cyc}} \left(\frac{COP_{cyc} - 1}{COP_{ss} - 1} \right) \text{ for } COP > 1 \quad 4.6.6$$

This ratio will be equal to 1.0 when $COP_{cyc} = COP_{ss}$ and less than 1.0 when $COP_{cyc} < COP_{ss}$. When Equation 4.6.6 is applied as an extension of the method utilizing Equation 4.6.3, it has the effect of minimizing the reduction in overall performance caused by cycling to a point where the total electrical energy consumed for the cyclic case

Table 4.6.2

Effect of Cycling Rate on COP-- $C_D = .25$

COP_{ss}	Q_L/Q_{ss}	COP_{cyc}	Q_{cyc}/Q_{ss}	f_{cyc}/f_{ss}
2.5	1.0	2.5	1.0	1.0
2.5	0.75	2.34	1.07	0.94
2.5	0.50	2.19	1.14	0.88
2.5	0.25	2.03	1.23	0.81
2.5	.0	1.88	1.33	0.75

in this derivation equals the energy consumed with zero degradation. An example is shown in Table 4.6.2. In actuality, this will never be the case and the real heat pump performance will be somewhere between the two cases.

4.7 Economic Considerations

It has been shown in Section 4.1 that the uncovered collector heat pump system achieves better performance than the conventional heat pump at a reasonably small collector area for space heating applications. Since there is additional capital expenditure required for any collector area increase in actual systems, it would be beneficial to estimate what this additional cost is in order to obtain a life-cycle return on investment. In this section a simple economic analysis to arrive at a "break-even" collector cost as a function of collector area will be made. The non-purchased fraction performance results for the uncovered collector and conventional heat pumps for Madison in Figure 4.1.1 will be used to determine energy savings for the uncovered collector system.

The economic analysis calculations are based on the P_1 , P_2 method outlined in [11]. The total life-cycle savings for this comparison is:

$$LCS = P_1 C_{F1} L (F_{np-s} - F_{np-c}) - P_2 (E_s - E_c) \quad 4.7.1$$

where F_{np-s} is the annual non-purchased fraction for the solar-assisted (uncovered collector) heat pump. F_{np-c} is the non-purchased fraction for the conventional heat pump, and $(E_s - E_c)$ is

the difference in initial system cost between the uncovered and conventional systems. The remaining terms are defined in the source [11] for this work. In order to determine a "break-even" point, when the life-cycle cost of energy savings of the uncovered system equals the additional initial investment in the system, the life-cycle savings in Equation 4.7.1 is set to zero. The terms in the equation can be rearranged to solve for the difference in system costs. Both sides are divided by the uncovered system collector area to arrive at a relation for the additional cost of the uncovered system as a function of its collector area.

$$\frac{(E_s - E_c)}{A_c} = \frac{P_1 C_{Fl} L}{P_2 A_c} (F_{np-s} - F_{np-c}) \quad 4.7.2$$

The value of P_1 was determined assuming a fuel inflation rate of 12% annually, a discount rate of 10% and a system life of 15 years, to be 15.5. P_2 was estimated at 0.6, which accounts for the total initial investment of the solar assisted heat pump after the 40% Federal tax credit has been applied. The two first year fuel costs considered in this study are 5¢/KWH and 10¢/KWH. Figure 4.7.1 shows the "break-even" additional system cost per square meter of collector area plotted against collector area for the uncovered collector system vs. the conventional heat pump. There are separate curves for each first year electrical fuel cost. The curves cross the additional system cost value of zero at about 12.5 m² of collector area. The annual "free energy" fractions of the two systems are

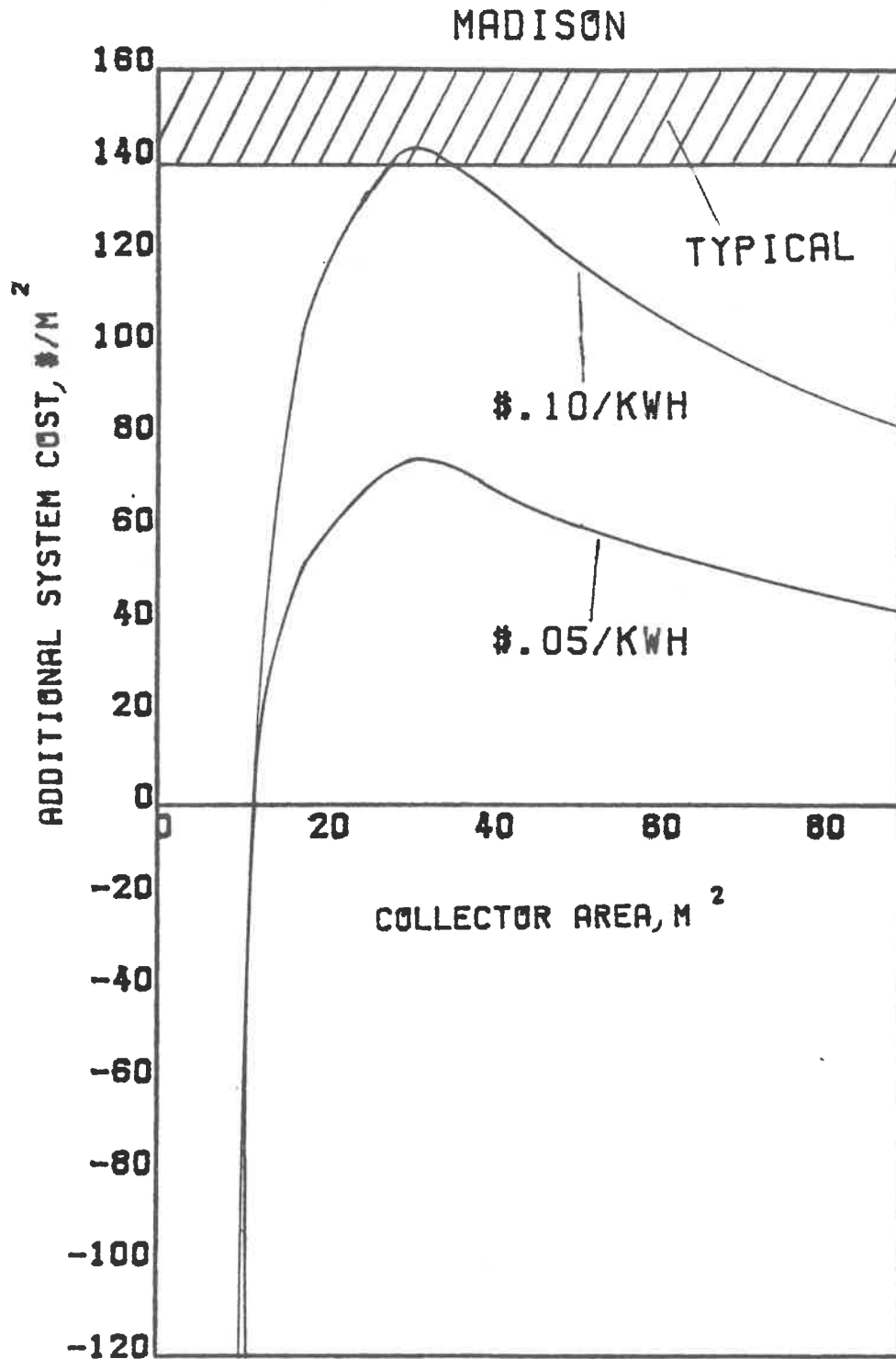


Figure 4.7.1 Additional Cost for Uncovered Collector System Collector Cost for Zero Life Cycle Savings vs. Conventional Heat Pump--Madison

equal at this point. The high slopes of the curves at collector areas less than 15 m^2 indicate that any increase in collector area will result in significant improvement in economic performance of the uncovered collector system.

Also shown in Figure 4.7.1 is the range of values for the initial installed collector cost for systems currently on the market. The economic performance results for $5\text{¢}/\text{KWH}$ indicate that the uncovered system has no economic advantage over the conventional heat pump at all collector areas. The "break-even" additional collector area cost for all collector areas is below the range of actual installed costs. At a fuel price of $10\text{¢}/\text{KWH}$ the uncovered collector system is also not economical. The curve enters the range of typical installed cost only at a collector area of approximately 30 m^2 .

The collector area size which is typically installed with the heat pump size used in this application (25.3 MJ) is approximately 17 m^2 . This is below the most economic collector area of 30 m^2 obtained from this study.

5.0 SPACE COOLING APPLICATIONS

The versatility and added value of the conventional heat pump lies in its ability to switch from heating to cooling upon demand from the room thermostat. The potential for using the refrigerant-filled collector heat pump in the cooling mode without altering the heating mode design or orientation of the collector will be discussed. The cooling performance might be expected to be reduced due to high condenser temperatures in this mode. Only the uncovered collector system is considered due to the low convection coefficient of the covered collector which results in its low heating performance relative to the uncovered collector system. During air conditioning the performance of the covered system will be low because of its inability to reject sufficient heat due to its low convection coefficient.

5.1 System Model for Cooling Performance

The model development of this system for cooling is similar to the model for heating operation. The basic collector equation (2.2.1) is used as a starting point to account for radiation and convection heat transfer. In the cooling mode, the collector plate is used as the refrigerant condenser. Refrigerant leaving the compressor is in a superheated state and a significant amount of the condenser heat exchanger is needed to desuperheat the refrigerant before condensation at constant temperature occurs. To insure that only liquid enters the expansion device, the refrigerant is subcooled. In conventional residential heat pump heat exchangers, the process

of desuperheating, condensation and subcooling is typically performed within the same refrigerant passage for condenser design simplicity. The same simplification can be extended to the operation of the collector/condenser. An extension of the heating mode model to the cooling mode allows the use of the refrigerant temperature as the plate temperature under the assumption that the collector efficiency factor, F' , is unity. The heat removal factor, F_R , is also assumed to be unity because most of the collector plate will be at the condensing temperature. The vapor phase will have high refrigerant velocities and high inside film coefficients. The average plate temperature, however, may not be equal to the saturation condensing temperature, due to the portion of the heat exchanger devoted to desuperheating (approximately 20%) and subcooling (0-10%). Due to the uncertainty in estimating the overall heat transfer coefficient between the refrigerant and the ambient air for the processes of desuperheating, condensing and subcooling the plate temperature can only be estimated. In the model, lower and upper bounds for average plate temperature as a function of condensing temperature are used. The lower bound is

$$T_p = T_c \quad 5.1.1$$

where T_c is the saturated condensing temperature. The upper bound for plate temperature is estimated as

$$T_p = 1.15 T_c - 1.0 \quad 5.1.2$$

Equation 5.1.2 was empirically derived from manufacturer's data for conventional heat pumps. The assumption made for this equation is that the plate temperature is equal to the average refrigerant temperature in the condenser/collector. The collector equation was used to generate the model:

$$Q_u = A_c F_R [(\tau\alpha) I_T - U_L (T_{f,i} - T_a)] \quad 2.2.1$$

Upon substitution of T_p for $T_{f,i}$, letting F_R equal unity and replacing Q_u with Q_{REJ} (heat rejected), the collector equation becomes:

$$Q_{REJ} = A_c [U_L (T_p - T_a) - (\tau\alpha) I_T] \quad 5.1.3$$

The remaining system equations for COP and total cooling capacity (Q_{COOL}) are empirically derived from manufacturer's data for conventional heat pumps.

$$COP = a_3 T_c + a_4 \quad 5.1.4$$

$$Q_{COOL} = (b_4 + b_3 T_c + b_6 T_c^2) Q_{NOM} \quad 5.1.5$$

The values assigned to these constants for cooling mode simulations are in Table 5.1.1. The maximum condensing temperature allowed in simulations was 80°C, above which the system will be turned off by the compressor overload switch.

The model for a conventional heat pump in the cooling mode includes Equations 5.1.4 and 5.1.5 in addition to the following approx-

Table 5.1.1

System Simulation Parameters—Cooling

Collector Properties

U_L (w/m ² C)	20.0	Heat Pump Size (MJ)	38.0
($\tau\alpha$)	0.80	Room Temperature (°C)	23
Collector Slope	60°, 90°	Collector Orientation	South
Collector Area (m ²)	10-100	Period of Simulation: June-Aug.	
Locations: Madison, WI and Albuquerque, NM			

Empirical Constants

a_3	-0.041/C
a_4	4.44
b_4	9.97 MJ/hr
b_5	0.16 MJ/C-hr
b_6	-0.0026 MJ/C ² -hr
c_3	16.7 C

imation for T_c :

$$T_c = T_a + c_3 \quad 5.1.6$$

where c_3 is an empirical constant. The component written for use with TRNSYS for space cooling calculations is in Appendix B.

5.2 TRNSYS Simulation Results

Performance results were obtained with TRNSYS simulations using the same building model employed in the capacitance effects of heating discussed in Section 4.5. The cooling load is dependent on solar heat gain and thermal capacitance of the building in these simulations. Table 5.1.1 contains the parameters used for cooling performance calculations.

Figures 5.2.1 and 5.2.2 show the potential range of overall COP as a function of collector area for Madison and Albuquerque during June through August. The simulations show that the upper bound for plate temperature also corresponds to the upper limit for cooling performance. This is due to the fact that the upper bound plate temperature case allows more heat to be rejected by the plate at the same condensing temperature as the lower bound plate temperature situation. At the same ambient condition the upper bound plate temperature situation will be able to reject nearly the same amount of heat to the ambient at a lower condenser temperature than the lower bound case. The lower condenser temperature allows the upper bound case to be more efficient.

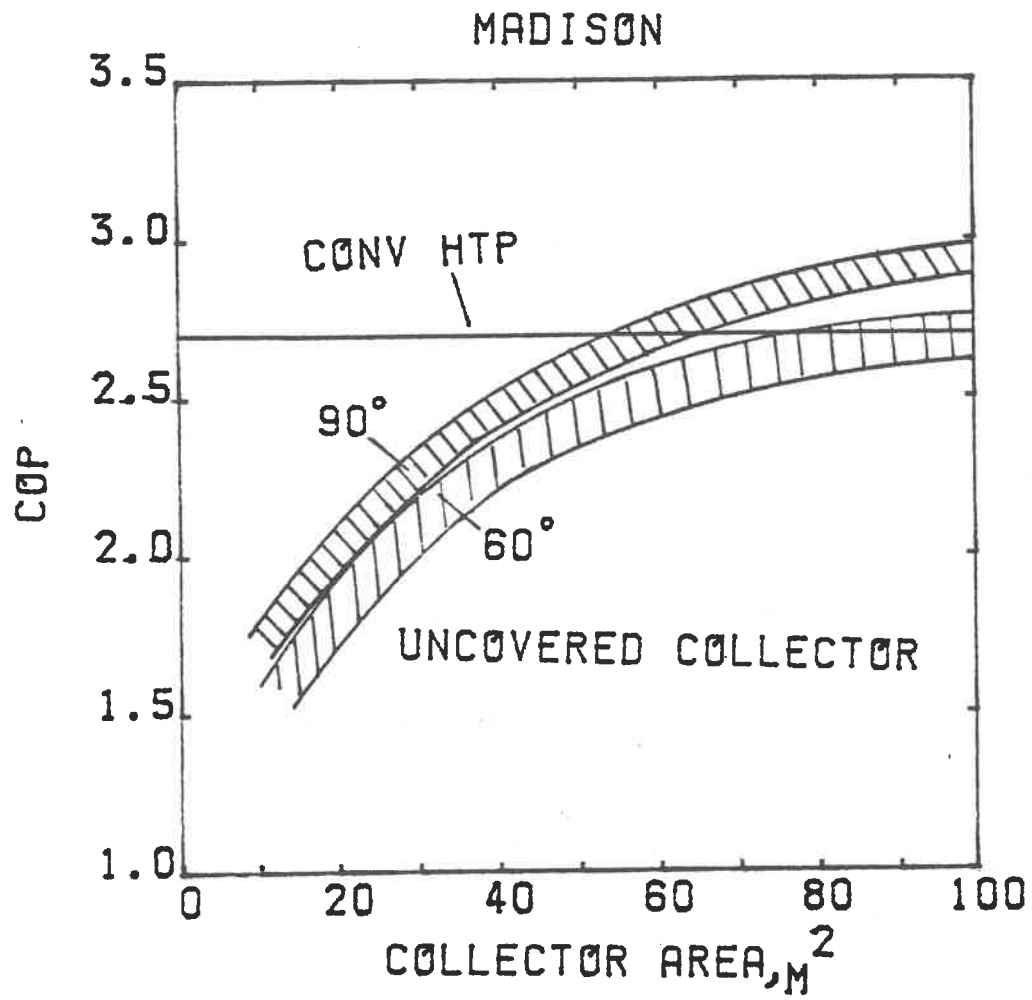


Figure 5.2.1 Overall Cooling COP--Madison

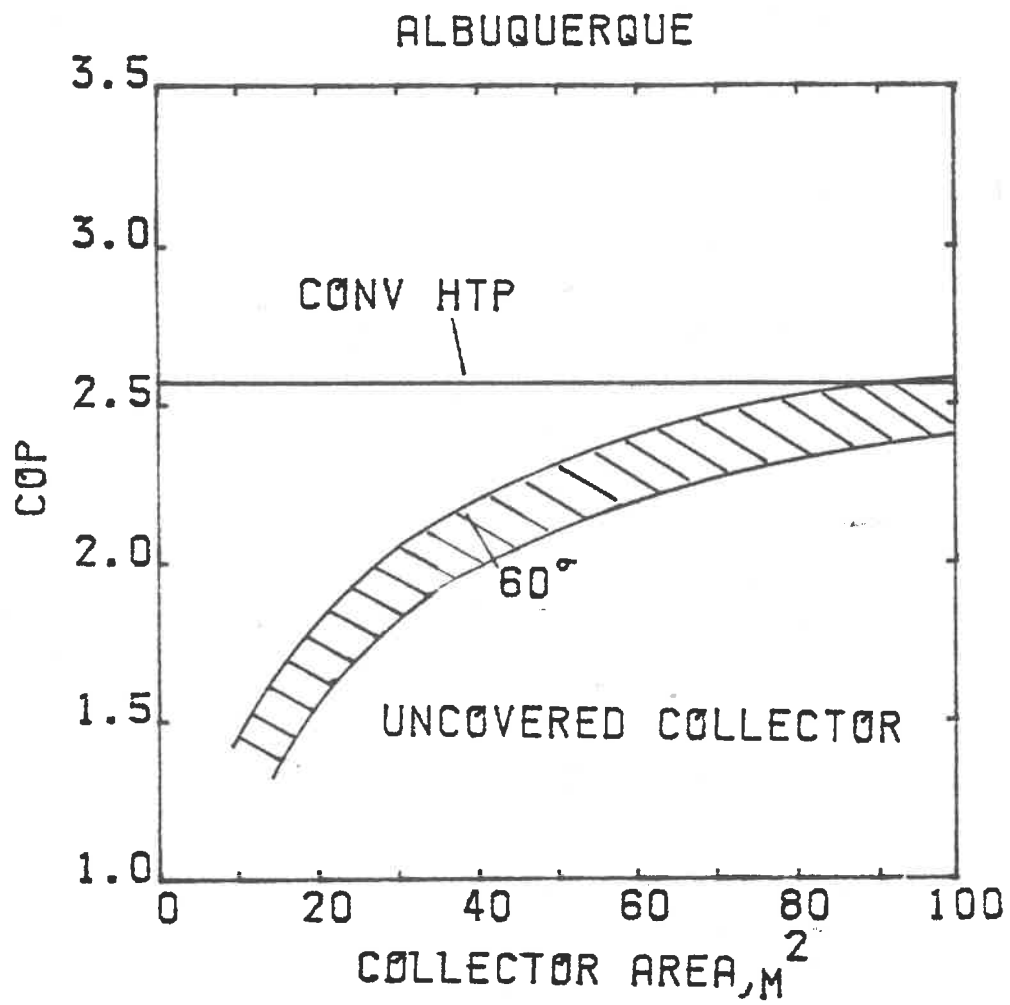


Figure 5.2.2 Overall Cooling COP--Albuquerque

Also shown in both Figures is a horizontal line representing conventional unit cooling performance during the same period. These results show that the performance of collector/condenser systems is poorer at small collector areas. In Madison, the collector system uses a minimum of 24% and 14% more electrical energy than the conventional heat pump at 30 m² and 60° and 90° collector slope, respectively. In Albuquerque the 30 m² collector system at 60° tilt requires at least 27% more electrical input than the conventional system to meet the load. The cooling performance for uncovered collector heat pumps is substantially worse than that of conventional heat pumps in the cooling mode. This detracts from any benefits gained in the heating performance.

6.0 HIGH TEMPERATURE PROCESS WATER HEATING APPLICATIONS

Another application for refrigerant-filled collector heat pumps is high temperature process water heating for commercial and industrial use. The heat pump has the ability to upgrade low grade energy to the required temperature for delivery on a continuous basis. The additional benefit of low grade solar energy on the collector/evaporator during daytime periods with process heat loads will further enhance the performance of the heat pump by increasing its efficiency and capacity. Since the load is continuous and usually predictable in process heat applications, the nominal capacity of the heat pump can be picked to match the load. Cycling losses can be reduced by a considerable amount in these applications and energy storage has great potential. In this Chapter, a 12 hour, daytime and continuous load is used for performance analysis. The sol-air temperature bin method outlined in Chapter 3 was used in all evaluations. The same heat pump model as was used in the space heating applications reported in Chapter 4 was utilized in this application. It is assumed that the system would be designed to operate efficiently at the high condensing temperatures required in process water heating.

6.1 Base Case Process Heat Applications

Table 6.1.1 lists the appropriate parameters for the four system types compared in these simulations. F-chart [15] was used to generate conventional solar system results.

Table 6.1.1

System Simulation Parameters--Process Heating

<u>System Type</u>	$F_R - U_L$ (W/m^2C)	$F_R(\tau\alpha)$	<u>Collector Slope</u>	<u>Collector Area (m^2)</u>	<u>Heat Pump Size (MJ)</u>
Covered Collector	3.0	.72	60°	0-100	25.3
Uncovered Collector	20.0	.80	60°	0-100	25.3
Conventional Heat Pump	-	-	-	-	25.3
Conventional Solar (Liquid System)	4.22	.70	60°	0-100	-
Collector Plate Emissivity					0.1
Load Requirement--24 MJ/hr, 12 hrs/day (6 A.M.-6 P.M.), 7 days/week, 52 weeks/year					
Storage Capacity for Conventional Solar (KJ/m^2C)					350.0
Minimum Delivery Temperature ($^{\circ}C$)					43
Collector Orientation					South Facing
Locations: Madison, WI and Albuquerque, NM					

For larger heating loads the heat pump and collector area sizes may be scaled appropriately to obtain corresponding results. The collector tilt angle used was 60° instead of the angle-equal-latitude recommendation for year-round heating loads of this type with conventional solar collectors. During the winter months, convection by the colder air causes heat pump performance to be lower than during summer months. The additional low-grade energy source of the solar radiation with the steeper sloped collector is important to heat pump performance during the colder months and less important during the warmer months when convection heat transfer is adequate.

Figures 6.1.1 and 6.1.2 show the simulation results for Madison and Albuquerque. The yearly non-purchased fraction is plotted against collector area for both locations. In this application, the uncovered collector system achieves superior performance over the other two heat pump systems at a small collector area, approximately 12 m^2 in both Madison and Albuquerque. The covered collector system performance improves relative to the other systems as compared to the space heating application shown in Figures 4.1.1 and 4.1.2. The yearly non-purchased-fraction for the covered system equals that of the conventional heat pump at 30 m^2 collector area, while in the space heating application the values are the same near a collector area of 55 m^2 for both locations. The conventional solar system has better performance in Albuquerque, where solar radiation levels are higher and the advantage of storage is utilized more.

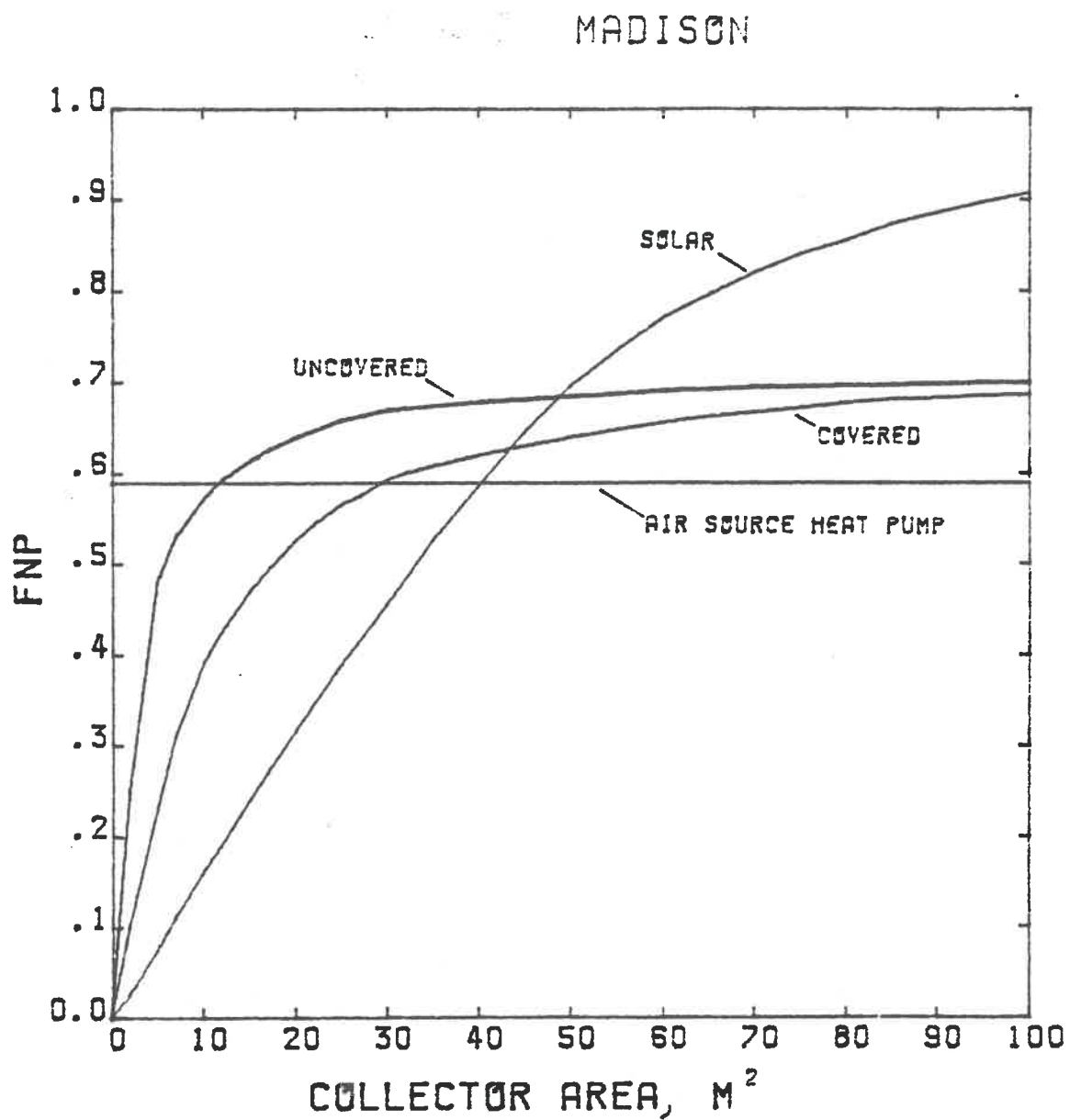


Figure 6.1.1 Base Case Process Heating Performance--Madison

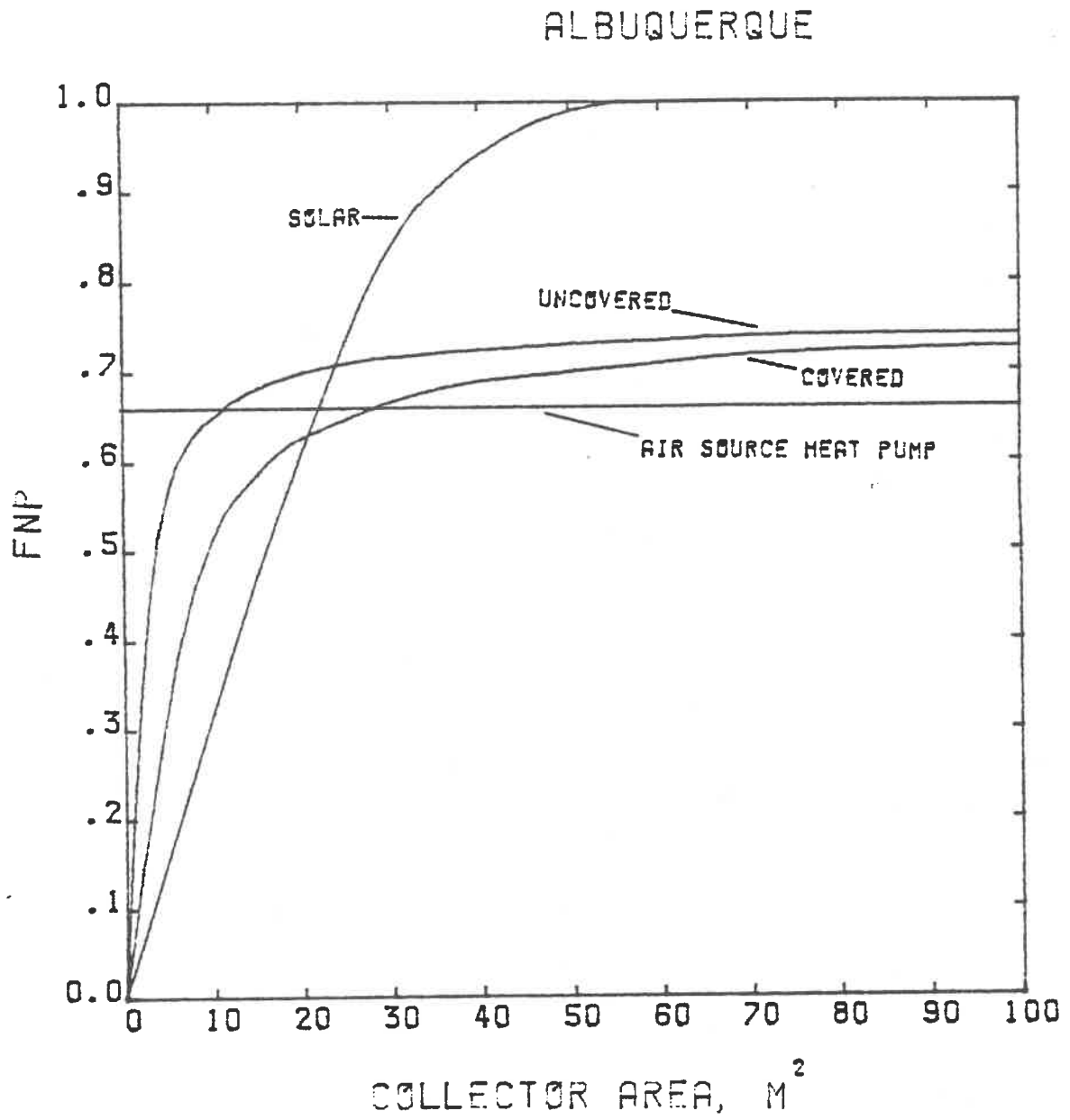


Figure 6.1.2 Base Case Process Heating Performance--Albuquerque

Although there is some relative performance improvement of the covered collector system in this daytime application, it is still significantly less than the uncovered collector system. Apparently, convection is more important than incident radiation to the solar-aided heat pumps without energy storage even in this daytime application. The uncovered system has better performance when convection is the primary low-grade energy source. When all of the available radiation is removed from the uncovered collector system during a yearly evaluation, the performance is reduced by the amount shown in Figure 6.1.3. The difference between the results with radiation and the results without radiation is approximately 8% at small collector areas and 5% at large collector areas. The overall non-purchased fraction for the uncovered system without radiation exceeds that of the conventional heat pump at collector areas greater than 25 m^2 , indicating that the uncovered collector heat pump system will be able to perform adequately with no incident radiation.

The ability of the collector heat pumps to deliver energy to meet the load is exhibited in Figures 6.1.4 and 6.1.5. The horizontal lines correspond to the total yearly process heat load. The uncovered collector heat pump system is able to meet over 90% of load at 10 m^2 collector area while a 200% larger collector area for the covered collector system, 30 m^2 , is needed to deliver at least 90% of the load.

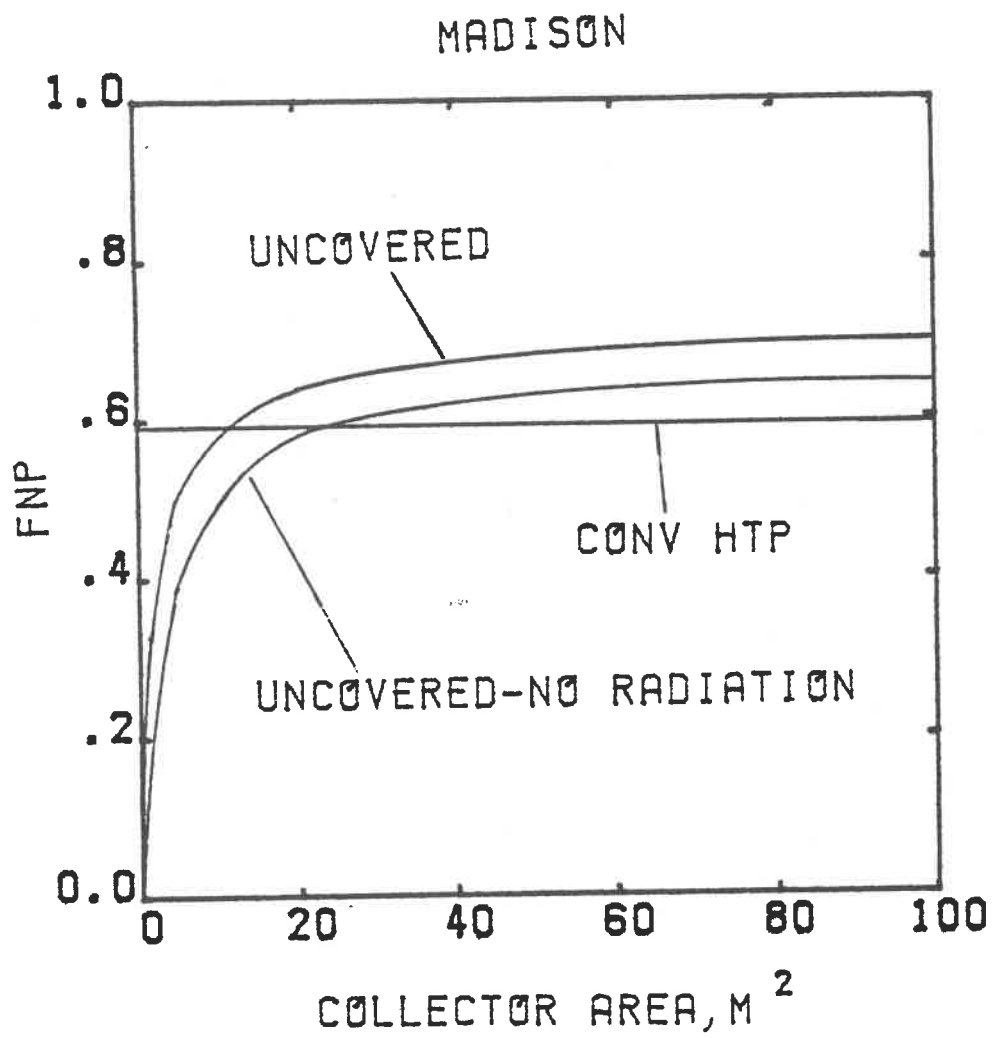


Figure 6.1.3 Effect of Shading Incident Radiation on Uncovered Collector Process Heat Performance--Madison

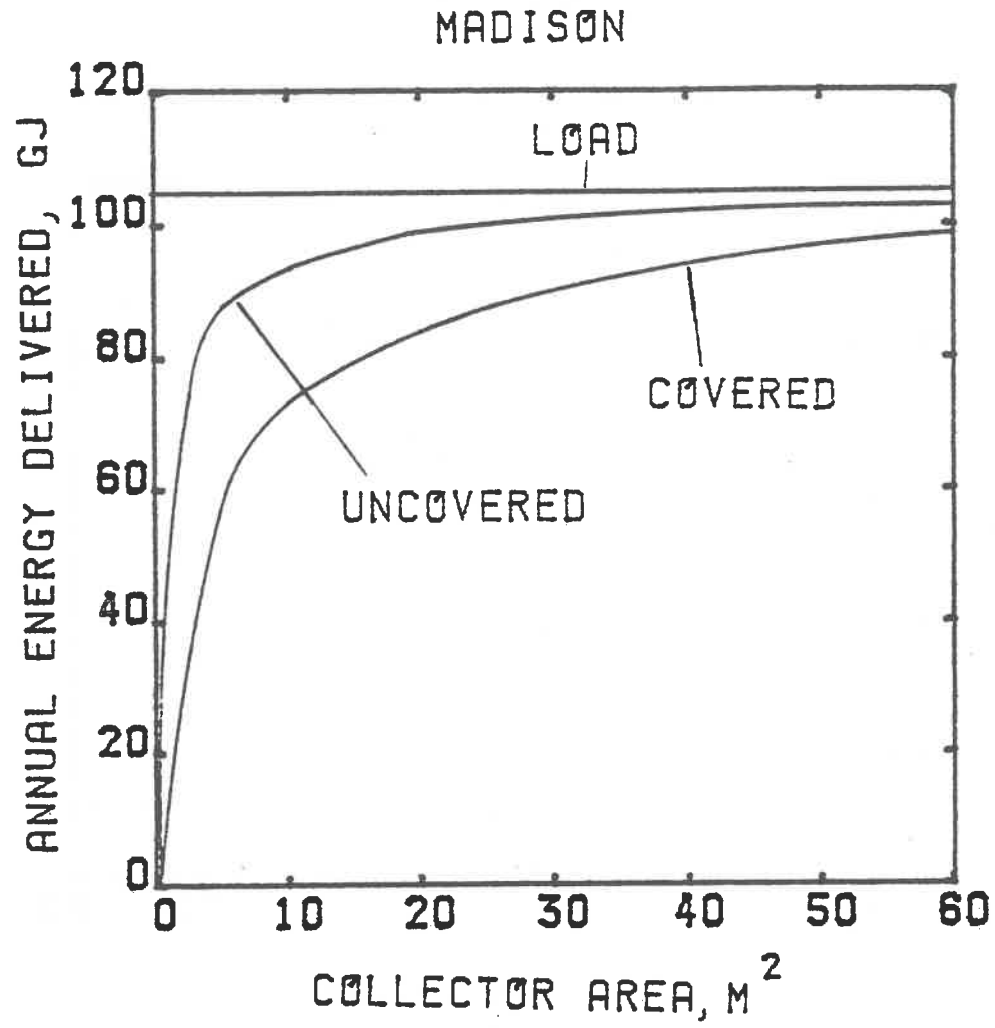


Figure 6.1.4 Energy Delivered to Load by Collector Heat Pumps--
Madison

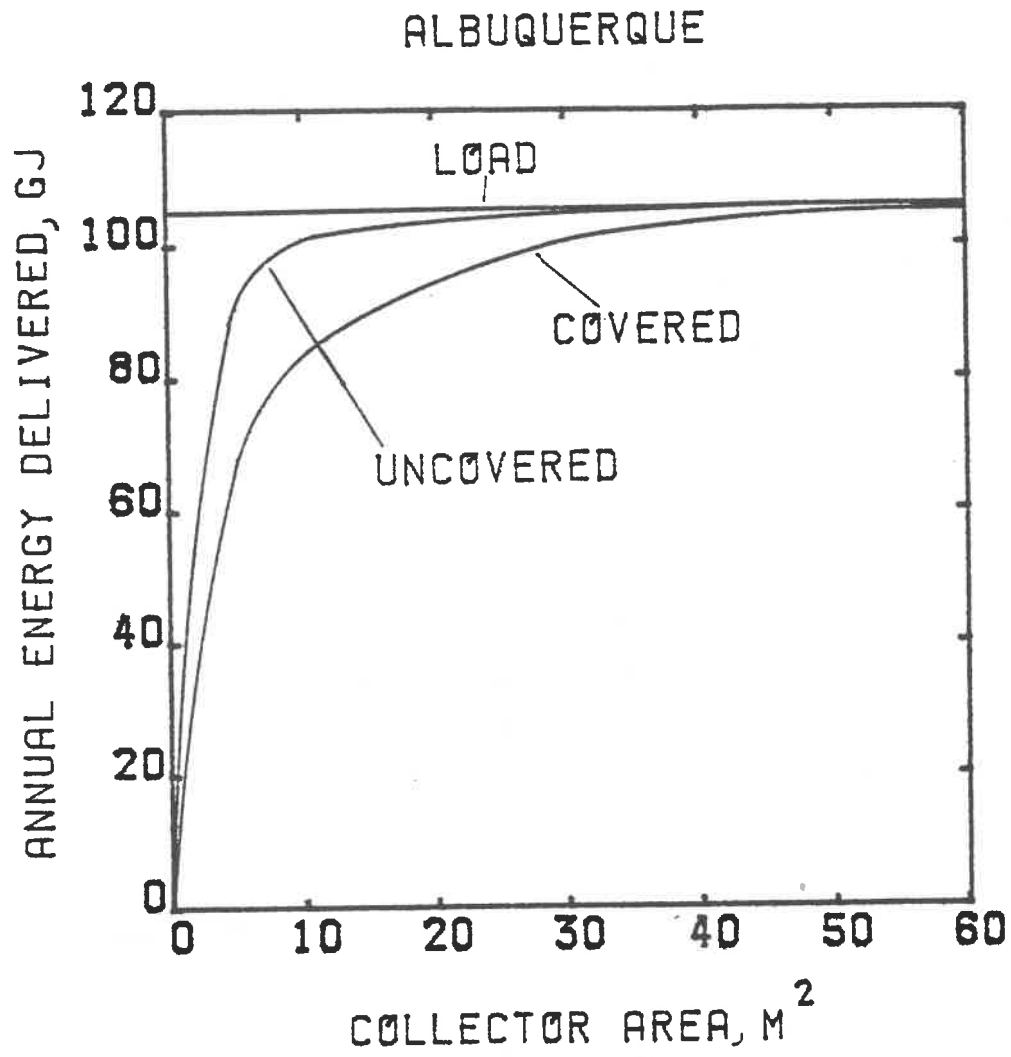


Figure 6.1.5 Energy Delivered to Load by Collector Heat Pumps--
Albuquerque

6.2 Collector Control

The possibility of increasing yearly performance of refrigerant-filled collector heat pumps by combining the uncovered and covered collector options into one system has been outlined and discussed in Section 4.2 for space heating applications. Control of collector performance results for the Madison process heat evaluation are shown in Figure 6.2.1. The overall performance improvement with this design is also slight, as it was in the space heating application. Although the fraction of hours of covered mode usage was increased due to the elimination of operation during night-time hours, the overall effect was not significant.

A major factor which restrains the improvement of overall performance with the collector performance control application is the constancy of hourly heat load. The restriction of the load rate limits the amount of "free" energy transferred from the collector to the load by the heat pump. Even though load is constant in this application, heat pump capacity increases with higher COP and higher levels of low-grade energy. Heat pump "on" time is thus reduced, limiting the utilizability of increased performance

6.3 Performance Upper Bound with Storage

In this section the method for obtaining upper bound performance with energy storage is applied to the daytime process water heat application. The general procedure and discussion for space heating applications is in Section 4.4. Results for process heating are obtained in the same manner as for space heating. Heat pump

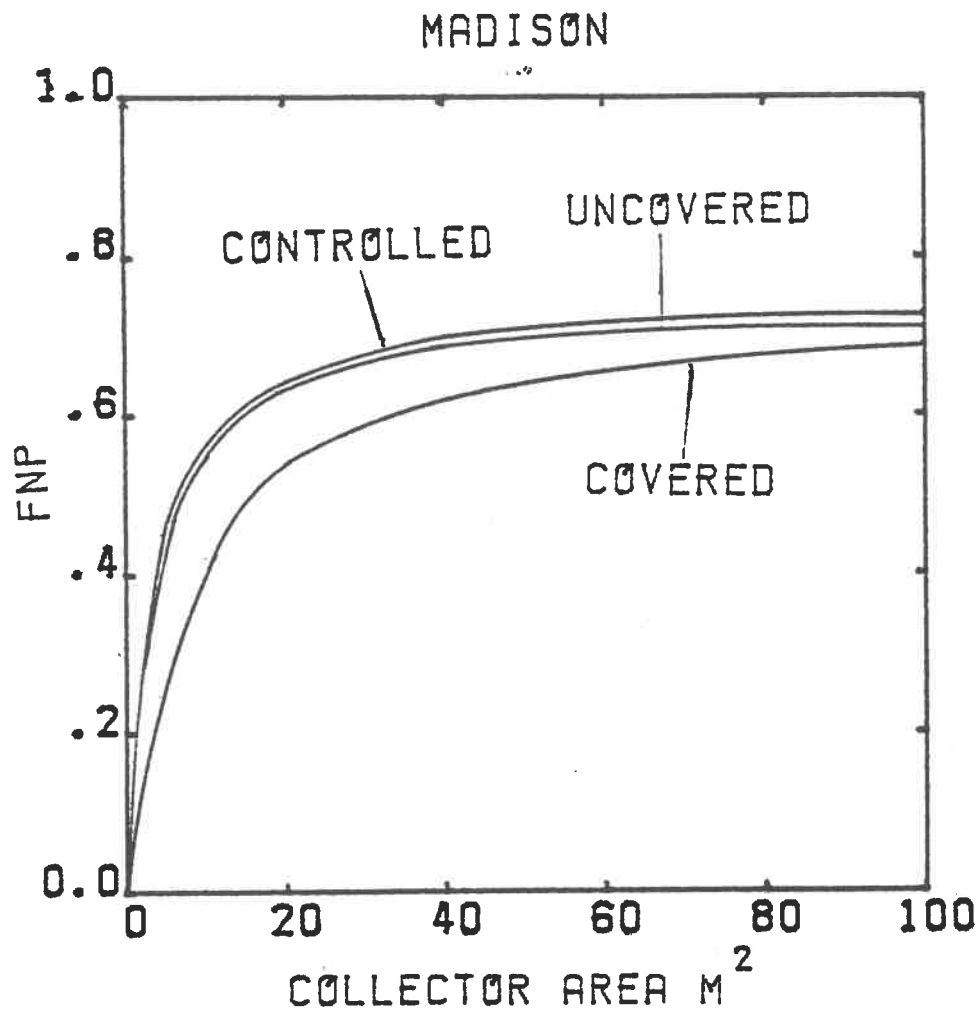


Figure 6.2.1 Effect of Collector Performance Control for Process Heating Load--Madison

operation is allowed only during the 12 hour daytime period when there is a load. Allowing operation of the heat pump outside of this time period has no effect on the upper bound performance for the process heat application. All of the hours with the high solar air temperatures and system COP occur during the day.

The yearly results for the uncovered and covered collector systems in Madison are indicated in Figure 6.3.1. As expected the greatest performance increase is seen with the covered system. In fact the covered system upper bound performance exceeds the uncovered system upper bound performance at collector areas greater than 35 m^2 , which is a reasonably small area for the heat pump size (25.3 MJ) used in the simulations. Performance improvement is not as great for the process heat system as for the space heating application. The primary reason for this is the maximum COP restriction. With a maximum allowable COP at 4.0, the highest non-purchased fraction in any hour (or bin) is 0.75. The even year-round distribution of the load allows more daytime summer hours and less winter hours to be coincident with process heat loads. The heat pump operates at maximum efficiency during most of the hours used for upper bound storage, hence the non-purchased fraction approaches the maximum value of 0.75 for both systems. The actual performance with storage will be somewhere between the no-storage and upper bound results.

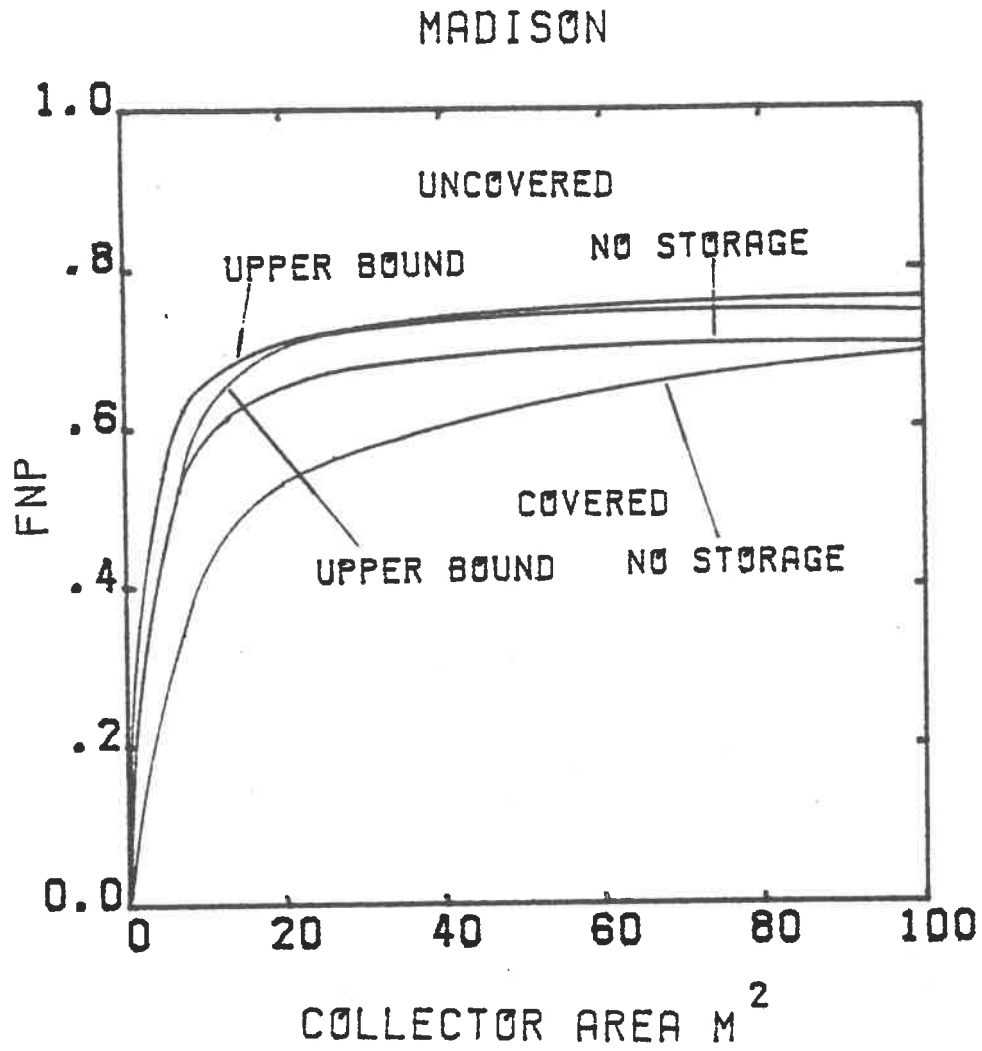


Figure 6.3.1 Upper Bound with Storage for Process Heat Load--
Madison

7.0 CONCLUSIONS

A computer simulation model and the sol-air temperature bin method for predicting the seasonal performance of refrigerant-filled collector heat pumps has been developed. The bin method is suitable for space heating loads for which thermal storage or capacitance is not a major factor and constant process heat loads. The method is simpler and faster than transient simulation routines such as TRNSYS, but requires access to a mainframe computer.

The performance evaluations for space heating and process water heating show that uncovered collector heat pumps have a performance advantage over conventional heat pumps over a wide range of collector areas and have consistent performance superiority over covered collector heat pump systems. These result comparisons held for all of the locations studied. The locations included Madison, WI, Albuquerque, NM, Seattle, WA and New York, NY. The uncovered performed better than the covered system in Madison, which is considered to have a cold climate. This is in disagreement with the conclusion reached by Krakow and Lin [7]: "For cold climates it does not appear practical to use a solar-source heat pump to justify using unglazed collectors..... Solar-source heat pump systems with glazed collectors are better suited for cold climates." The performance of the covered ("glazed") collector heat pump systems without storage is generally inferior to the other systems. Due to the nighttime operation which occurs with a heat pump without storage in space heating applications, convection is the primary means of energy transfer to the

evaporator/collector in these systems. Overall heating performance increases at higher collector convection heat transfer coefficient values. However, incremental increases in convection coefficient result in less increase in performance.

Altering the maximum attainable COP to exceed a practical limit will not significantly change the seasonal performance of the system. A slight improvement occurs with the covered collector heat pump, which is more able to take advantage of high levels of incident radiation. Increasing the average steady-state system COP improves the performance of the uncovered system more than the covered system.

For a given collector area the covered collector system experiences greater COP increases with decreasing nominal heat pump size than the uncovered system. Small collector areas and large heat pump compressor sizes work well for uncovered collector systems while large collector areas and small heat pump compressor sizes are more suitable for covered systems. 60° is the preferred collector slope for heating applications with these systems.

The design of a system in which collector performance can be controlled to utilize the covered collector mode or a forced convection mode similar to uncovered collector performance results in little performance improvement over the uncovered collector system in heating applications. Most of the load occurs during periods of low radiation when the uncovered mode would be used.

Performance of collector heat pump systems can be improved considerably with energy storage. In applications studied in this re-

port the nonpurchased fraction may have a potential 20% increase for uncovered collector systems and 50% increase for covered collector systems. Simulations using only building thermal capacitance as storage show substantial performance improvement over zero-storage applications.

Performance degradation due to compressor cycling and start-up transients downgrades overall performance of the heat pump system. Overall COP's suffer significantly if the collector area-heat pump size combination is large enough to cause persistent compressor cycling. The effect of degradation slightly reduces the relative performance differences between different heat pump types. In general there is no relative difference in performance reduction due to degradation between the two types of collector heat pumps and conventional heat pumps.

An economic analysis of the uncovered collector system based on its performance in Madison shows that the attractiveness of such a system relative to a conventional heat pump is reduced. The results show that the uncovered system is uneconomical, based on the selection of appropriate economic parameters.

The cooling performance of refrigerant-filled collector heat pumps is low compared to conventional heat pumps in the cooling mode. This suggests that some detraction in year-round utility exists with collector heat pump systems.

In daytime process heating applications, the uncovered system achieves superior performance at a small collector area, as it did

in the space heating applications. The performance of the covered collector heat pump system improves relative to the uncovered system in the process heat applications. Both types of collector heat pumps are able to meet 90% of the annual load at a reasonably small collector area. This may be one reason why efforts to improve system performance, such as controlling collector performance and energy storage do not benefit the system in process heat applications as much as they could in space heating applications.

APPENDIX A: DESIGN METHOD PROGRAMS

A.1 Sol-Air Temperature Bin Generation Method

A.2 Performance Simulation--Space and Process Water Heating

A.1 Sol-Air Temperature Bin Generation Method

```

C PROGRAM BINS
  REAL KT
  INTEGER BIN(22,100)
  DIMENSION TMIN(12),TA(24),IH(24),ITA(24)
C READ MINIMUM MONTHLY AMBIENT TEMPERATURES
  READ(*,*)(TMIN(I),I=1,12)
C READ SYSTEM CHARACTERISTICS
  READ(*,*)BETA,PHI,UL,ALPHA,TAU,ICOV,HR1,HR2,JP,NTSA
C BETA = COLLECTOR SLOPE (DEGREES)
C (COLLECTOR IS SOUTH-FACING)
C PHI = LOCAL LATITUDE (DEGREES)
C UL = COLLECTOR LOSS COEFFICIENT
C TAU = COVER TRANSMITTANCE (UNITY IF UNCOVERED)
C ICOV = 1 IF COVERED, 0 IF UNCOVERED
C HR1 = FIRST HOUR OF DAY FOR BIN DATA
C HR2 = LAST HOUR OF DAY FOR BIN DATA
C JP = 1 IF PRINTOUT IS TO BE SUPPRESSED
C NTSA = NUMBER OF SOL-AIR TEMPERATURE BINS
C
C CONVERT DEGREES TO RADIANS
  BETA=BETA/57.296
  PHI=PHI/57.296
  IF(ICOV.EQ.0)TAU=1.
  N=0
  J=1
C RESET BINS TO ZERO
51 IOBU=0
C INCREMENT AMBIENT TEMP BINS
  DO 55 I=1,22
C INCREMENT SOL-AIR TEMP BINS
  DO 55 J=1,NTSA
  BIN(I,J)=0
55 CONTINUE
  IF(IDAY.EQ.1)GO TO 91
60 CONTINUE
C READ HOURLY WEATHER DATA FROM TMY WEATHER TAPE FOR 24 HOURS
  DO 90 I=1,24
  READ(*,99,END=700)IMO,IDAY,IH(I),ITA(I)
99 FORMAT(10X,I2,1X,I2,9X,I4,1X,I4)
  TA(I)=ITA(I)/10.
90 CONTINUE
  IF(.J.LT.IMO)GO TO 600
91 J=IMO
  N=N+1
C CALCULATE DECLINATION ANGLE
  DEL=.4093*(SIN(.01721*(284.+N)))
  DO 100 I=HR1,HR2
C TITO = TOTAL INCIDENT RADIATION ON COLLECTOR SURFACE
  TITO=0.
C DETERMINE INCIDENT RADIATION ON COLLECTOR SURFACE
  IF(IH(I).EQ.0.)GO TO 75
56 CONTINUE
  W2=(15*I-180.)/57.296
  W1=(15*I-195.)/57.296
  WS=ACOS(-TAN(DEL)*TAN(PHI))
  WSR=-WS
  IF(I.GT.12.AND.WS.LT.W2)W2=WS
  IF(I.LT.12.AND.WSR.GT.W1)W1=WSR
  W=(W1+W2)/2.
  D=(W2-W1)/.2618
C TIO = TOTAL EXTRA-TERRESTRIAL RADIATION
  TIO=(12.*3.6/3.14159)*1353.*(1+.033*(COS(360.*N/365.
  C/57.296)))*(COS(PHI)*COS(DEL))*(SIN(W2)-SIN(W1))+
  C((W2-W1)*SIN(PHI)*SIN(DEL))
  TIO=TIO/D

```

```

      KT=FLOAT(IH(I))/TIO
      IF(KT.LE.1.)GO TO 57
      IH(I)=FLOAT(IH(I)/KT)
      KT=1.
57  CONTINUE
      IF(KT.LT..8)GO TO 61
C   TID = DIFFUSE RADIATION
      TID=.165*IH(I)
      GO TO 70
61  IF(KT.LT..22)GO TO 65
      TID=(.7511-.1604*KT+4.388*KT**2-16.638*KT**3
      C+12.336*KT**4)*IH(I)
      GO TO 70
65  TID=(1.-.09*KT)*IH(I)
70  CONTINUE
C   TIR = BEAM RADIATION
      TIR=IH(I)-TID
C   RB = RATIO OF BEAM RADIATION ON TILTED SURFACE TO BEAM
C   RADIATION ON A HORIZONTAL SURFACE
      RB=(COS(PHI-BETA)*COS(DEL)*COS(W)+SIN(PHI-BETA)*SIN(DEL))
      C/(COS(PHI)*COS(DEL)*COS(W)+SIN(PHI)*SIN(DEL))
      TITO=TIR*RB+TID*(1.+COS(BETA))/2.42*IH(I)*(1.-COS(BETA))/2.
75  CONTINUE
C   DETERMINE SOL-AIR TEMPERATURE
      TSA=TA(I)+TIT*ALPHA*TAU/UL/3.6
C   DETERMINE BIN LOCATION
      IBTA=IFIX((TA(I)-TMIN(J))/2.41)
      IBTSA=IFIX((TSA-TMIN(J))/2.41)
      IF(IBTA.GT.0.AND.IBTA.LT.23)GO TO 80
C   IOBO = NUMBER OF HOURS OUT OF ROUNDS
      IOBO=IOBO+1
      GO TO 100
80  CONTINUE
      IF(IBTSA.GT.NTSA)IBTSA=NTSA
85  BIN(IBTA,IBTSA)=BIN(IBTA,IBTSA)+1
100 CONTINUE
      GO TO 60
600 CONTINUE
      IF(JP.EQ.1)GO TO 605
C   PRINT OUT BIN DATA FOR MONTH
      WRITE(*,800)J,IOBO
      WRITE(*,801)((BIN(I,J),J=1,22),J=1,NTSA)
C   WRITE BIN DATA INTO STORAGE FILE FOR LATER USE
605  WRITE(7,802)((BIN(I,J),I=1,22),J=1,NTSA)
      IF(IDAY.EQ.1)GO TO 51
      GO TO 51
700 CONTINUE
      IF(IMO.EQ.12.AND.IDAY.EQ.31)GO TO 605
800  FORMAT('1',' MONTH NUMBER = ',I3,
      C' NUMBER OUT OF ROUNDS = ',I5)
801  FORMAT(22I5)
802  FORMAT(22(1X,I3))
      STOP
      END

```

A.2 Performance Simulation--Space and Process Water Heating

```

C PROGRAM KINPER
  DEFINE FILE 7(SDF,,132)
  DIMENSION TMIN(12),IBINS(22,100),TE(3),F(3),INO(12)
C READ SYSTEM PARAMETERS
C QHNM = NOMINAL HEAT PUMP SIZE (TONS)
C A1,A2 AND A3 ARE HEAT PUMP CAPACITY PARAMETERS
C B1 AND B2 ARE HEAT PUMP COP PARAMETERS
C AC = COLLECTOR AREA
C UL1 = UNCOVERED COLLECTOR CONVECTION COEFFICIENT
C UL2 = COVERED COLLECTOR LOSS COEFFICIENT
C (LEAVE ZERO IF COVERED COLLECTOR RESULTS ARE NOT DESIRED)
C TAU2 = COVER TRANSMITTANCE FOR COVERED COLLECTOR
C COPM = MAXIMUM ALLOWABLE COP
  READ(*,*)QHNM,A1,A2,B1,B2,B3,AC,UL1,UL2,TAU2,COPM
  READ(*,*)UA,ILOAD,QLOAD,NTSA,N,NS,I1,12
C UA = BUILDING HEAT TRANSFER COEFFICIENT
C ILOAD = CONSTANT LOAD FLAG (ILOAD = 1 CORRESPONDS TO CONSTANT LOAD)
C QLOAD = VALUE OF CONSTANT HOURLY LOAD (M.J)
C NTSA = NUMBER OF SOL-AIR TEMPERATURE BINS
C N = NUMBER OF MONTHS IN SIMULATION
C N = NUMBER OF MONTHS IN SIMULATION
C
C READ MONTH NUMBERS
  READ(*,*)(INO(I),I=1,N)
C READ MINIMUM AMBIENT TEMPERATURES CORRESPONDING TO EACH MONTH
  READ(*,*)(TMIN(I),I=1,N)
C INCREMENT BY MONTHS
  KK=1
  DO 150 K=1,12
C READ THE NUMBER OF HOURS IN EACH BIN
  READ(7,*)((IBINS(I,J),I=1,22),J=1,NTSA)
  IF(INO(KK).NE.K)GO TO 150
  DO 100 I=1,22
    TAMB=TMIN(KK)+2.*I-1.
C DETERMINE HEATING LOAD
    IF(ILOAD.EQ.1)GO TO 20
    QLOAD=UA*(20.-TAMB)
    IF(QLOAD.LE.0.)GO TO 100
  20 CONTINUE
C CONVERT BIN LOCATION INTO SOL-AIR TEMP FOR UNCOVERED COLLECTOR
  DO 100 J=1,NTSA
    IF(IBINS(I,J).EQ.0.)GO TO 100
    TSA=TMIN(KK)+2.*J-1.
    UL=UL1
C CONVERT SOL-AIR TEMP FOR UNCOVERED COLLECTOR INTO SOL-AIR TEMP
C FOR COVERED COLLECTOR IF COVERED COLLECTOR SPECIFIED
    IF(UL2.EQ.0.)GO TO 40
    TSA=(TSA-TAMB)*TAU2*UL1/UL2+TAMB
    UL=UL2
C DETERMINE TEVAP FOR HEAT PUMP BALANCE POINT
  40 QHNP=0.
    TE(2)=TAMB
  55 TE(1)=TE(2)-.5
    TE(3)=TE(2)+.5
    DO 60 N=1,3
C COLLECTOR EQUATION
    QL=AC*UL*(TSA-TE(N))*0.036
C HEAT PUMP PERFORMANCE
    COP=A1*TE(N)+A2
    QH=(B1+B2*TE(N)+B3*TE(N)**2)*QHNM
    W=QH/COP
    F(N)=QL/W+1.-COP
    IF(ABS(F(N)).GE..01)GO TO 60
    IF(COP.LT.COPM)GO TO 58
    QH=QH*COPM/COP

```

```

COP=COPM
58 QHTP=QH
   QELE=QH/COP
60 CONTINUE
   IF(QHTP.GT.0.)GO TO 65
C  RESET TEVAP FOR NEWTON'S ITERATION
   TE(2)=TE(2)-F(2)/(F(3)-F(1))
   GO TO 55
65 CONTINUE
C  SUMMARIZE HOURLY RESULTS
   QAUX=0.
   IF(QLOAD.GT.QHTP)QAUX=QLOAD-QHTP
   TO=QLOAD/(QHTP+QAUX)
   QHTP=TO*QHTP
   QELE=TO*QELE
C  ADD HOURLY TOTAL INTO MONTHLY RESULTS
   QMHTP=QMHTP+QHTP*IBINS(I,J)
   QMLD=QMLD+QLOAD*IBINS(I,J)
   QMW=QMW+QELE*IBINS(I,J)
   QMX=QMX+QAUX*IBINS(I,J)
100 CONTINUE
   TCOP=QMHTP/QMW
   FNP=1.-(QMW+QMX)/QMLD
C  WRITE MONTHLY RESULTS
   WRITE(*,200)K
   WRITE(*,201)
   WRITE(*,202)QMLD,QMHTP,QMW,QMX,TCOP,FNP,ITE,ITO
   TLD=TLD+QMLD
   TW=TW+QMW
   TX=TX+QMX
   THP=THP+QMHTP
   IF(K.NE.12)GO TO 110
   SCOP=THP/TW
   TFNP=1.-(TW+TX)/TLD
C  WRITE YEARLY TOTALS
   WRITE(*,203)
   WRITE(*,201)
   WRITE(*,202)TLD,THP,TW,TX,SCOP,TFNP,ITTE,ITTO
C  RESET MONTHLY TOTALS
110 QMLD=0.
   QMHTP=0.
   QMW=0.
   QMX=0.
   KK=KK+1
150 CONTINUE
200 FORMAT(' MONTH NUMRER = ',I3)
201 FORMAT(6X,'QLOAD',7X,'QHTP',7X,'QHTP',7X,'QAUX',7X,'COP',
   C7X,'FNP')
202 FORMAT(5X,F7.0,4X,F7.0,4X,F7.0,4X,F7.0,6X,F4.2,7X,F4.3,
   C4X,I4,4X,I4)
203 FORMAT(' SEASONAL TOTALS ')
   STOP
   END

```

APPENDIX B: COOLING MODEL TRNSYS COMPONENT

```

C COOLING PERFORMANCE ROUTINE
  SUBROUTINE TYPE21(TIME,XIN,OUT,T,DTDT,PAR,INFO)
  DIMENSION PAR(20),OUT(4),XIN(10),TC(3),F(3)
  IMODE=PAR(1)
  QNDM=PAR(2)
  A1=PAR(3)
  A2=PAR(4)
  B1=PAR(5)
  B2=PAR(6)
  B3=PAR(7)
  TAU=PAR(8)
  ALPHA=PAR(9)
  UL=PAR(10)
  AC=PAR(11)
  COPM=PAR(12)
  CAPAC=PAR(13)
  TSET=PAR(14)
  TAMB=XIN(1)
  GT=XIN(2)
  ISWCH=XIN(3)
  TROOM=XIN(4)
  QCOOL=0.
  QELE=0.
C ISWCH INDICATES WHETHER UNIT IS ON
  IF(ISWCH.NE.1)GO TO 100
  IF(IMODE.NE.1)GO TO 10
C IMODE = 1 CORRESPONDS TO CONVENTIONAL HEAT PUMP
  TCOND=TAMB+16.7
C COOLING CAPACITY
  QCOOL=QNDM*(B1+B2*TCOND+B3*TCOND**2)*1000.
C COOLING COP
  COP=A1*TCOND+A2
  QELE=QCOOL/COP*1000.
  GO TO 60
10 TALF=TAU*ALPHA
  TC(2)=TAMB
20 TC(1)=TC(2)-.5
  TC(3)=TC(2)+.5
  DO 50 N=1,3
  TPLATE=TC(N)
C COLLECTOR EQUATION
  QH=AC*(UL*(TPLATE-TAMB)*.0036-TALF*GT/1000.)
C COOLING PERFORMANCE CALCULATIONS
  COP=A1*TC(N)+A2
  QL=QNDM*(B1+B2*TC(N)+B3*TC(N)**2)
  W=QL/COP
  F(N)=1.+COP-QH/W
  TCOND=TC(N)
  IF(ABS(F(N)).GE..01)GO TO 50
  IF(COP.LT.COPM)GO TO 40
  QL=QL*COPM/COP
  COP=COPM
C CONVERT MJ TO GJ
40 QCOOL=QL*1000.
  QELE=QL/COP*1000.
50 CONTINUE
  IF(QCOOL.GT.0.)GO TO 60
C RESET TCOND FOR NEWTON'S METHOD
  TC(2)=TC(2)-F(2)/(F(3)-F(1))
  GO TO 20
60 CONTINUE
C LIMIT MAXIMUM VALUE OF TCOND
  IF(TCOND.GT.80.)GO TO 100
C DETERMINE 'ON'TIME DURING SIMULATION HOUR
  TO=CAPAC*(TROOM-TSET)/QCOOL

```

```
      IF(TO.GT.1.)TO=1.  
      IF(TO.LT.0.)TO=0.  
C   OUTPUT RESULTS  
100 OUT(1)=-TU*QCOOL  
    OUT(2)=TO*QELE  
    OUT(3)=TO  
    RETURN  
    END  
:
```